

DOE Environmental Management Science Program

Final Report

Title: Characterization of Changes in Colloid and DNAPL Affecting Surface Chemistry and Remediation

Project ID: 0009572

Project Manager: Roland F. Hirsch, Phone: 301-903-9009 Division: SC-75

Award Register#: ER63660 0009572

Primary EM Problem Area: Subsurface Contamination

Report: Final report, December 15, 2006

Principal Investigators:

Lead PI:	Co-PI:	Co-PI:
Dr. Susan E. Powers Clarkson University Potsdam NY 13699-5710 315-268-6542 (PN) 315-268-7985 (FN) sep@clarkson.edu	Dr. Stefan Grimberg Clarkson University Potsdam NY 13699-5710 315-268-6490 (PN) grimberg@clarkson.edu	Dr. Miles E. Denham Westinghouse Savannah River Company Building 773-42A Aiken SC 29808 803-725-5521 (PN) miles.denham@srs.gov

Researchers:

Wenqian Dou, Ph.D. Candidate (DNAPL characterization) (Clarkson)
Laura Bertrand, M.S. Candidate (microbial characterization) (Clarkson)
Margaret Millings, Senior Scientist (sample preparation and grain size analysis) (WSRC)
Jay Noonkester, Senior Scientist (drilling preparations and oversight during drilling) (WSRC)

Prepared for the U.S. Department of Energy Under Contracts No.
DE-FG02-03ER63660 and DE-AC09-96SR18500

Disclaimers

Any opinions, findings, and conclusions or recommendations expressed in this material are those of the authors and do not necessarily reflect the views of the Department of Energy.

Portions of this report were prepared by Westinghouse Savannah River Company (WSRC) and Clarkson University for the United States Department of Energy under Contract Nos. DE-AC09-96SR18500 and DE-FG02-03ER63660 and is an account of work performed under that contract. Neither the United States Department of Energy, nor WSRC, nor any of their employees makes any warranty, expresses or implied, assumes any legal liability or responsibility for accuracy, completeness, or usefulness, of any information, apparatus, or product or process disclosed herein or represents that its use will not infringe privately owned rights. Reference herein to any specific commercial product, process, or service by trademark, name, manufacturer or otherwise does not necessarily constitute or imply endorsement, recommendation, or favoring of same by WSRC or by the United States Government or any agency thereof. The views and opinions of the authors expressed herein do not necessarily state or reflect those of the United States Government or any agency thereof.

Executive Summary

The waste disposal to the M-area basin and A-14 outfall at the Savannah River Department of Energy facility in Aiken SC (USA) included a wide variety of inorganic aqueous flows and organic solvents in the form of dense non-aqueous phase liquids (DNAPL). The DNAPL has migrated through the subsurface resulting in widespread groundwater contamination. The goal of this research was to identify and quantify processes that could have affected the migration and remediation of the DNAPL in the subsurface. It was hypothesized that the variety of waste disposed at this site could have altered the mineral, microbial and DNAPL properties at this site relative to other DNAPL sites.

The DNAPL was determined to have a very low interfacial tension and is suspected to be distributed in fine grained media, thereby reducing the effectiveness of soil vapor extraction remediation efforts. Although the DNAPL is primarily comprised of tetrachloroethene and trichloroethane, it also contains organic acids and several heavy metals. Experimental results suggest that iron from the aqueous and DNAPL phases undergoes precipitation and dechlorination reactions at the DNAPL-water interface, contributing to the low interfacial tension and acidity of the DNAPL. Biological activity in the contaminated region can also contribute to the low interfacial tension. PCE degrading bacteria produce biosurfactants and adhere to the DNAPL-water interface when stressed by high tetrachloroethene or low dissolved oxygen concentrations. The presence of iron can reduce the interfacial tension by nearly an order of magnitude, while the PCE degraders reduced the interfacial tension by nearly 50%. Abiotic changes in the mineral characteristics were not found to be substantially different between contaminated and background samples.

The research completed here begins to shed some insight into the complexities of DNAPL fate and migration at sites where co-disposal of many different waste products occurred. Quantifying the low interfacial tension of the SRS DNAPL helps to formulate a new conceptual picture of the subsurface DNAPL migration and provides an explanation of the limited effectiveness of remediation efforts. Alternative designs for remediation that are more effective for sites with DNAPL in fine grained media are required.

Table of Contents

Disclaimers.....	i
Executive Summary.....	ii
Table of Contents.....	iii
List of Figures.....	v
List of Tables	viii
Project Report	1
1.0 Research Basis and Objectives	2
2.0 Research Approach.....	4
3.0 Activities Completed to Meet the Objectives.....	5
4.0 Properties of Subsurface Sediments near the A-14 Outfall (Task 1)	6
4.1 Introduction	6
4.2 Sediment Properties and DNAPL Behavior.....	6
4.3 Background	7
4.4 Methods.....	10
4.5 Results	11
4.6 Conclusions Task 1	20
4.7 References Task 1	21
5.0 Microbial Distribution in Field Samples (Task 2).....	23
5.1 Methods.....	23
5.2 Bacterial Distribution within the Background Cores	24
5.3 Comparison of Contaminated & Uncontaminated Borings	26
5.4 Conclusions - Task 2	28
6.0 Effect of microorganisms on DNAPL interfacial properties (Task 2)	29
6.1 Abstract	29
6.2 Introduction	29
6.3 Materials and Methods	30
6.4 Results	37
6.4.1 Base Case Scenarios	38

6.4.2 Abiotic Controls.....	39
6.4.3 Stressed Culture Results	40
6.5 Discussion	46
6.6 Conclusions – Task 2	48
6.7 References	48
7.0 Characterization of DNAPL from DOE Savannah River Site (Task 3).....	51
7.1. Introduction	51
7.2. Experimental Approach.....	53
7.3. Results and Discussion.....	56
7.4. Conclusions and Implication – Task 3	63
7.5 Acknowledgements	64
7.6 References	64
8.0 Mechanisms for interfacial tension reductions in the presence of metals and metal-ligand complexes (Task 4).....	68
8.1 Introduction	68
8.2 Materials and Methods	70
8.4 Results and Discussion.....	72
8.5 Conclusions – Task 4	81
8.5 Acknowledgements	82
8.6 References	82
9.0 Research Products.....	86
9.1 Papers:	86
9.2 Presentations at Conferences:.....	86
9.3 Invited Lectures.....	86
9.4 Graduate Thesis.....	87

List of Figures

Figure 4.1: Map of the study location.....	9
Figure 4.2: Photograph showing hollow stem augering at the A-14 Outfall.	10
Figure 4.3: Photograph showing sampling of split spoon core.....	10
Figure 4.4: Location of background soil borings relative to A-14 Outfall.	11
Figure 4.5: Comparison of various sediment properties in the SB-01 core. Each bar represents a sample.	12
Figure 4.6: Comparison of various sediment properties in the MHS-03 core. Each bar represents a sample.....	12
Figure 4.7: Plots of grain size variation with depth in cores from A-14 Outfall. SB-04 through SB-06 are background samples.....	13
Figure 4.8: Ternary diagram of x-ray fluorescence data plotted as fraction of quartz, kaolinite, and hematite. Open circles are samples from SB-01, open squares are from MHS-03, triangles are from background cores P-16, P-28, and P-30 (Strom and Kaback, 1992).	14
Figure 4.9: Fe_2O_3 versus Al_2O_3 (wt. %). Open circles are samples from SB-01, open squares are from MHS-03, closed triangles are from background core SB-04.	15
Figure 4.10: TiO_2 versus Fe_2O_3 (wt. %). Open circles are samples from SB-01, open squares are from MHS-03, closed triangles are from background core SB-04.	15
Figure 4.11: TiO_2 versus Al_2O_3 (wt. %). Open circles are samples from SB-01, open squares are from MHS-03, closed triangles are from background core SB-04.	15
Figure 4.12: Al_2O_3 versus SiO_2 (moles/kg). Open circles are samples from SB-01, open squares are from MHS-03, triangles are from background cores P-16, P-28, and P-30 (Strom and Kaback, 1992).	15
Figure 4.13: Solubility of gibbsite and kaolinite versus pH. Solubility expressed as total dissolved aluminum.	16
Figure 4.14: Specific surface area versus wt.% fines for A-14 Outfall samples compared to samples from other studies.	17
Figure 4.15: Calculated versus measured surface areas using the model discussed in the text.	18
Figure 4.16: Scanning electron photomicrograph of sample SB-01-16.5 (left) and SB-01-23.5 (right) ...	19
Figure 4.17: Thin-section photomicrographs of three samples from in SB-01: a) weathered grain; b) typical sediment texture; and, c) cemented nodule. White grains are quartz, fine grained matrix is brown to black, porosity is blue. Scale is about 200 um across the bottom.	20
Figure 5.1: Location of soil boring and soil vapor extraction wells at the A-14 outfall, SRS	24
Figure 5.2: Total cell concentration as a function of depth in wells upstream of the contamination.....	25
Figure 5.3: Cell viability as a function of depth in SB-04 (NW upstream of contamination)	25
Figure 5.4: Spatial distribution of total cell counts in contaminated vs un-contaminated cores.....	26
Figure 5.5: Characterization of soil borings SB-01 (a) and MHS-03 (b).....	27

Figure 5.6: Cell concentration measured using the acridine orange direct count method as a function of VOC concentrations in boring MHS-03 below 20 feet.	28
Figure 6.1: Celstir reactor	33
Figure 6.2: Microcosm preparation schematic	35
Figure 6.3: Mineral colloids, and pure media controls effect on interfacial tension	39
Figure 6.4: ST and IFT of particulate sample from Cornell butyrate culture stressed with 190 mg/L PCE for 1-week. Error bars represent one standard deviation of three replicate measurements	40
Figure 6.5: Effect of PCE (190 mg/L) and oxygen (1.5 mg/L) stress on SRS2 IFT at a cell concentration of $8.9 \times 10^8 \text{ #/mL}$ (5X). (1 μm Filtered (particulate samples))	41
Figure 6.6: Effect of oxygen stress on interfacial properties (ST: a, b) and IFT: c, d)) of Cornell Culture after one-week of incubation. DO concentrations in mg/L. Media filtered through 1 μm filter paper (particulate samples: a, c)) and 0.22 μm (particulate free samples: b, d)). Error bars of one standard deviation included	43
Figure 6.7: IFT for SRS2 sample - Original Concentration, 0.22 μm Filtered	46
Figure 7.1: Pendent drop ST/IFT measured by OCA 15+	55
Figure 7.2: SRS DNAPL chromatography from GC/MS	57
Figure 7.3: ^1H NMR spectra for SRS DNAPL (a) and TCE with hydraulic oil (b)	57
Figure 7.4: Dynamic changes of IFT between DNAPL/water over time. Error bars are standard deviation calculated from triplicate measurements	60
Figure 7.5: Pendant drops from tensiometer (IFT in mN/m). Left column – time series of DNAPL droplets in water show little change with time. Right column – time series of water droplets in DNAPL show more significant changes and the formation of a semi-rigid film as white precipitate (not visible in photo) accumulates at the interface	61
Figure 7.6: Electrophoretic mobility of SRS soils and DNAPL	62
Figure 7.7: Electromotive force measured during non-aqueous titration of SRS DNAPL spiked with stearic acid. The derivative of this curve is used to determine the inflection point and acid number	63
Figure 8.1: Interfacial tension of TCE/water with surfactants TBP and DBBP	72
Figure 8.2: Interfacial tension of PCE (with oxine) and water (with Cu(II)). The interfacial tensions were measured 20 minutes after the drops dispense in order for the equilibration of the two phases. Sample numbers are defined in Table 3	74
Figure 8.3: Interfacial tension of PCE (with oxine) and water (with Fe(III)). The interfacial tensions were measured 20 minutes after the drops dispense in order for the equilibration of the two phases. Sample numbers are defined in Table 2	75
Figure 8.4: PCE solubility in metal complex solutions. Sample numbers are defined in Table 8.5	77
Figure 8.5: Percentage change in the interfacial tension of NAPLs contacted with a) and b) 0.01 mol/L Fe(III) or c) and d) 0.01 mol/L Fe(II) solutions	78
Figure 8.6: Film formation when dispense 0.01 mol/L a) Fe(III) and b) Fe(II) aqueous solution droplets in PCE. A semi-rigid surface film is apparent on drops that aged at least 60 minutes. The white center of the droplets is an artifact of the light reflected from the liquid surface during photography	78

Figure 8.7: Fe(III) aqueous solution droplets suspended in NAPLs: a) 3-chlorotoluene; b) toluene; and, c) heptane at 0 mins (left) and 120 mins (right).....	80
Figure 8.8: Precipitate formation observed when a 0.01 mol/L Fe(III) aqueous solution drop was dispensed in 4-chlorotoluene.	80
Figure 8.9: PCE degradation with 0.01 mol/l Fe^{3+} and 0.01 mol/l Fe^{2+}	81
Figure 8.10: pH change of PCE degradation with 0.01 mol/l Fe^{3+} and 0.01 mol/l Fe^{2+}	81

List of Tables

Table 4.1: Zero Point of Charge of various minerals present in SRS subsurface sediments (from Stumm, 1992).....	7
Table 4.2: Soil Vapor Extraction wells at the A-14 Outfall.....	9
Table 4.3: Specific surface areas for various minerals from Langmuir (1997).	17
Table 4.4: Sample Descriptions and results of sediment acidification	19
Table 6.1: Cornell Culture Basal Media Constituents (DiStefano et al. 1992).....	31
Table 6.2: Cornell Culture Trace Metals Solution (TMS) Constituents (DiStefano et al. 1992).....	31
Table 6.3: SRS Culture Media Constituents	32
Table 6.4 : SRS Culture Trace Metals Solution (TMS) Constituents	32
Table 6.5: Carbon Sources for SRS Enrichment Cultures	33
Table 6.6: Stressors and concentrations tested on enrichment cultures	34
Table 6.7: Base-case culture interfacial activity after 48 hrs (mean±standard deviation).	38
Table 6.8: Comparison of ST and IFT of non-stressed Cornell and Concentrated SRS Cultures at similar cell concentrations.	39
Table 6.9: EDTA and Carbon Source Amendments Results for Cornell Culture.....	40
Table 6.10: Effect of PCE (190 mg/L) and Oxygen (1.5 mg/L) Stress on SRS2 at a cell concentration of $8.9 \times 10^8 \text{#/mL}$. Statistical Significance IFT Measurements, 1 μm Filtered	42
Table 6.11: Base Case Comparison of Mean Values of ST and IFT (dynes/cm) at 0, 24, 48 hrs for Varying Cell Concentrations	45
Table 7.1: Overview of experimental approach	53
Table 7.2: Detected metals in SRS DNAPL	58
Table 7.3: SRS DNAPL solubility in water (mg/kg; mean \pm standard deviation)	58
Table 7.4: Surface tension of water equilibrated with the DNAPLs and water-DNAPL interfacial tensions measured with a ring tensiometer (average \pm standard deviation).....	59
Table 8.1: Overall plan for research.....	70
Table 8.2: Properties of organic solvents tested.....	71
Table 8.3: Variable matrix of Oxine-Cu interfacial tension experiment.....	73
Table 8.4: Variable matrix of Oxine-Fe interfacial tension experiment	74
Table 8.5: Variable matrix of PCE solubility experiment.....	76

Project Report

1.0 Research Basis and Objectives

The remediation of DNAPLs in subsurface environments is often limited by the heterogeneous distribution of the organic fluid. The fraction of DNAPL that is in the high conductivity regions of the subsurface can often be recovered relatively easily, although DNAPL in lower conductivity regions is much more difficult to extract, either through direct pumping or remediation measures based on interface mass transfer. Most current conceptual models describing DNAPL infiltration and redistribution attribute heterogeneities in the DNAPL distribution to heterogeneity in the pore size distribution. DNAPLs are generally expected to accumulate in layers of high conductivity above lower conductivity strata due to the high capillary entry pressure of these fine-grained layers. There is a growing body of evidence that suggests that this conceptual model is insufficient - DNAPL does indeed enter the lower permeability layers, ultimately resulting in reduced remediation efficiencies. **The fundamental basis for the work summarized here is that there are other sources of heterogeneities in the subsurface that significantly affect the migration and entrapment of DNAPL** and, therefore, our ability to remove it from the subsurface. These heterogeneities include variable properties of the DNAPL itself and the presence of colloidal matter – including bacteria, mineral colloids, and organic macromolecules – that can alter the pore size distribution or accumulate on interfaces. Localized heterogeneity in oxidation state and/or pH affects the DNAPL and mineral composition and the generation and accumulation of colloids in the subsurface. The co-disposal of a wide range of organic and aqueous solutions at DOE sites might have created conditions that are uniquely important at these sites.

The work completed under this grant was a direct extension of the findings and results of a current EMSP grant (DNAPL Surface Chemistry: Its Impact on DNAPL Distribution in the Vadose Zone and its Manipulation to Enhance Remediation, project number 70035). The original grant provided a focused study predominantly on biological processes that affect interfacial properties and thus DNAPL migration. Detailed characterization of soil cores from SRS, coupled with the laboratory assessment, supported the basic premise that biological systems can indeed alter interfacial properties and multiphase flow. Characterization of the field samples suggested, however, that these biologically induced alterations were insufficient to describe the observed correlation between the DNAPL distribution and subsurface properties. A few of the key findings from the original that directly led to the work summarized here are highlighted below.

- The surface area of subsurface soils is significantly greater than predicted by the particle size distribution and mineralogy, suggesting the presence of a significant fraction of very fine or colloidal particles.
- Highest DNAPL concentrations are not correlated with coarse sand layers as would be predicted by most conceptual models. It is not yet clear if these concentrations represent the original DNAPL distribution or the results of effective remediation only in the coarser layers.
- DNAPL at the site has a very low interfacial tension (<2 dynes/cm) relative to the value calculated based on its primary components (~40 dynes/cm). Hydraulic oil and surfactants known to have been contaminants in the DNAPL cannot account for the very low interfacial tension.
- The DNAPL is very acidic. Leaching of the acidic components from the DNAPL into water causes a significant decrease in the aqueous phase pH.
- PCE degrading microorganisms that are stressed with increasing PCE or dissolved oxygen concentrations cause the production of compounds that reduce TCE-water interfacial tensions (IFT). The decrease in IFT can be as much as 50%

Although the findings of the original grant do indeed show that a complex system that includes microbial interactions with the soil and DNAPL does affect the fundamental interfacial properties of the

subsurface, it does not explain the extreme conditions found at the SRS facility. Thus, we are proposing to complete this investigation with a focused effort to better characterize the DNAPL properties and surface area of fine-grained materials at this site. We hypothesize that these unique observations are the result of the co-disposal of a wide range of fluids into the M-area basin and the A-14 outfall area. Understanding the phenomena that contribute to these observations will help to identify challenges – which may be unique to DOE facilities - in locating and remediating DNAPL sites.

The general objectives of this project are to:

1. Obtain core samples from uncontaminated areas near the A-14 outfall area to characterize the distribution of biotic and abiotic colloidal material to determine if the observations related to biological interactions at surfaces and the high surface area of the fined grained media near the outfall are common to the native sediments or the result of past disposal practices.
2. Characterize the organic and inorganic constituents in the DNAPL and in water with leached constituents from the DNAPL to better understand the components that contribute to the low IFT and the mechanisms for partitioning these components into the DNAPL.

2.0 Research Approach

A multi-task approach involving experimental measurements at both laboratory and field scales was designed to meet the objectives of this research. Materials for this research were chosen to be applicable to vadose zone contamination problems at the Savannah River site (SRS). This research offered a unique opportunity to develop our fundamental understanding of the fate of DNAPLs in the vadose zone through both laboratory scale testing and evaluation of field samples collected at SRS. The fieldwork during this phase of the overall project provided a detailed assessment of the distribution of microbial populations, mineral characterization, and heterogeneous grain size distribution in background samples. Concurrent laboratory testing provided an understanding of the fundamental mechanisms governing these distributions. The close coupling between lab and field was designed to provide a deeper understanding of NAPL behavior in the vadose zone.

Specific objectives included in this continuation grant include:

1. Discern whether trends in surface area and bulk chemistry result from waste disposal or depositional history
2. Determine if the observed surface activity of the stressed soil organisms is specific to PCE dechlorinating cultures or can also be observed for microbial communities in uncontaminated SRS sediments.
3. Identify the constituents in the DNAPL that affect its acidic and interfacial behavior
4. Determine if the co-disposal of acids, bases, aluminum and other effluent contaminants could cause chemical reactions or the partitioning of constituents into the DNAPL

3.0 Activities Completed to Meet the Objectives

Four tasks were established to meet these objectives:

Task 1: Analysis of Background Samples – Surface Area Issues

Task 2: Analysis of Background Samples – Microbial Accumulation and Surface Activity

Task 3: Characterize SRS DNAPL

Task 4: Partitioning/Reaction Experiments

The research work included additional field sample collection that occurred in 2003 to provide sufficient samples for Tasks 1 and 2. Following characterization of these samples, the results were compared to the results from samples collected at the contaminated A-14 outfall area. Tasks 3 and 4 were completed in the laboratory.

The background analyses work completed for Task 1 and Task 2 are integrated here with prior results for contaminated A-14 outfall samples to provide the most relevance for this work (Sections 4.0 and 5.0). Task 2 was extended to include a laboratory analysis of the effects of background microbial communities on interfacial properties. These results are included in Section 6. Tasks 3 and 4 are presented as two separate manuscripts that are currently in preparation for publication (Sections 7.0 and 8.0).

4.0 Properties of Subsurface Sediments near the A-14 Outfall (Task 1)

4.1 Introduction

The migration, accumulation, and remediation of DNAPL (dense non-aqueous phase liquid) is strongly dependent on the nature of the subsurface material in which it occurs and the composition of the DNAPL. The original project, funded by the Environmental Management Science Program (Project No. 70035), was a collaboration between the Savannah River Technology Center (SRTC) and Clarkson University to investigate these factors that influence DNAPL behavior. Subsurface samples were collected from 2 sites with known DNAPL (PCE and TCE) contamination at the Savannah River Site. These were split between Clarkson University and SRTC for analysis. Clarkson University concentrated on investigating the influences of microbiology and DNAPL chemistry, as well as simulating DNAPL behavior in the laboratory. SRTC measured PCE and TCE concentrations in the samples and investigated the sediment properties that may influence DNAPL behavior. The subsequent grant allowed background samples to be collected and analyzed. This section covers the SRTC portion of the project.

The objectives of the SRTC portion of this project were to:

- Provide support to Clarkson University in obtaining SRS subsurface sediment samples, DNAPL samples, and information pertinent to their studies,
- Characterize the properties of subsurface sediment samples that may influence DNAPL migration, accumulation, and remediation in a typical coastal plain setting.

Analysis of the background samples suggest that the hypothesis that corrosive fluids disposed at the A-14 Outfall caused significant changes in the properties of the sediments is false. The chemical and textural trends observed in the background samples are identical to samples taken at the A-14 Outfall. If corrosive fluids did affect the properties of the sediments, the changes are too minor to be detected in these types of bulk analyses.

4.2 Sediment Properties and DNAPL Behavior

Migration and accumulation of DNAPL in the subsurface is controlled, in large part, by gravitational and capillary forces. Sediment properties play no role in the gravitational forces, but are fundamentally important to the capillary forces. In a system containing multiple fluids and a solid surface the capillary forces are a balance of interfacial tensions between the different media. Thus, any factor that affects interfacial tension can influence DNAPL behavior.

The property that has received the most attention is grain size distribution. The capillary forces in sediments have been compared to those in a bundle of straws with different diameters (Cohen and Mercer, 1993; Looney and Falta, 2000). If the straws are placed in a liquid, the level of the liquid rises highest in the smallest diameter straws because the capillary forces are greatest. The analogy to sediments is that capillary forces tend to be stronger in fine grained sediments than in coarse grained sediments. If DNAPL is the wetting phase, these forces can draw DNAPL into fine grained sediments and hold it there. If water is the wetting phase, capillary forces may exclude DNAPL from fine grained sediments, confining its migration and accumulation to coarse sediments.

Mineralogy is an important influence on the wetting properties of sediment surfaces because interfacial tension of a liquid on a mineral surface varies with the surface charge of the mineral. For example, a hydrophobic substance such as perchloroethylene (PCE) will have a minimum interfacial tension when the bulk surface charge of the mineral is zero. The pH at which this occurs is different for different minerals and is referred to as the zero point of charge (ZPC). Table 1 shows the ZPC for several minerals common to sediments. They vary from a pH of 2 for quartz to a pH of 8.5 for hematite. This

suggests that for a given groundwater pH the capillary forces controlling DNAPL behavior depend, in part, on the identity of the dominant mineral at sediment grain surfaces.

Table 4.1: Zero Point of Charge of various minerals present in SRS subsurface sediments (from Stumm, 1992).

Mineral	Formula	Zero Point of Charge
Gibbsite	$\text{Al}(\text{OH})_3$	5.0
Kaolinite	$\text{Al}_2\text{Si}_2\text{O}_5(\text{OH})_4$	4.6
Hematite	Fe_2O_3	8.5
Goethite	FeOOH	7.8
Quartz	SiO_2	2.0

Surface area of sediment may also play a role in migration and accumulation of DNAPL. Surface area is strongly correlated to grain size distribution, but may also reflect microporosity and surface roughness of mineral grains. Burdon (1949) indicates that increases in surface roughness, and hence in surface area, can further decrease the interfacial tension of a wetting liquid on a surface. Dissolution pitting or adherence of colloidal sized particles to mineral surfaces may increase surface roughness of mineral grains.

The main sediment property that controls DNAPL remediation is permeability of sediments to fluids designed to destroy or mobilize DNAPL. For heating technologies this would be permeability to steam or other heating media. For surfactant and oxidation technologies permeability to injected reagents would be important. In the vadose zone, permeability of air would be important to sediment vapor extraction (SVE).

This study concentrated on measurement of grain size, mineralogy, and surface area. In addition, it focussed on demonstrating the types of heterogeneities in these properties that are common to coastal plain sediments. Permeability was not measured, but its variation can be qualitatively inferred from the other properties.

4.3 Background

Chlorinated solvents and other chemicals were used and released to the subsurface during operations within the A/M-Area of the Savannah River Site from the early 1950's through the mid 1980's. Solvents, primarily trichloroethylene (TCE), tetrachloroethylene (PCE), and 1,1,1-trichloroethane (1,1,1-TCA), were used in degreasing processes in facilities that fabricated reactor fuel and target assemblies for SRS reactors, laboratory facilities within Savannah River Technology Center (formerly the Savannah River Laboratory), and other support facilities within the A/M-Area.

The majority of the chlorinated solvents were used during fabrication processes in M-Area where fuel and target elements were dipped in degreasing vats and cleaned with hot caustic and hot acidic solutions at various processing stages. The spent solvent and chemical wastes were disposed via underground vitrified clay process sewer lines to the M-Area Settling Basin and the A-014 Outfall (Figure 1). Historical investigations estimate that from 1952 through 1982 approximately 13 million pounds of chlorinated solvents were used in M-Area. Of this total, 1.5 million pounds of solvent were estimated to have been released to the A-014 Outfall and 2 million pounds of solvent were estimated to have been released to the M-Area Settling Basin (Marine and Bledsoe, 1984; Pickett et al., 1987; Looney et al., 1992).

In 1952 the A-014 Outfall began receiving waste from the fabrication facilities in M-Area. The outfall feeds an unnamed tributary of Tim's Branch, which flows into Upper Three Runs Creek and eventually discharges to the Savannah River. In 1979 solvent discharges to the process sewer ended (Jackson et al., 1999). The A-014 Outfall currently receives stormwater runoff and water from a groundwater pump and treat system (M1 Stripper). The M-Area Settling Basin is an 8 million gallon unlined surface impoundment and was constructed in 1958 to settle and contain flocculated aluminum and other particulate metals released from M-Area fabrication processes. During high water, the basin discharged to a 3-acre seepage area and then to Lost Lake, a natural Carolina bay. In 1985 discharge to the basin ceased, the basin was backfilled, and a RCRA-style cap was installed (Looney et al., 1992).

In addition to the chlorinated solvents, waste streams to the M-Area Settling Basin and the A-014 Outfall also included metal hydroxide precipitates (e.g. aluminum, uranium, nickel and lead), acids (e.g. nitric, phosphoric, boric and sulfuric), caustics (e.g. sodium hydroxide), and industrial lubricant (e.g. lead oil) and cleaning compounds (Pickett et al., 1987; Jackson et al., 1996). Variations in operation schedules together with changes in products used through time resulted in varying waste stream chemistries and volumes discharged to the basin and outfall. Results from a 1985 study of the M-Area Settling Basin show some of the extreme pH's of the process streams. During this 9-week study, influent waters to the basin ranged from 9.2 to 12.4 with an average pH of 11 (Pickett et al., 1987). Historical records of discharges to the A-014 Outfall also show that the frequency and magnitude of the different types of wastes could vary dramatically. A 1970 memo regarding the discharges to the A-014 Outfall for the 1969-1970 period documents the releases of acidic, caustic, organic and other wastes. During this time period, tetrachloroethylene (PCE) and methanol were discharged to the outfall in batches once and twice a week (1750 pounds PCE and 350 pounds methanol per release). In contrast, trichloroethylene (TCE) was released in a single event (12,000 pounds). This memo also provides some details of acidic and caustic releases to the outfall during this time. A total of 173,000 pounds of nitric acid were reported to have been discharged in weekly and biweekly batches of 700-1300 pounds. Discharges of sodium hydroxide wastes totaled 23,700 pounds in weekly batches of 380 pounds and monthly batches of 300 pounds. Although these chemical concentrations were reported as 100%, they most likely were discharged at more dilute concentrations (Jackson et al., 1996; Jackson et al., 1999). Available disposal information gives some insight into the magnitude and variety of waste streams at A/M-Area. However, records of disposal are not detailed or complete enough to fully discern contaminant pathways or distributions in the subsurface. In addition, little is known about the diagenetic impact of the waste on subsurface sediments.

Various characterization studies and investigations have been conducted since soil and groundwater contamination was first identified in the A/M-Area in 1981 (Marine and Bledsoe, 1984; Pickett et al., 1987; Looney et al., 1992; Jackson et al., 1996; Jackson et al., 1997; Jackson et al., 1999; Jerome et al., 1999; Jackson et al., 2000; Vangelas, 2000). Remediation strategies have been developed and applied to meet the needs and remediation goals of the various parts of the DNAPL plume in the A/M-Area. Technologies implemented include conventional pump and treat systems and a series of vertical recirculation wells (in-well vapor stripping) to address the dissolved phase of DNAPL contamination in the groundwater. Soil vapor extraction and barometric pumping systems have been installed to help remove solvent in the vapor phase from the vadose zone. In addition to these programs, other remediation technologies, such as phytoremediation, Dynamic Underground Stripping, six phase heating, radiofrequency heating, and in-situ oxidation using Fenton's reagent have been demonstrated or implemented as pilot treatment systems to target particular parts of the plume (Jerome et al., 1997; Jackson et al., 2000; Vangelas, 2000; Jackson and Looney, 2001).

Beginning in 1987 soil vapor extraction was implemented in various stages for vadose remediation within A/M Area (Jackson et al., 1999). During the first year of operation more than 39,000 pounds of solvent were removed by the soil vapor extraction units (Jackson et al., 1996). Currently at the A-014 Outfall the soil vapor extraction system (782-3M) consists of seven wells screened at various depths within the vadose zone. More specifically, MVE-13, MVE-17, and MVE-19 target shallow

contaminants (16-26 feet below land surface) close to the outfall whereas MVE-4, MVE-9, MVE-10, and MRS-34 are screened deeper within the vadose zone. Table 2 lists the wells, their installation dates, and approximate depths of their screen zones.

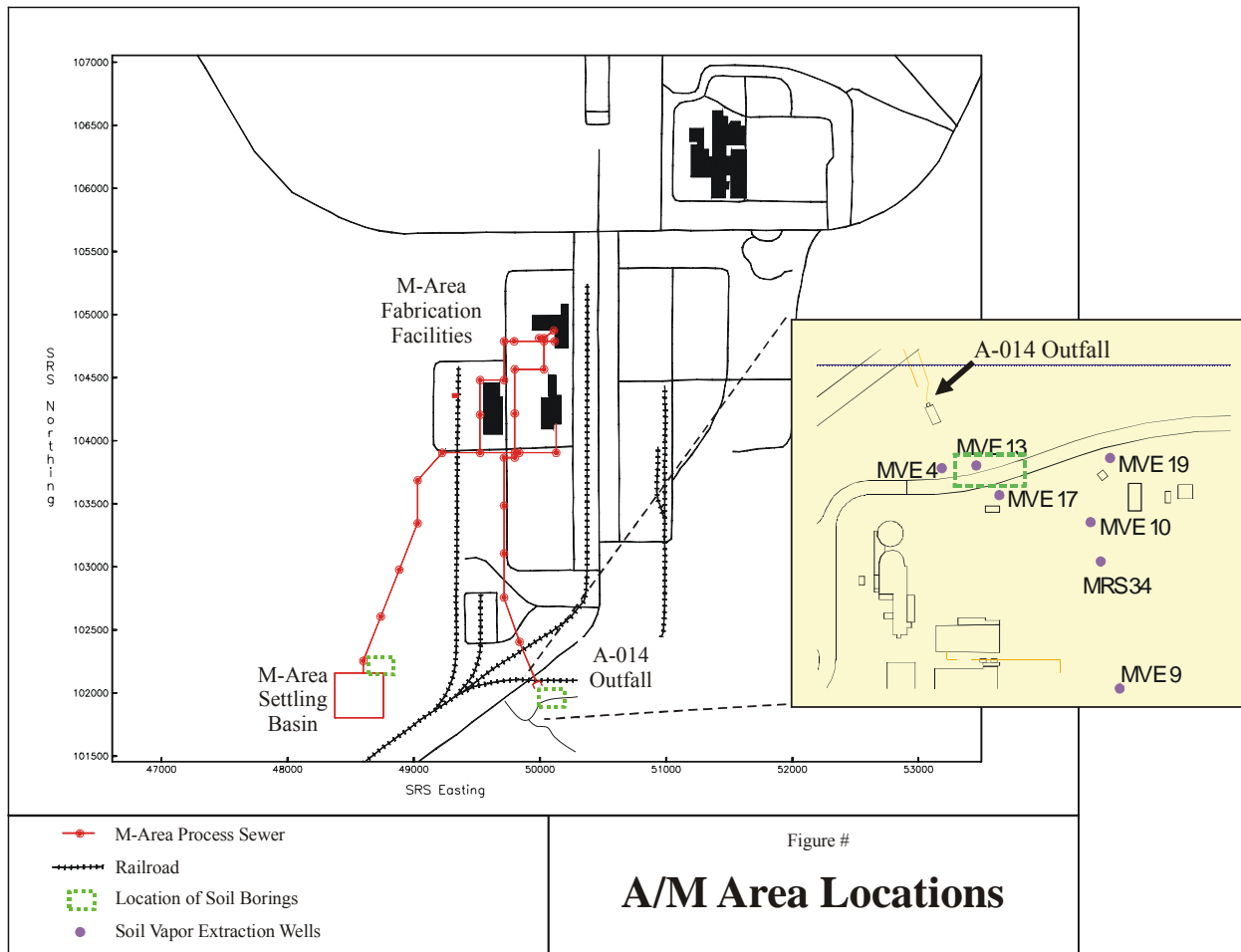


Figure 4.1: Map of the study location.

Table 4.2: Soil Vapor Extraction wells at the A-14 Outfall.

Well ID	Well Installation Date	Approximate Screen Zone (ft bbls)
MVE-4	9/1990	54-115
MVE-9	3/1994	35-102
MVE-10	3/1994	43-109
MVE-13	4/1999	17-27
MVE-17	4/1999	16-26
MVE-19	4/1999	14-24
MRS-34	4/2000	95-115

4.4 Methods

In March 2000 four soil borings were collected from A/M-Area, two from the M-Area Settling Basin and two from the A-014 Outfall, using hollow stem augers and split spoons (Figures 4.1-4.3). Depth discrete sediment samples were collected at approximately 1-foot intervals for TCE and PCE analysis. Based on these analytical results, two more soil borings were collected at the A-014 Outfall in May 2001 using direct push/rotary hammer (GeoProbe®) techniques. This method was used to collect continuous core samples in 4-foot long, 1 $\frac{3}{4}$ -inch diameter polycarbonate sleeves (Gregg In-Situ MacroCore™). Once collected the polycarbonate sleeves were split and depth discrete soil samples were collected at approximately 1-foot intervals for TCE and PCE analysis.



Figure 4.2: Photograph showing hollow stem augering at the A-14 Outfall.



Figure 4.3: Photograph showing sampling of split spoon core.

PCE and TCE concentration data from the original grant and other studies were used to delineate a zone of contamination around the A-14 Outfall. Four locations outside of this area were selected for depth discrete sampling, two on either side of the outfall (Figure 4.4). These were sampled on March 15, 2003 by direct push methods. Continuous cores were collected from each location to a depth of 30 feet below ground surface. Samples for microbiological and VOC analyses were taken in the field. Samples for chemical and textural analyses were taken from the cores in the laboratory. Grain-size analyses were done on 3 of these (SB-04, SB-05, and SB-06) and one (SB-04) was selected for detailed chemical, textural, and mineralogical analysis.

The method for TCE and PCE analysis is a modified version of EPA Method 5021 and has been an effective analytical technique used in environmental characterization at SRS since 1991. The method involves collecting approximately a 2 cubic centimeter plug of sediment from the core using a modified plastic syringe. The plug is placed in a 22 mL headspace vial with 5 mL of deionized pure water. The glass vial is then sealed with a crimped Teflon-lined septum top for headspace analysis. Duplicate samples are collected at each sample depth. Volatile analysis is performed at SRTC laboratories using a Hewlett Packard 5890 or 6890 Series II gas chromatograph with electron capture (ECD) and flame ionization detectors (FID) in parallel with an automated headspace sampler at 70°C.

The two soil borings (SB-01 and MHS-03) with the highest concentrations of TCE and PCE were chosen for more extensive analyses to investigate the interrelations between soil properties that may be important to DNAPL accumulation and remediation. Both soil borings were collected from the A-014 Outfall, and the high concentrations of TCE and PCE in these borings indicate that they were both in the path of migrating DNAPL.

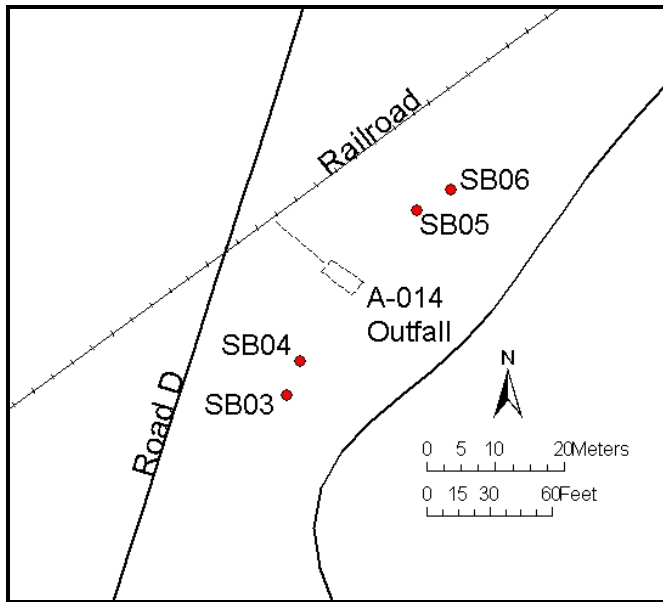


Figure 4.4: Location of background soil borings relative to A-14 Outfall.

Analyses of soil properties for the two soil borings included grain size distribution, surface area, bulk chemistry, bulk mineralogy, soil pH, petrographic and scanning electron microscopy and gravimetric moisture. Grain size analyses were conducted according to an internal SRTC dry sieving procedure (Manual WSRC-L14.1, Procedure 2-43 Rev. 1, issued 10/30/92) with modifications to sieve sizes and disposition of samples. Surface area was determined by BET nitrogen adsorption method using a Micromeritics ASAP2010 (Accelerated Surface Area and Pore volume analyzer) precision gas adsorption instrument. For bulk chemistry analysis, sediment samples were fused in a lithium tetraborate/lithium fluoride mixed flux and a Rigaku 3271 wavelength dispersive x-ray fluorescence spectrometer was used to determine the elemental compositions. Bulk mineralogy of ground sediment samples was analyzed using a Siemens D500 diffractometer by step scanning over the 2Θ ranges of $3\text{--}70^\circ$ with a step size of 0.02° and a dwell time of 1s. Soil pH was determined using ASTM Standard Test Method for pH of Soils (ASTM D4972-01). Petrographic thin sections made using standard commercial methods were examined using Leitz and Zeiss petrographic microscopes. Sediments were also analyzed using a Cambridge 250 scanning electron microscope to determine mineral morphology and distribution. Gravimetric moisture was determined by weight difference before and after oven drying. Further details regarding grain size distribution, surface area, bulk chemistry, and bulk mineralogy analyses can be found in the appendices.

4.5 Results

4.5.1 General Relationships among Sediment Properties

Figures 4.5 and 4.6 show sediment properties plotted with depth for both sediment borings at the A-14 Outfall. In general, grain size increases with depth, and consequently, surface area of the sediments decreases with depth. Iron and aluminum concentrations also decrease with depth because they are associated with the fine grained matrix of the sediments. In both sediment borings the median grain size is largest in the depth interval from 18-23 feet. In sediment boring SB-01 this corresponds to a significant decrease in the concentrations of TCE and PCE. This pattern is not observed in sediment boring MHS-03; TCE and PCE concentrations are nearly constant with depth.

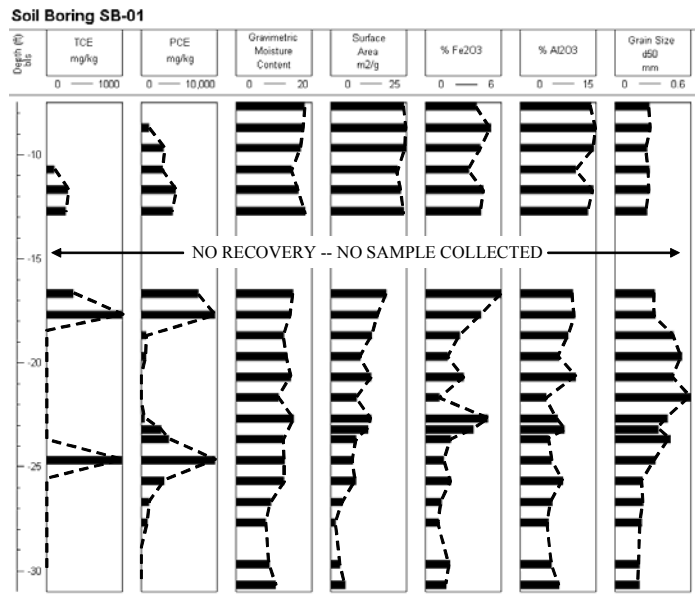


Figure 4.5: Comparison of various sediment properties in the SB-01 core. Each bar represents a sample.

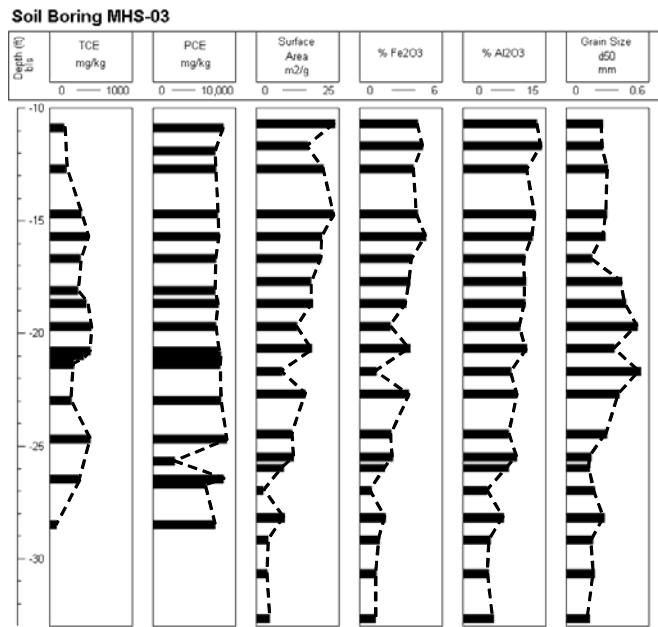


Figure 4.6: Comparison of various sediment properties in the MHS-03 core. Each bar represents a sample.

4.5.2 Grain Size

The sediments in the top 30 feet near the A-14 Outfall can be classified as coarse to fine grain sands with minor fine-grained material. The silt and clay fraction (<0.075 mm) varies from 4.4 to 15.7 wt % in boring SB-01 and from 5.3 to 13.8 wt. % in boring MHS-03. A much greater variation is observed in the relative abundances of the sand-sized fractions. Figure 4.7 shows grain size in both borings classified as coarse sand (>0.6 mm), medium sand (0.25-0.6 mm), fine sand (0.15-0.25 mm), very fine sand (0.075-0.15 mm), and silt + clay (<0.075 mm). The largest variation in grain size is from the medium/coarse sand

compared to very fine/fine sand. Much of this variation is associated with an increase in the coarse/medium fraction at a depth interval of 17.5 to 23.5 feet in sediment boring SB-01. A similar feature occurs in sediment boring MHS-03 at a depth interval of 15.5 to 25.5 feet.

Grain-size analysis of the 3 background cores show similar trends (Figure 4.7). The coarsening of grain-size in the middle interval is less pronounced in the background cores than in cores from the A-14 Outfall. However, the analyses of the background cores should not be quantitatively compared with SB-01 and MHS-03 because they were done by different analysts using slightly different procedures.

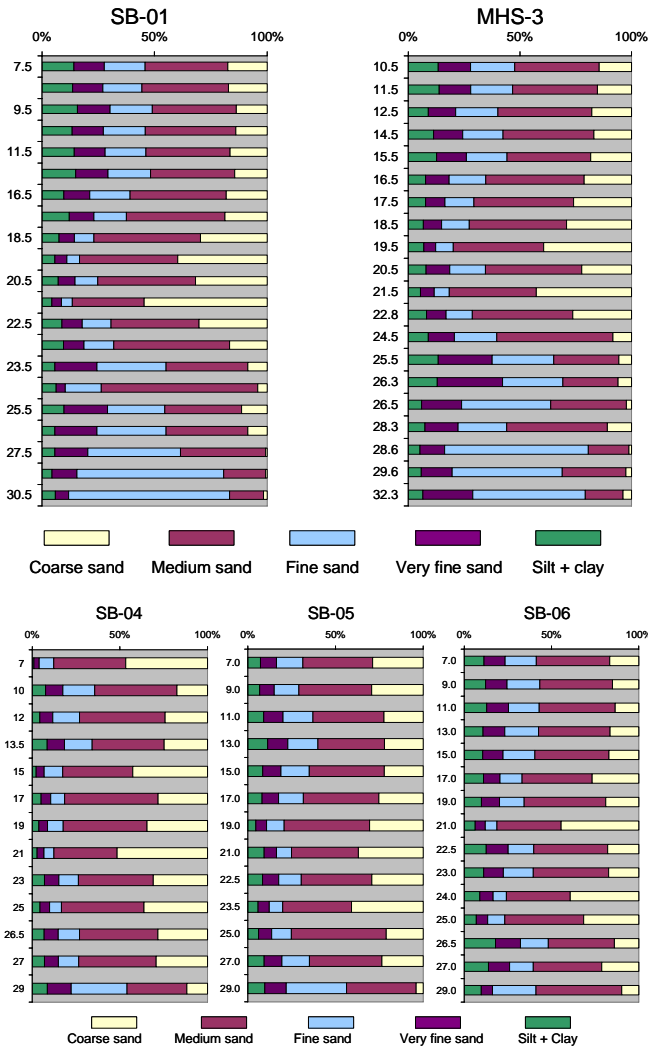


Figure 4.7: Plots of grain size variation with depth in cores from A-14 Outfall.
SB-04 through SB-06 are background samples

4.5.3 TCE and PCE Concentrations

The one parameter for which there is a marked difference between the two sediment cores is concentration of solvents (Figures 4.5 and 4.6). The highest concentrations in these cores are indicative of the presence of DNAPL. The concentrations of TCE and PCE in boring MHS-03 are relatively constant throughout the sampled depth interval. In contrast, there is a sharp decrease in TCE and PCE concentrations at a depth interval of 17.5 to 25.0 feet in boring SB-01. This depth interval corresponds to

the screen intervals of the shallow vapor extraction wells (Table 4.2) suggesting efficient removal of DNAPL within this depth interval. This depth interval also corresponds to the increase in the fraction of medium-coarse sand relative to finer grain-size fractions present in both borings. Both borings were also in close proximity to vapor extraction wells, so the reason for efficient DNAPL removal in one relative to the other is unclear. Nevertheless, it does highlight the heterogeneity that makes DNAPL clean-up in coastal plain sands difficult.

4.5.4 Mineralogy/Chemistry

The mineralogy of the sediment borings, as determined by powder x-ray diffraction, is dominated by quartz, kaolinite, and hematite. This is consistent with the bulk chemistry determined by x-ray fluorescence spectroscopy. Figure 4.8 shows Si, Al, and Fe x-ray fluorescence data plotted as the fraction of quartz, kaolinite, and hematite in the sediments. The observed pattern is typical of SRS sediments that are composed of quartz sand with a pore-filling matrix of fine-grained kaolinite and hematite. The linear trend of the A-14 Outfall data indicates that the fraction of hematite (0.18) to kaolinite (0.82) is relatively constant across most of the samples. Figure 4.9, a plot of Fe_2O_3 versus Al_2O_3 , confirms this. Thus, variations in bulk chemistry are the result of variations in the amount of matrix relative to quartz, rather than variations in the mineralogy of the matrix. This may have implications for DNAPL migration because it suggests that the pH at which the net surface charge on the matrix is zero is constant throughout the sediment column.

There are other trends in the chemical composition of these samples that are useful to note. Titanium is highly resistant to chemical weathering, and thus differences in the Fe/Ti and Al/Ti ratios between A-14 samples and background samples might reflect the effects of corrosive fluids disposed at the A-14 outfall. Figure 4.10 and 4.11 show that these ratios are similar in A-14 and background samples, suggesting that there was no significant leaching of Fe and Al from disposal of corrosive fluids.

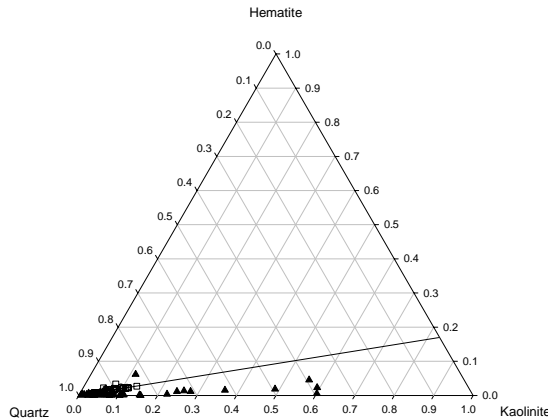


Figure 4.8: Ternary diagram of x-ray fluorescence data plotted as fraction of quartz, kaolinite, and hematite. Open circles are samples from SB-01, open squares are from MHS-03, triangles are from background cores P-16, P-28, and P-30 (Strom and Kaback, 1992).

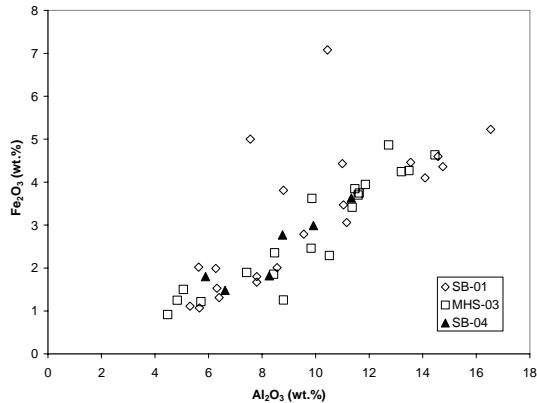


Figure 4.9: Fe_2O_3 versus Al_2O_3 (wt. %). Open circles are samples from SB-01, open squares are from MHS-03, closed triangles are from background core SB-04.

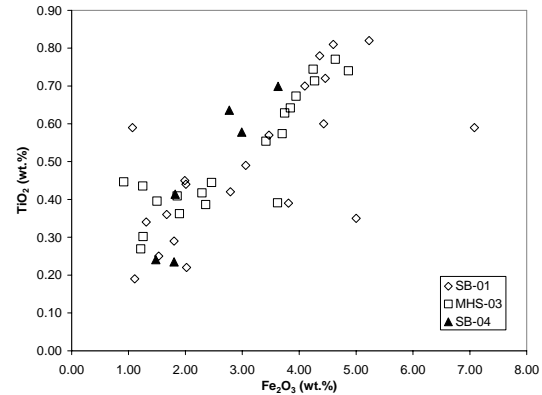


Figure 4.10: TiO_2 versus Fe_2O_3 (wt. %). Open circles are samples from SB-01, open squares are from MHS-03, closed triangles are from background core SB-04.

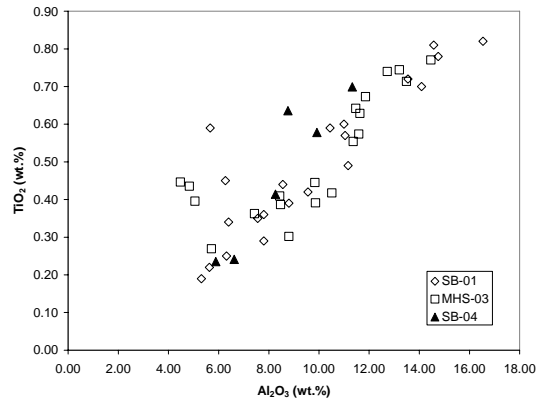


Figure 4.11: TiO_2 versus Al_2O_3 (wt. %). Open circles are samples from SB-01, open squares are from MHS-03, closed triangles are from background core SB-04.

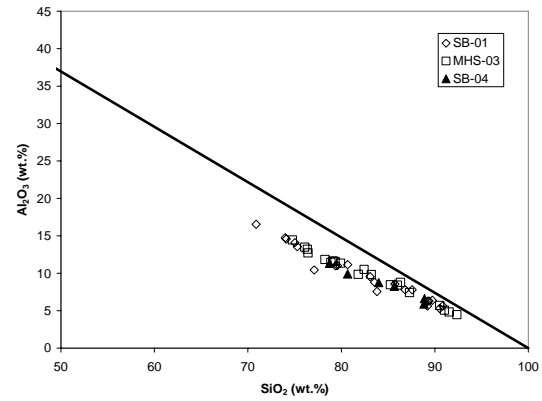


Figure 4.12: Al_2O_3 versus SiO_2 (moles/kg). Open circles are samples from SB-01, open squares are from MHS-03, triangles are from background cores P-16, P-28, and P-30 (Strom and Kaback, 1992).

Sediment samples from SRS, including those from the A-14 Outfall, show an excess of aluminum over an ideal mixture of quartz and kaolinite. Figure 11 shows the Al_2O_3 concentrations plotted versus the SiO_2 concentrations for A-14 Outfall samples and SRS background samples. The solid line represents the trend for a mixture of quartz and kaolinite. Samples that plot below this line have an excess of aluminum that is probably the result of the highly weathered nature of South Carolina coastal plain sediments. Under these weathering conditions kaolinite typically weathers to gibbsite because of preferential leaching of silica.

The potential effect of corrosive solutions on sediment chemistry can be examined by comparing solubilities of pertinent phases. Figure 4.13 shows the calculated solubilities of kaolinite and gibbsite versus pH. At normal groundwater conditions (pH between 5 and 7) gibbsite is the less soluble phase, indicating that kaolinite will ultimately weather to gibbsite. The solubilities converge at alkaline conditions suggesting that disposed alkaline solutions would not alter the aluminum silica ratios of a

mixture of quartz, kaolinite, and gibbsite. Thus, the effects of corrosive fluid disposal may be indistinguishable from natural weathering if the fluids were dominated by high pH.

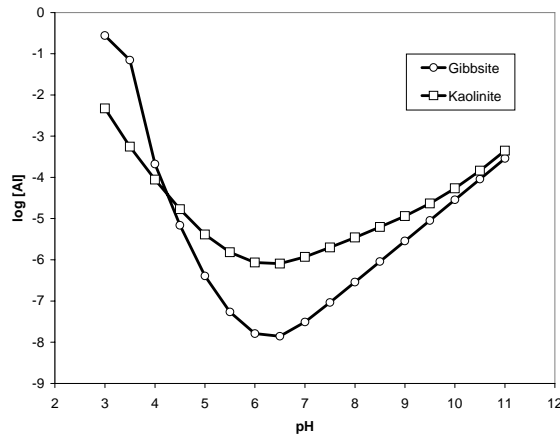


Figure 4.13: Solubility of gibbsite and kaolinite versus pH.
Solubility expressed as total dissolved aluminum.

4.5.5 Surface Area

The fine-grained fraction in most sediments and soils is the dominant contributor to surface area. This holds true for samples from the A-14 Outfall. Figure 4.14 shows a comparison of the relationship between surface area and per cent fine-grained material in A-14 Outfall samples and other studies. Samples from the A-14 Outfall have a significantly steeper slope than the other sets of samples. This suggests that the fine-grained matrix in A-14 Outfall samples has a higher specific surface area than the fine-grained material in the other studies reported here. Extrapolating the regression line for A-14 Outfall samples to 100% fine-grained matrix, yields a specific surface area of $151 \text{ m}^2/\text{g}$ for this matrix. Given that the extrapolation is from a narrow range of values near the origin, a reasonable range of specific surface area values would be 100 to $200 \text{ m}^2/\text{g}$. This is higher than many other studies, but is in the range of values reported for kaolinitic tropical soil by Chorover and Sposito (1995).

To examine the relationship of mineralogy to specific surface area, it was assumed that the total surface area is the sum of the surface area contributed by each mineral phase. Thus, the following equation allows surface areas to be calculated from mineralogical composition and values of specific surface for each mineral phase.

$$SA_{\text{total}} = SA_k * f_k + SA_h * f_h + SA_q * f_q$$

In this equation the total surface area of a sample (SA_{total}) is equal to the sum of the individual specific surface areas of kaolinite, hematite, and quartz (SA_k , SA_h , and SA_q respectively) times the fraction of each mineral in the sample (f_k , f_h , and f_q). Mid-points in the ranges of specific surface area values reported by Langmuir (1997) were used for each mineral (Table 4.3).

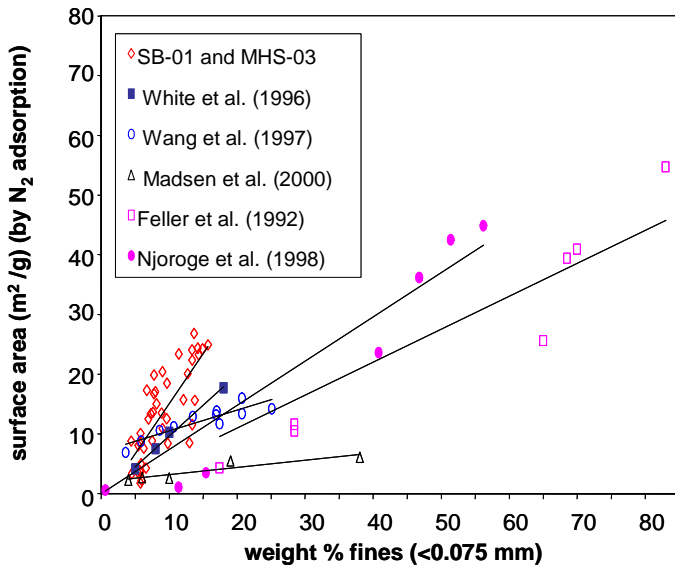


Figure 4.14: Specific surface area versus wt.% fines for A-14 Outfall samples compared to samples from other studies.

Table 4.3: Specific surface areas for various minerals from Langmuir (1997).

Mineral	Specific Surface Area (m ² /g)
Kaolinite	24
Hematite	2
Quartz	0.14

The fraction of each mineral was calculated from bulk chemical compositions of A-14 Outfall samples. Figure 4.15 shows how these calculated values relate to measured values. There is a strong linear trend in the calculated versus measured values, but it is well below the 1:1 line. This suggests that the model for calculating specific surface areas is valid, but that at least one phase used in the calculations has a specific surface area significantly higher than that reported in the literature. Of the three minerals, kaolinite requires the minimum increase in specific surface area values to give reasonable calculated values. The solid symbols in Figure 4.15 are the result of using a specific surface area for kaolinite of 200 m²/g, rather than 24 m²/g. The specific surface area of hematite would have to be about 900 m²/g to achieve a similar result.

Weathering tends to increase the specific surface area of natural sands. This may be because of an increase in surface roughness (White et al., 1996) or an increase in porosity from mineral dissolution (Kieffer et al., 1999). Yet, relatively pure Georgia kaolinite used in experiments by Huertas et al. (1998) had a specific surface area of only 8.16 m²/g. A large difference in grain size could explain the difference between this value and specific surface areas of fine-grained matrix in A-14 Outfall samples. But, this difference may also be consistent with exposure of the A-14 Outfall samples to corrosive solutions. Both acidic and caustic solutions may increase microporosity in kaolinite. Likewise, incongruent dissolution of kaolinite in acid may result in an amorphous silica gel at the surface (Xie and Walther, 1992). The specific surface areas of such gels are high; Langmuir (1997) reports literature values ranging up to 292 m²/g.

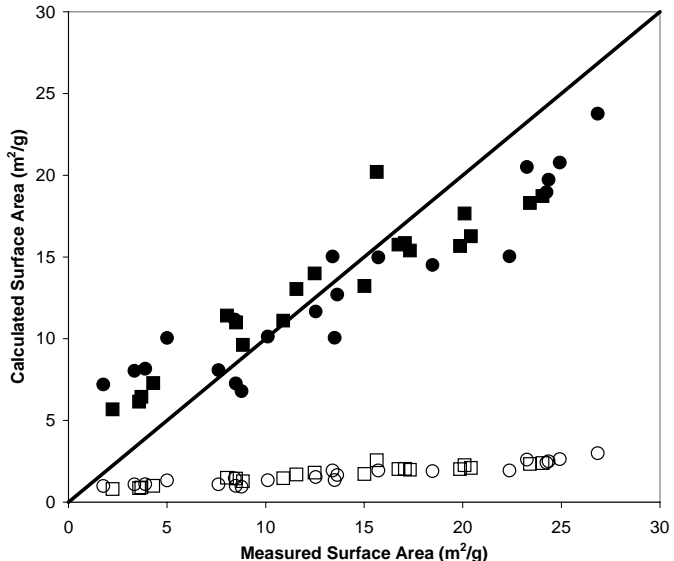


Figure 4.15: Calculated versus measured surface areas using the model discussed in the text.

To test how acidic fluids would affect surface areas of sediments in the A-14 Outfall area, laboratory leaching tests were done. Vadose zone sediments collected near the A-014 Outfall and kaolin purchased from a quarry local to the Savannah River Site were used. Soil boring SB-04 was considered representative of background conditions since it was located outside the zone of influence from the outfall. SB-04 sediments were collected from 11 feet below land surface (bls) and 16 feet bls. The sediments were then air dried and carefully disaggregated prior to the experiments.

For the experiments, sediments were mixed with DI water or an acidic (pH ~2) solution and allowed to equilibrate (Table 4.4). The acidic solution was prepared using DI water and HCl. The pH of each mixture was measured after 24 and 72 hours. After 72 hours, the liquid portion of each mixture was decanted. Sediments equilibrated with the acidic solutions were washed twice with DI water. All sediments were allowed to air dry.

The surface area of the dried sediments was measured using the BET method of surface area measurement. This method entailed using nitrogen gas and a Micromeritics ASAP 2010 (Accelerated Surface Area and Pore volume analyzer) precision gas adsorption instrument. The surface areas of the two kaolin samples were not appreciably different (Table 4.4). However, results from the vadose zone sediments indicate that the acidic solution increased the surface area of the sediments relative to the samples exposed to water at a neutral pH. The difference between the neutral and acidic samples was not, however, as substantial as the differences between the measured and calculated surface areas (open symbols, surface area $\sim 2 \text{ m}^2/\text{g}$) presented in Figure 4.15.

Table 4.4: Sample Descriptions and results of sediment acidification

Description	Sediment (g)	Solution	pH after		BET surface area (m ² /g)
			24 hrs	72 hrs	
SB-04-11	25.2	60 mL DI water	5.07	5.30	10.41
SB-04-11	25.7	60 mL acidic solution	2.09	2.12	16.31
SB-04-16	25.3	60 mL DI water	5.04	5.16	10.97
SB-04-16	25.7	60 mL acidic solution	1.67	1.63	15.85
Kaolin	25.4	60 mL DI water	7.21	7.20	11.80
Kaolin	25.6	60 mL acidic solution	1.91	1.80	10.84

Textures revealed in scanning electron photomicrographs are consistent with high specific surface areas for A-14 Outfall samples. Figure 4.16 shows the abundance of microporosity and microstructures in the fine-grained matrix. The presence of highly weathered grains also contributes to surface area (Figure 4.17a). It should also be noted that micro-scale heterogeneties in the distribution of matrix complicate interpretation and prediction of behavior of fluids in these samples. For example, Figures 4.17b and 4.17c show very different distribution of matrix in two samples. The sample in Figure 4.18c may have a higher specific surface area as measured in the laboratory, but the surface area in contact with migrating fluids in the subsurface may actually be less than that in Figure 4.17b.

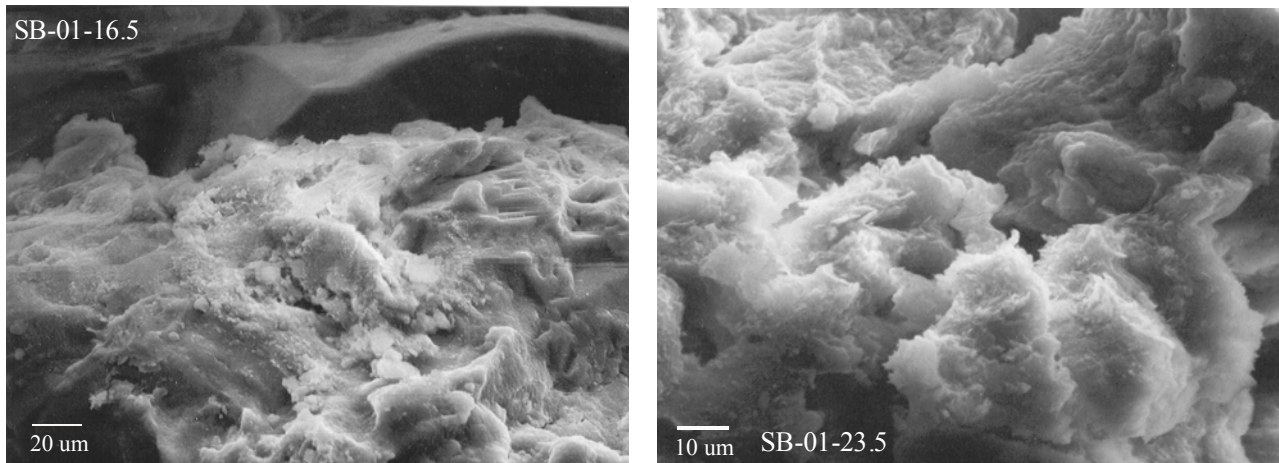


Figure 4.16: Scanning electron photomicrograph of sample SB-01-16.5 (left) and SB-01-23.5 (right)

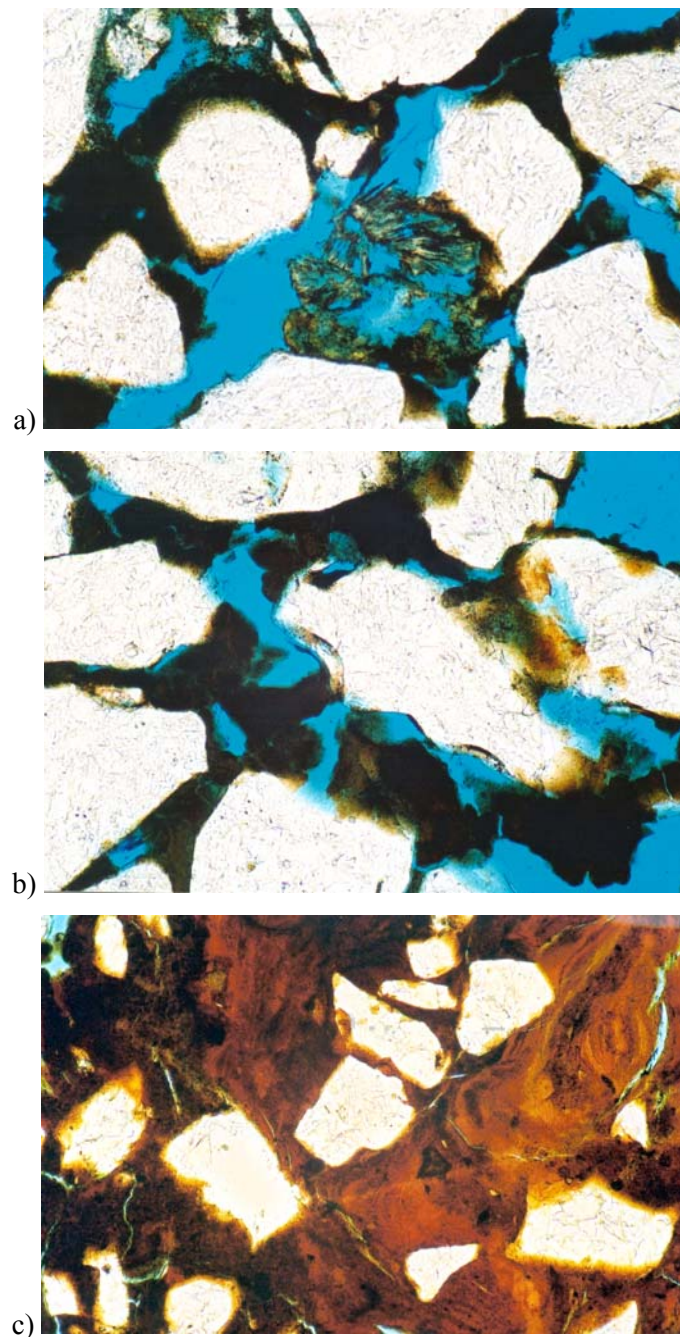


Figure 4.17: Thin-section photomicrographs of three samples from in SB-01: a) weathered grain; b) typical sediment texture; and, c) cemented nodule. White grains are quartz, fine grained matrix is brown to black, porosity is blue. Scale is about 200 um across the bottom.

4.6 Conclusions Task 1

The data presented here provide important information for designing realistic laboratory and modeling studies of DNAPL behavior in coastal plain sediments. In particular, they emphasize the complexity of the system and the need to integrate field based studies into these types of investigations.

The sediment samples are highly weathered quartz sands with minor clay matrix dominated by kaolinite and hematite. The bulk chemistry suggests that the A-14 Outfall samples are slightly enriched in iron and depleted in aluminum relative to other SRS samples.

The fine-grained matrix accounts for most of the specific surface area of the A-14 Outfall samples. These samples have higher specific surface areas per wt% fine-grained matrix than other sediments reported in the literature. Thus, the fine-grained matrix in the A-14 Outfall samples must have a higher specific surface area than fine-grained material in other sediment samples. Extrapolation of these data yields an estimate of between 100 and 200 m²/g for the fine-grained matrix in A-14 Outfall samples. This may be the result of extreme weathering or could be an effect of disposal of corrosive fluids.

The TCE and PCE concentrations indicate the presence of DNAPL. Yet there is a distinct difference in the pattern of concentrations in the two borings from the A-14 Outfall. At a depth interval 17.5 to 25 feet in boring SB-01 there is decrease in TCE and PCE concentrations. This coincides with the screen interval of near-by vapor extraction wells. It is also coincident with an increase in the coarse to medium fraction of sand. In contrast, TCE and PCE concentrations are consistently high throughout the entire depth interval of boring MHS-03, despite close proximity to vapor extraction wells and a similar pattern of grain-size distribution. This suggests that heterogeneity in the subsurface results in heterogeneous removal of DNAPL during vapor extraction. Yet, in this case the heterogeneity is not readily apparent from bulk sediment properties.

Analysis of the background samples suggest that the hypothesis that corrosive fluids disposed at the A-14 Outfall caused significant changes in the properties of the sediments is false. The chemical and textural trends observed in the background samples are identical to samples taken at the A-14 Outfall. If corrosive fluids did affect the properties of the sediments, the changes are too minor to be detected in these types of bulk analyses.

4.7 References Task 1

Burdon, R.S. (1949). *Surface Tension and the Spreading of Liquids*, Cambridge University Press, London, England.

Chorover, J. and G. Sposito (1995). "Dissolution behavior of kaolinitic tropical soils." *Geochimica et Cosmochimica Acta* **59**(15): 3109-3121.

Cohen, R. M. and J. W. Mercer (1993). *DNAPL Site Evaluation*. Boca Raton, Florida 33431, CRC Press Inc.

Denham, M.E., J.R. Kastner, K.M. Jerome, J. Santo Domingo, B.B. Looney, M.M. Franck, and J.V. Noonkester (1999). Effects of Fenton's Reagent on Aquifer Geochemistry and Microbiology at the A/M Area, Savannah River Site, WSRC-TR-99-00428. Aiken, South Carolina 29808, Westinghouse Savannah River Company.

Huertas, F. J., L. Chou, et al. (1998). "Mechanism of Kaolinite Dissolution at Room Temperature and Pressure: Part 1. Surface Speciation." *Geochimica et Cosmochimica Acta* **62**(3): 417-431.

Jackson, D. G. and B. B. Looney (2001). Evaluating DNAPL Source and Migration Zones: M-Area Settling Basin and the Western Sector of A/M Area, Savannah River Site (U). Aiken, South Carolina 29808, Westinghouse Savannah River Company.

Jackson, D. G., B. B. Looney, et al. (1997). Assessment of Chlorinated Solvent Contamination in the Crouch Branch Aquifer of the A/M Area (U). Aiken, South Carolina 29808, Westinghouse Savannah River Company.

Jackson, D. G., J. V. Noonkester, et al. (2000). Characterization Activities to Evaluate Chlorinated Solvent Discharges to Tims Branch from the A/M Area of the Savannah River Site (U). Aiken, South Carolina 29808, Westinghouse Savannah River Company.

Jackson, D. G., T. Payne, et al. (1996). Estimating the Extent and Thickness of DNAPL within the A/M Area of the Savannah River Site (U). Aiken, South Carolina 29808, Westinghouse Savannah River Company.

Jackson, D. G., W. K. Hyde, et al. (1999). Characterization Activities to Determine the Extent of DNAPL in the Vadose Zone at the A-014 Outfall of A/M Area (U). Aiken, South Carolina 29808, Westinghouse Savannah River Company.

Jerome, K. M., B. D. Riha, et al. (1997). Final Report for Demonstration of In-Situ Oxidation of DNAPL Using Geo-Cleanse Technology. Aiken, South Carolina, Westinghouse Savannah River Company.

Jerome, K. M., J. V. Noonkester, et al. (1999). A/M Area DNAPL Characterization Report for Cores Collected in 2Q99. Aiken, South Carolina 29808, Westinghouse Savannah River Company.

Kieffer, B., C. F. Jové, et al. (1999). "An experimental study of the reactive surface area of the Fontainebleau sandstone as a function of porosity, permeability, and fluid flow rate." *Geochimica et Cosmochimica Acta* **63**(21): 3525-3534.

Langmuir, D. (1997). *Aqueous Environmental Geochemistry*. Upper Saddle River, NJ, Prentice-Hall, Inc.

Looney, B. B. and R. W. Falta (2000). *Vadose zone science and technology solutions*. Columbus, OH, Battelle Press.

Looney, B. B., J. Rossabi, et al. (1992). Assessing DNAPL Contamination, A/M-Area, Savannah River Site: Phase I Results (U). Aiken, South Carolina 29808., Westinghouse Savannah River Company.

Marine, I. W. and H. Bledsoe (1984). Supplemental Technical Data Summary: M-Area Groundwater Investigation. Aiken, South Carolina 29808., Savannah River Laboratory, E. I. duPont de Nemours & Company.

Pickett, J. B., W. P. Colven, et al. (1987). Environmental Information Document: M-Area Settling Basin and Vicinity. Aiken, South Carolina 29808., Savannah River Laboratory, E. I. duPont de Nemours & Company.

Strom, R. and D. Kaback (1992). Groundwater Geochemistry of the Savannah River Site and Vicinity, WSRC-RP-92-450, Aiken, South Carolina, Westinghouse Savannah River Company.

Vangelas, K. M. (2000). Summary and Status of DNAPL Characterization and Remediation Activities in the A/M Area, Savannah River Site. Aiken, South Carolina 29808, Westinghouse Savannah River Company.

White, A. F., A. E. Blum, et al. (1996). "Chemical Weathering Rates of a Soil Chronosequence on Granitic Alluvium: I. Quantification of Mineralogical and Surface Area Changes and Calculation of Primary Silicate Reaction Rates." *Geochimica et Cosmochimica Acta* **60**(14): 2533-2550.

Xie, Z. and J. V. Walther (1992). "Incongruent dissolution and surface area of kaolinite." *Geochimica et Cosmochimica Acta* **56**: 3357-3363.

5.0 Microbial Distribution in Field Samples (Task 2)

5.1 Methods

Subsurface samples collected from uncontaminated soil near the A-14 outfall area were cultured and then used to determine if the reduction of interfacial tension (IFT) due to the accumulation of bacteria at the dense non-aqueous phase liquid (DNAPL) interface is specific to tetrachloroethylene (PCE) dechlorinating cultures or whether all “stressed” cells present in the soil would respond similarly. Methods to determine the concentration of bacteria as a function of depth was also a focus of this research. Soil samples collected as part of the March 2004 field work at SRS were preserved and shipped to Clarkson University, stored at 4°C where they awaited analysis until quality control measures were completed. Details describing the sample collection, preparation, quality control, and other materials and methods are described in detail in the following section.

Subsurface Sampling. In preparation for soil sampling, glass liquid 20-mL scintillation vials were autoclaved and filled with 10-mL of 2% particle free formalin solution. Each vial was then numbered and weighed prior to shipping to Savannah River Site (SRS). Four soil borings, SB-03, SB-04, SB-05, SB-06, located in uncontaminated areas near the A-14 Outfall were taken March 15, 2004. Sampling from each boring began at 6 feet below the surface. Soil samples were taken at every foot, until 30 feet was reached. At each foot, approximately 4 cubic centimeters of soil were collected from the coring tube using a 5-cm³ sterile syringe and placed in vials with 2% formalin. The depth and time of sample was recorded for each. Two anaerobic samples were taken at each boring site between 23 and 30 feet. Each anaerobic sample was placed in an inflatable glovebox supplied with 100% nitrogen. Anaerobic samples were then placed in 250-mL amber jars purged with 100% nitrogen. All samples were kept on dry ice and shipped the next day to Clarkson University where they were placed in a cold constant temperature room at 4 °C.

Bacterial Enumeration. In order to measure the number of cells per gram of soil as a function of depth, a Live/Dead® BacLight™ Kit L-7007 (Molecular Probes, Inc.) was used. This kit contains SYTO® 9 green-fluorescent nucleic acid stain and a red-fluorescent stain containing propidium iodide. The SYTO® 9 will stain all cells, while propidium stains only those with a compromised membrane (i.e. “dead” organisms). The soil at the SRS site contains extremely orange clay which provides a challenge to enumerate dead cells. In order to optimize the analysis and reduce the interference of orange clay particles in the measurements the relative concentration of stains (red versus green) and dilution ratios were varied. The kit recommends a stain ratio of 1:1, but suggests that this ratio may need to be changed in certain situations. In order to determine the correct ratio of the green and red fluorescent stains, several samples from the same vial were taken and prepared using different ratios of the stains.

Each sample was diluted 1/200 from its original slurry concentration. Stain ratios of 1:1, 2:1, 1:2, 1.75:1.25 (Component A (green) to Component B (red)) were considered. Ten milliliters of diluted sample were stained and filtered onto black 0.22 micron filter paper. The filter was then placed on a slide and viewed using fluorescent microscopy at 1250X magnification using an optical filter for live/dead fluorescent stains. The Olympus BX51 microscope is equipped with a Photometrics Cool SNAP™ ES digital camera linked to a computer. Image analysis was performed using Universal Imaging Corporation™ MetaMorph® Software in order to obtain the live and dead cell counts. The correct stain ratio was then determined based on how visible the red cells were for each stain ratio. It was determined that the original 1:1 stain ratio best fit our needs.

Original slurry samples preserved with formalin contained on average 5 grams of soil per 10 milliliter 2% particle free formalin solution. Several different dilutions were compared in order to determine a dilution that made viewing the bacteria accessible. Dilutions from the original slurry included: 1/125, 1/200, 1/500, 1/1000, and 1/10000. Due to the presence of soil particles, more concentrated dilutions (1/125, 1/200) hid attached bacteria and caused the total cell per gram count to be

slightly lower than that found for the more dilute sample (1/500 and 1/1000). At a very high dilution, the error associated with the analysis becomes large. A dilution of 1/500 (0.002) was ultimately chosen for shallower depths and 3/1000 (0.003) for deeper samples. In order to estimate the representative number of cells on the filter paper the ideal number of locations counted on each slide had to be determined. As the number of locations counted on the filter is increased the standard error (variability) is reduced. Twenty locations were taken from several slides. For each slide, averages were done and compared for 5, 10, 15, and 20 locations. The variability could be significantly reduced by analyzing 15 instead of 10 locations. There was however less improvement between 15 and 20 locations. Ultimately, 30 locations were counted for each slide. Three slides were produced for each sample. Reagent blanks were conducted with each counting sequence to ensure the purity of all reagents.

5.2 Bacterial Distribution within the Background Cores

Cell counts to determine the spatial distribution of bacteria in the subsurface of the uncontaminated portion of the site allowed for a comparison between the uncontaminated and contaminated portion of the site to assess if the distribution seen in the contaminated portion was unique. Bacterial concentrations were measured from samples taken at one foot intervals to approximately thirty feet in depth. The samples were preserved using a 2% formalin solution and were analyzed using fluorescent microscopy as discussed in Section 5.1. Three soil borings from the vadose zone (water table at 130 to 140 ft (Grimberg et al. 2000) in the uncontaminated portion of the site were analyzed. All three showed a higher amount of bioactivity near the surface (10^6 – 10^7 cells/g wet soil) with a decline as depth increased ($\sim 10^4$ cells/g wet soil). This is to be expected since there tends to be more organic material that can be utilized by the organisms near the surface compared to that at increasing depths. However, in an environment with organic contamination such as PCE or TCE, at non-toxic concentrations, this may not hold true. The presence of anaerobic dechlorinating organisms would relate to an increase at depths containing contamination due to the organisms' ability to utilize the substrate.

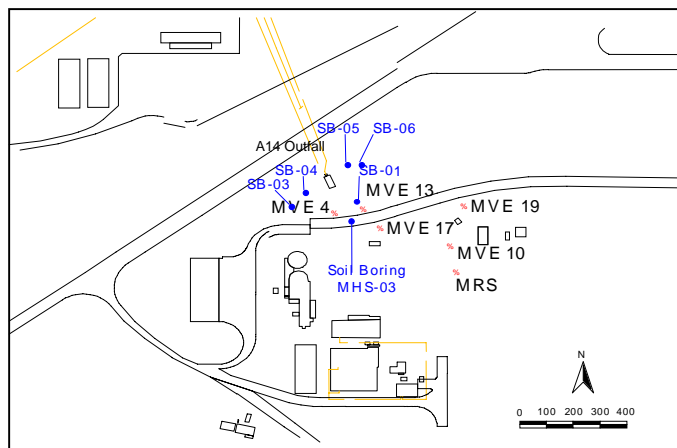


Figure 5.1: Location of soil boring and soil vapor extraction wells at the A-14 outfall, SRS

Figure 5.1 illustrates the outfall area and the locations of both the soil borings and the soil vapor extraction wells. Borings SB-03, 04, 05, and 06 are all located in the uncontaminated portion of the site, while SB-01 and MHS-03 are located in the DNAPL contaminated portion. Soil boring SB-05 cell counts were not performed. Figure 5.2 illustrates the decrease of total cell concentrations as depth of the samples for all three soil borings. Cell viability is defined as the ratio of live to total cells. Cell viability decreased with increasing depth in each of the three cores (Figures 5.3). Zero viability indicates that no live cells were accounted for at the corresponding depth during the enumeration process.

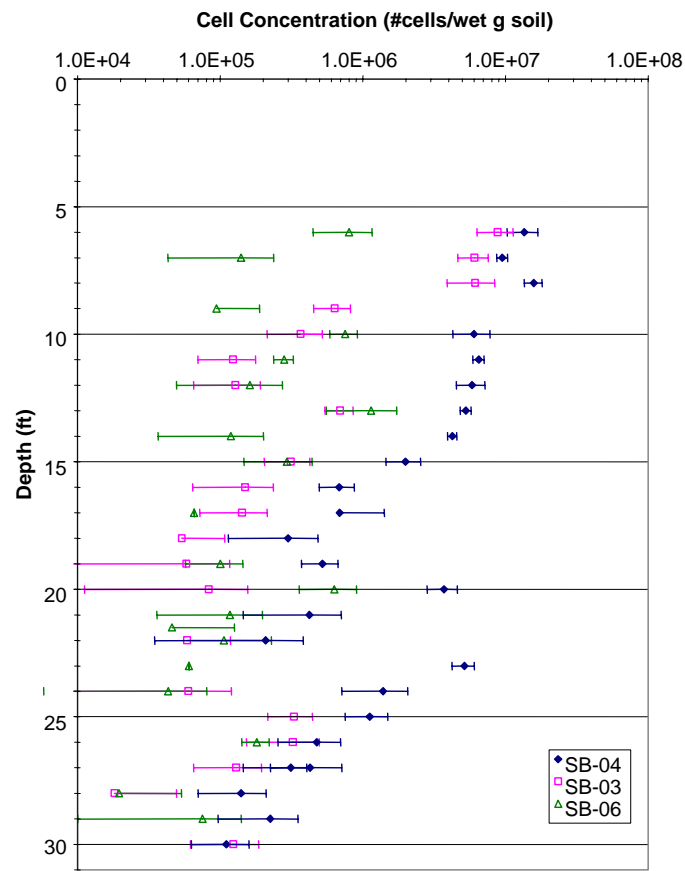


Figure 5.2: Total cell concentration as a function of depth in wells upstream of the contamination

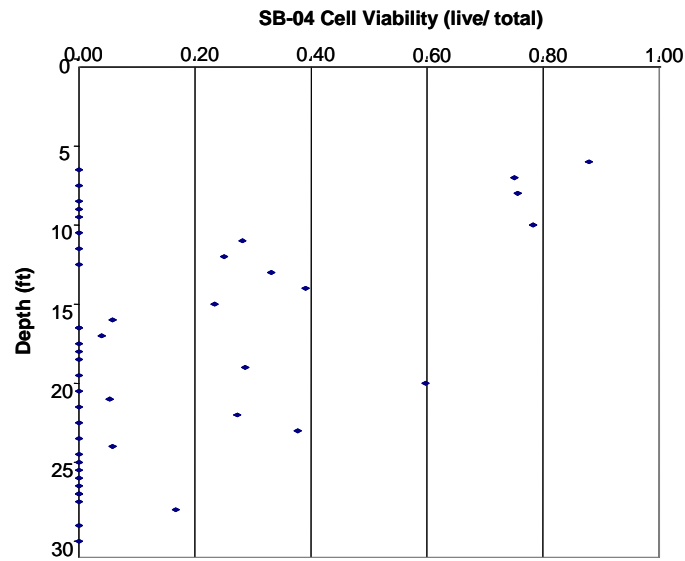


Figure 5.3: Cell viability as a function of depth in SB-04 (NW upstream of contamination)

5.3 Comparison of Contaminated & Uncontaminated Borings

Sampling events were conducted at SRS during the spring of 2000 and 2001. As part of these events, soil boring SB-01 was taken from the contaminated A-14 Outfall Area of SRS. Enumerations conducted were used to determine the distribution of bacteria in the subsurface for this contaminated portion of the site. In order to compare the contaminated bacterial distributions with that from the uncontaminated soil borings, methods used were kept similar to that of prior research.

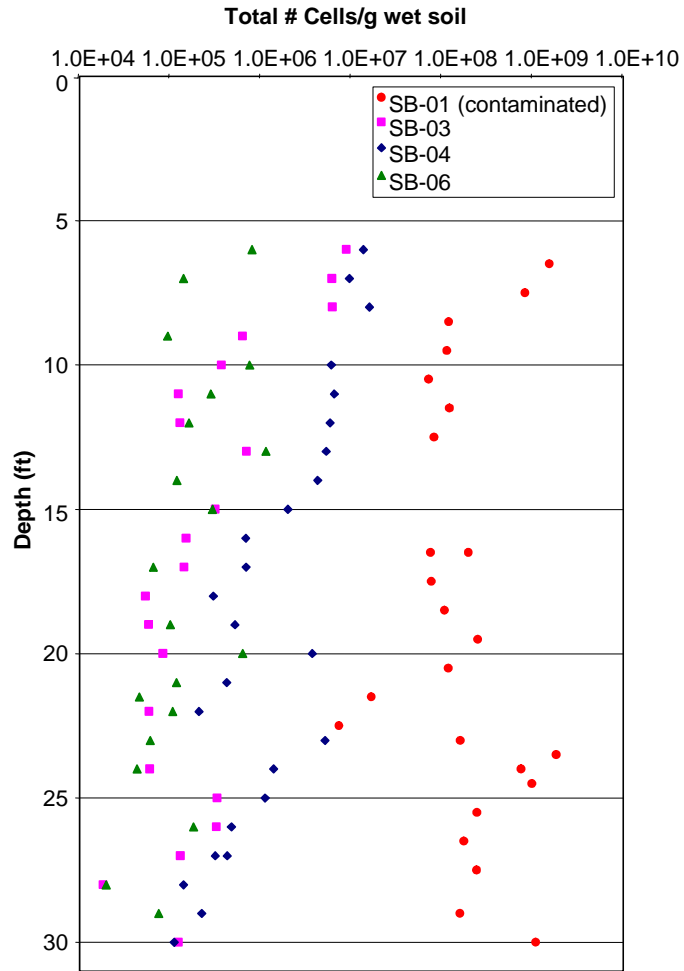


Figure 5.4: Spatial distribution of total cell counts in contaminated vs un-contaminated cores

Figure 5.4 shows the substantially higher cell concentrations in the contaminated soil boring SB-01 compared to that of the soil borings from the uncontaminated area near the A-14 Outfall. The highest concentrations observed in the uncontaminated borings, 10^6 - 10^7 cells per gram, were similar to that of the lowest observed concentrations from the contaminated boring. Overall there was an approximately 2 to 3 orders in magnitude difference between concentrations in the uncontaminated and contaminated borings. Results indicate an increased level of bioactivity in the contaminated area, which supports the notion that the local microbial community utilized the DNAPL to support microbial growth. Overall, the distribution of organisms in the subsurface at higher concentrations was unique to the contaminated portion of SRS (Figure 5.5 a,b). At depths affected most by the ongoing soil vapor phase extraction system (SVE), bacterial concentrations remained low (e.g. at a depth of 20 ft, Figure 5.5 a). Due to the extraction, soil moisture content decreased significantly and thus inhibited bacterial growth. At depths with lower hydraulic conductivity (i.e. smaller average particle diameter, d_{50}), SVE was ineffective in removing

DNAPL contamination even after decade-long operation illustrating the need to develop alternate remediation processes. Bacterial concentrations within the contaminated cores correlated well with contaminant concentrations measured in the cores (Figure 5.6).

Since the surface area of the soil declined gradually in both cores as a function of depth but the d_{50} remained similar (with the exception of the 20-25 feet interval in core SB-01) the observed weathering processes dominate at the top 20 feet of the soil cores (Figure 5.5). Concurrently, bacterial concentrations were relatively low at the top 20 feet and at least one order of magnitude higher below 22 feet. At this depth the bacterial concentrations were highest at high DNAPL concentrations (Figure 5.6). Furthermore, tests indicated that the microbial consortium was capable of co-metabolizing TCE under aerobic conditions as well as degrading PCE via reductive dechlorination pathways (Doty, 2003). A range of organisms has been known to produce biosurfactants that either reduce the toxicity or enhance the bioavailability of sparsely soluble substrates (Déziel et al. 1996; Sandrin et al, 2000). However, neither TCE- nor PCE- degrading organisms have been reported to produce biosurfactants. Under environmental stress some microorganisms excrete metabolic by-products that may exhibit surface-active properties. Betrand et al (submitted) have shown that two anaerobic PCE-degrading enrichment cultures will reduce the TCE/mineral media interfacial tension up to 50% when stressed by introducing oxygen at 1.5 mg/L. Heterogeneity in the vadose zone creates microscopic areas where dissolved oxygen concentrations are extremely low, allowing for anaerobic organisms to proliferate. Operational changes in the SVE system due to seasonal fluctuations may have impacted dissolved oxygen levels in the vadose zone, thereby exposing the anaerobic cells to varying concentrations of oxygen. It is conceivable, therefore, that microbial activity at the A-014 Outfall Area affected the distribution of DNAPL.

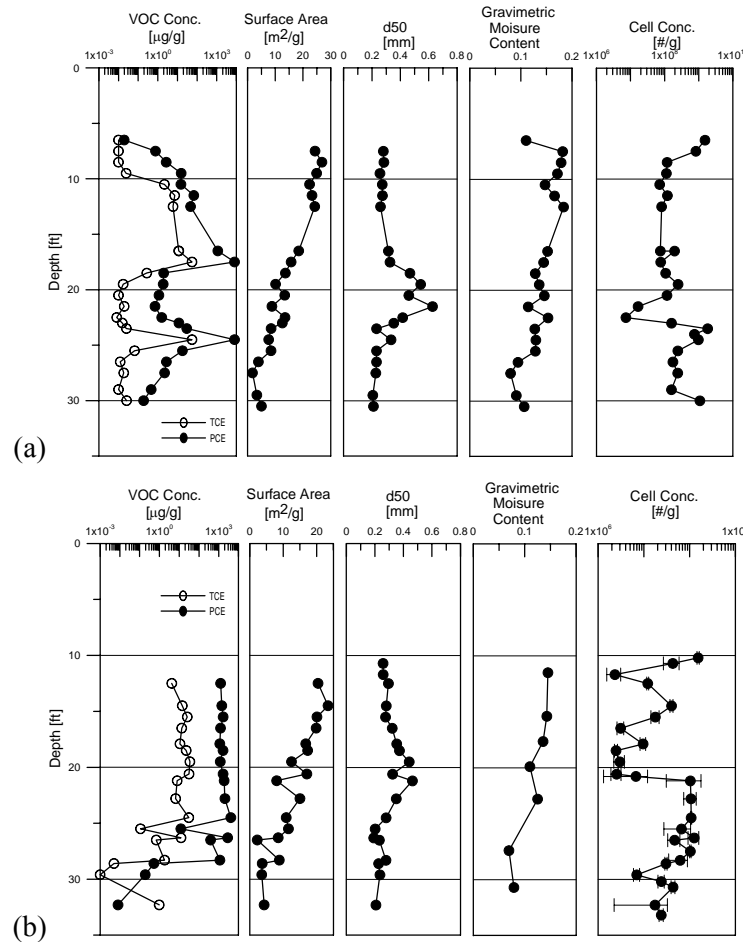


Figure 5.5: Characterization of soil borings SB-01 (a) and MHS-03 (b).

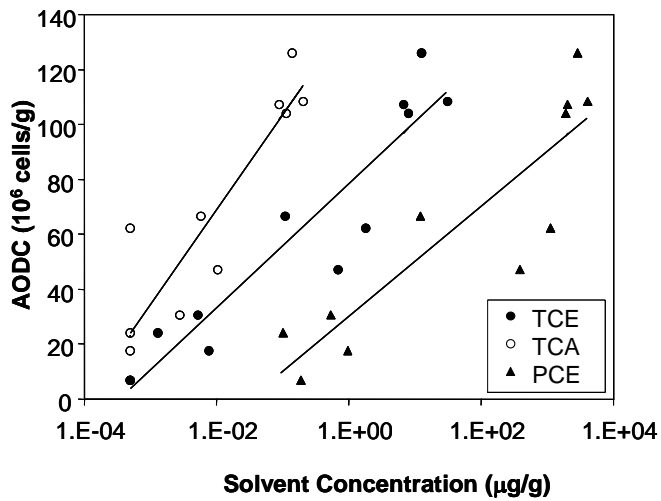


Figure 5.6: Cell concentration measured using the acridine orange direct count method as a function of VOC concentrations in boring MHS-03 below 20 feet.

5.4 Conclusions - Task 2

The collection and analysis of nearby uncontaminated sediments near the A-14 outfall area help to show the significant impact the presence of DNAPL in the subsurface has on the microbial community. Bacterial concentrations in the contaminated region were 2-3 orders of magnitude higher than in the uncontaminated region, which supports the notion that the local microbial community utilized the DNAPL to support microbial growth. In the uncontaminated region, cell counts were most closely correlated with depth, which in turn is correlated to organic carbon content, and moisture content. Overall, the distribution of organisms in the subsurface at higher concentrations was unique to the contaminated portion of SRS. At depths affected most by the ongoing soil vapor phase extraction system, bacterial concentrations remained low, most likely due to the low soil moisture content associated with this remediation technique.

6.0 Effect of microorganisms on DNAPL interfacial properties (Task 2)

6.1 Abstract

Previous research has shown that a number of organisms have the ability to anaerobically dechlorinate tetrachloroethylene (PCE) and other chlorinated solvents. However, the extent to which the presence of these organisms affects the interfacial properties of non-aqueous phase liquids (NAPLs) is largely unknown. Conversely, aerobic organisms have been studied and observed to change their adhesion properties and produce extracellular compounds or biosurfactants, particularly under stressed conditions. Either of these microbial mechanisms may significantly impact DNAPL interfacial properties, thereby altering its distribution in the subsurface. The objective of this research was to determine specific growth conditions under which DNAPL interfacial properties are altered. Several environmental stressors and three anaerobic enrichment cultures were studied in an attempt to stimulate changes in adhesion properties or biosurfactant production. Two of the cultures degraded PCE. The third was collected from an uncontaminated field site and could not metabolize PCE. This research showed that amending growth media with complexing agents and varying carbon sources had little effect on interfacial tension reduction. However, increased concentrations of PCE, or introducing low concentrations of dissolved oxygen (DO), to the culture medium created an environment causing the PCE degrading organisms to reduce DNAPL interfacial tension. The reduction in interfacial tension upon oxygen or PCE stress was only observed for the PCE degrading cultures and not for the background anaerobic culture suggesting that the observed response may be organism specific.

6.2 Introduction

Tetrachloroethylene (PCE) is a chlorinated solvent and suspected carcinogen, and is also a contaminant frequently present in groundwater. As a dense non-aqueous phase liquid (DNAPL), PCE migrates with relative ease through regions of high conductivity in the subsurface. Regions of lower conductivity, or smaller pore spaces, inhibit migration of PCE, although, once DNAPL enters these regions, it becomes extremely difficult to remediate (BHI 1996). The overall distribution and migration of DNAPLs in a natural system is affected by a number of variables. The most critical of these variables include heterogeneities in the porous matrix, and the corresponding interfacial properties, specifically surface tension (ST) and interfacial tension (IFT) of the system.

ST and IFT affect the capillary forces that define fluid and solid phase interactions, and ultimately the DNAPL distribution. When considering natural systems, the complexities of the porous media are often simplified and considered to be similar to a bundle of thin tubes, each with radius r , thus the equation (6.1) explaining capillary pressure is as follows:

$$P_c = \frac{2\sigma \cos \theta}{r} \quad 6.1$$

Where: P_c = Capillary pressure of a single pore; σ = Interfacial tension (IFT) between DNAPL & water; θ = Contact angle; and r = Capillary tube radius.

As illustrated in the above equation, the entry pressure of a single pore, P_c , varies directly with interfacial tension (σ). As IFT decreases, the entry pressure decreases. This decrease in entry pressure allows the NAPL to enter smaller pore spaces. The significance of this altered DNAPL distribution in the subsurface was apparent during soil vapor extraction efforts at the U.S. DOE Savannah River site in South Carolina (USA), where the efficiency of the extraction efforts were less than expected. Preliminary analysis suggested that this was due to the migration of the DNAPL into small pores (BHI 1996).

The goal of this research was to determine whether anaerobic microorganisms may alter NAPL interfacial properties, which would ultimately affect DNAPL distribution in the subsurface. It has previously been shown that anaerobic microorganisms can survive in PCE-contaminated environments, and have the ability to reductively dechlorinate tetrachloroethene completely to ethene (Maymo-Gatell et al. 1997; Yang and McCarty 2002). Such organisms have the ability to derive energy directly from PCE, using it as a respiratory electron acceptor. Similar organisms were used in this research for their obvious ability to survive and even thrive at PCE concentrations toxic to most other organisms.

Two possible mechanisms may promote the alteration of these interfacial properties. The first is microbial adhesion. Hydrophobic organisms have been observed to adhere to the DNAPL-water interface, enabling utilization of DNAPL components for energy and growth. Under some stressed conditions, such as starvation, many organisms increase their cell surface hydrophobicity, thereby increasing adhesiveness (Marshall 1991). The accumulation of organisms at the NAPL-water interface may result in a significant decrease in the NAPL-water interfacial tension. The second mechanism potentially affecting interfacial properties is the production of extracellular polymers or biosurfactants. During this process, the cell produces and excretes a chemical that acts as a surfactant in solution. Due to its amphiphilic nature, the biosurfactant will then accumulate at interfaces, thereby reducing the interfacial tension (IFT) of the system. Numerous organisms have been observed to produce biosurfactants, many of which have been found to exist in the subsurface (Chanmugathas 1988; Knox 1979). The production of these biosurfactants has previously been associated with imbalanced growth (Dohse 1994).

The objective of this research was to determine specific growth conditions under which these two mechanisms are promoted and the DNAPL-water interfacial tension reduced. In order to achieve imbalanced growth conditions to stimulate adhesion and/or biosurfactant production, a number of variables were investigated. These included altering preferred carbon sources, temporarily increasing PCE concentration in the growth media, introducing dissolved oxygen (DO) concentrations, and adding complexing agents to the anaerobic PCE dechlorinating enrichment cultures.

6.3 Materials and Methods

Chemicals and reagents. All chemicals were analytical grade. PCE and TCE (purity, >99%) were obtained from Sigma-Aldrich, St. Louis, MO.

Anaerobic enrichment cultures. Of the three enrichment cultures used in this research two were able to metabolize chlorinated solvents while one was not. Two cultures were developed using soil samples from the Savannah River site while one was obtained from the research laboratory of Dr. Gossett at Cornell University (Gossett 1996, 1997).

Cornell Culture. The culture initially chosen for use in this study was a mixed anaerobic culture that utilizes butyrate as a carbon source and was previously observed to dechlorinate PCE completely to ethene (Gossett 1996). This culture was chosen for its obvious ability to withstand concentrations of PCE toxic to most organisms. The culture was maintained as described by Gossett (1996), at a constant temperature of 30°C, and continuously stirred at 100 rpm.

Every 48 hours the enrichment culture was administered, including 110 µmol (18.2 mg) of neat PCE, 440 µmol (38.8 mg) of butyric acid, and 400 µl of a 50g/l yeast extract stock solution per liter of enrichment culture. Additionally, during every other feed (every fourth day), 510 µl of **vitamin solution** per liter of culture was also dispensed to the culture. Also, during every other feed, 300 ml of culture was wasted and replaced with fresh basal medium (DiStefano et al. 1992) (Table 6.1; 6.2), which translates to an average cell residence time of 40 days in the reactor. The culture and all associated media were purged with a 70% N₂/30% CO₂ gas mixture, which was first passed through a titanous chloride/sodium bicarbonate/sodium citrate solution (Zehnder 1976) in order to remove any trace amounts of oxygen. PCE and other chlorinated ethenes- trichloroethylene (TCE), cis- and trans- dichloroethylene (DCE), and

vinyl chloride (VC) concentrations were all tracked weekly via GC analysis, as explained below in greater detail.

Table 6.1: Cornell Culture Basal Media Constituents (DiStefano et al. 1992)

Constituent		Final Concentration (g/L)	
1	Distilled Water	H ₂ O	
2	Ammonium Chloride	NH ₄ Cl	0.2
3	Potassium Phosphate	K ₂ HPO ₄	0.1
4	Potassium Di-phosphate	KH ₂ PO ₄	0.055
5	Magnesium Chloride	MgCl ₂ .6H ₂ O	0.2
6	Rezasurin		0.001
7	Trace Metals Solution	TMS	10 ml
8	Ferric Chloride	FeCl ₂ .4H ₂ O	0.1
9	Sodium Bicarbonate	NaHCO ₃	6
10	Sodium Sulfide	Na ₂ S.9H ₂ O	0.5

Table 6.2: Cornell Culture Trace Metals Solution (TMS) Constituents (DiStefano et al. 1992)

Constituent		Final Concentration (g/L)	
1	Distilled Water	H ₂ O	
2	Manganese Chloride	MnCl ₂ .4H ₂ O	0.1
3	Cobalt Chloride	CoCl ₂ .6H ₂ O	0.17
4	Zinc Chloride	ZnCl ₂	0.1
5	Calcium Chloride	CaCl ₂ .2H ₂ O	0.251
6	Boric Acid	H ₃ BO ₃	0.019
7	Nickel Chloride	NiCl ₂ .6H ₂ O	0.05
8	Sodium Molybdate	Na ₂ MoO ₄ .2H ₂ O	0.02

SRS cultures. Two anaerobic enrichment cultures were developed using soil samples taken from the Savannah River Site. Anaerobic SRS soil samples for one enrichment culture were taken from depths of greater than 90 feet of a PCE/TCE contaminated soil at the SRS M-area. Eight microcosms containing 30 g soil, 50 mL of mineral media (Table 6.3; 6.4), a mixture of carbon sources (Table 6.5) and PCE were incubated at 30 °C, shaken at 100 rpm for one week. Subsequent GC analysis tracked PCE dechlorination in four of eight initial soil sample microcosms, which were then combined to create the SRS enrichment culture (SRS1).

A second anaerobic enrichment culture was developed using uncontaminated soil collected from the Outfall area of the Savannah River Site (SRS2). The objective of this background culture was to determine whether potential bacterial surface activity at the DNAPL was specific to dechlorinating organisms or nonspecific to anaerobic organisms. Soil samples, which were taken under anaerobic conditions from the SRS subsurface at depths below 20 feet, were used to create microcosms to seed the enrichment culture. Six initial microcosms were created consisting of 5 grams of soil, and 80 mL of anaerobic media as described by Hurst et al. (1997). Microcosms were fed an initial dose of the carbon

source described by Table 6.5, and maintained at 30°C and placed on an orbital shaker at 130 rpm, in a constant temperature room set at.

Table 6.3: SRS Culture Media Constituents

Constituent			Final Concentration (g/L)
1	Distilled Water	H ₂ O	
2	Rezasurin		0.001
3	Potassium Di-phosphate	KH ₂ PO ₄	0.138
4	Potassium Phosphate	K ₂ HPO ₄	0.176
5	Ammonium Phosphate	(NH ₄) ₂ HPO ₄	0.02
6	Ammonium Chloride	NH ₄ Cl	0.2
7	Magnesium Chloride	MgCl ₂ .6H ₂ O	0.6
8	Ferric Chloride	FeCl ₂ .4H ₂ O	0.2
9	Potassium Chloride	KCl	0.1
10	Calcium Chloride	CaCl ₂	0.1
11	Sodium Sulfide	Na ₂ S.9H ₂ O	0.1
12	Sodium Bicarbonate	NaHCO ₃	4.2
13	Trace Metals Solution	TMS	10 ml

Table 6.4 : SRS Culture Trace Metals Solution (TMS) Constituents

Constituent			Final Concentration (g/L)
1	Distilled Water	H ₂ O	
2	Potassium Iodide	KI	1
3	Manganese Chloride	MnCl ₂ *4H ₂ O	0.4
4	Cobalt Chloride	CoCl ₂ *6H ₂ O	0.4
5	Nickel Chloride	NiCl ₂ *6H ₂ O	0.05
6	Cupric Chloride	CuCl ₂	0.05
7	Zinc Chloride	ZnCl ₂	0.05
8	Boric Acid	H ₃ BO ₃	0.05
9	Sodium Molybdate	Na ₂ MoO ₄ *2H ₂ O	0.05
10	Sodium Metavanadate	NaVO ₃ *nH ₂ O	0.05
11	Sodium Selenite	Na ₂ SeO ₃	0.01

Table 6.5: Carbon Sources for SRS Enrichment Cultures

Constituent	Conc [mg/L]
Phenol	40
Butyrate	40
Acetone	40
Sodium Benzoate	40
Yeast Extract	30
DI Water	

Every 48 hrs, each of the two cultures received mixed carbon source and PCE (final concentration: 1.7 mg/L) for SRS1. After several weeks of allowing the culture to mature, active cultures (as indicated by gas production and PCE degradation for SRS1), were used as seed for the enrichment cultures. Each enrichment culture was placed in an autoclaved 1-gallon, Wheaton-cell stirred reactor (Figure 6.1). Approximately 60 mL from each of the active cultures were used along with one liter of media in the nitrogen-purged reactor.



Figure 6.1:Celstir reactor

The carbon source was fed to the culture in the same concentration as that of the initial cultures every 48 hours. 10% of enrichment culture was replaced every 96 hrs with new media resulting in an approximate 40-day mean cell residence time, which was maintained for several months prior to use in order to allow the enrichment culture to mature and reach steady state.

Microcosm experiments. The three enrichment cultures were used in a range of microcosm experiments. The hypothesis to be tested for these set experiments was whether stress induced due to changing growth conditions may induce microbial surface activity. A number of variables were tested with each of the cultures in order to determine which specific factors induced the most significant changes in interfacial properties (Table 6.6). In addition to the induction of oxygen (DO) and increased concentrations of PCE, the addition of complexing agents was also considered for the Cornell culture, which resulted in elevated dissolved inorganic compound concentrations, and changes in the carbon source for microbial growth.

Table 6.6: Stressors and concentrations tested on enrichment cultures

Variable	Conditions	Conc [mg/L]	Cornell	SRS1	SRS2
PCE	PCE low	27			X
	PCE high	190	X	X	X
Dissolved Oxygen	DO-1	0	X	X	
	DO-2	1.0		X	X
	DO-3	1.5	X	X	X
	DO-4	2.8	X		
Inorganic Compounds	EDTA	200	X		
Growth Substrate	Lactic Acid	440	X		
	Propionic Acid	440	X		

Unless specified otherwise, each microcosm consisted of 50 mL of anaerobic media and 10 mL of enrichment culture in a sterile 80-mL serum bottle with a rubber septa and aluminum crimp cap. All samples were incubated for one week at 30°C on an orbital shaker at 100 rpm, and, unless otherwise indicated, all were fed identical constituents to create at the same culture concentrations as in the main culture reactor. Base case microcosms (non-stressed control) were used to gauge the relative impact of the various stress factors on interfacial and surface tension. Figure 6.2 is a schematic of the microcosm preparation and measurement. During the initial experiments, it was noted that the interfacial activity depends on microbial concentration. Subsequent experiments for cultures SRS1 and SRS2 therefore were conducted at three cell concentrations (original, 5X and 20X). For the 5X samples, 50 mL of enrichment culture were combined with 10 mL of fresh media. For 20X samples, cell suspensions that were taken from the enrichment culture were centrifuged under anaerobic conditions for 15 min at 5000g. The cells were re-suspended in carbon-free media to yield a twenty (20X) times concentration. Cell concentrations were determined using the LIVE/DEAD baclight (see below) for each of the microcosms. Each microcosm was set up in triplicate.

Amendments were introduced to a number of sample sets in order to observe the effects of environmental variables on all cultures. These amended samples, as defined in Table 6.6, were compared to base case scenarios, and abiotic conditions, to determine the significance of each variable on DNAPL interfacial properties. Samples were incubated for one week at 30 °C, shaken at 100 rpm and then filtered twice - first to a particle size of 1 micron, to remove all inorganic particles present in the media, while allowing the organisms and any dissolved components (biosurfactants) to pass through the filter, creating a “particulate filtrate.” Microscopic observations of the particulate filtrate verified that this pore size was sufficient to selectively remove the vast majority of inorganic particulates, yet allow the bacteria to pass through the pores. A portion of this “particulate filtrate” was then further filtered to 0.22 microns to generate a “particle-free filtrate” in order to determine the effect of biosurfactants.

Surface tension (ST) and interfacial tension (IFT) measurements were completed on each filtrate after 0, 24, and 48 hours of equilibration of the interface. Initial ST and IFT measurements provided greater repeatability with TCE as the DNAPL, and therefore TCE was used as the model DNAPL in each subsequent IFT measurement. For the SRS2 samples, PCE was used in addition to TCE as a model DNAPL since the contamination at the Savannah River Site consists predominantly of PCE.

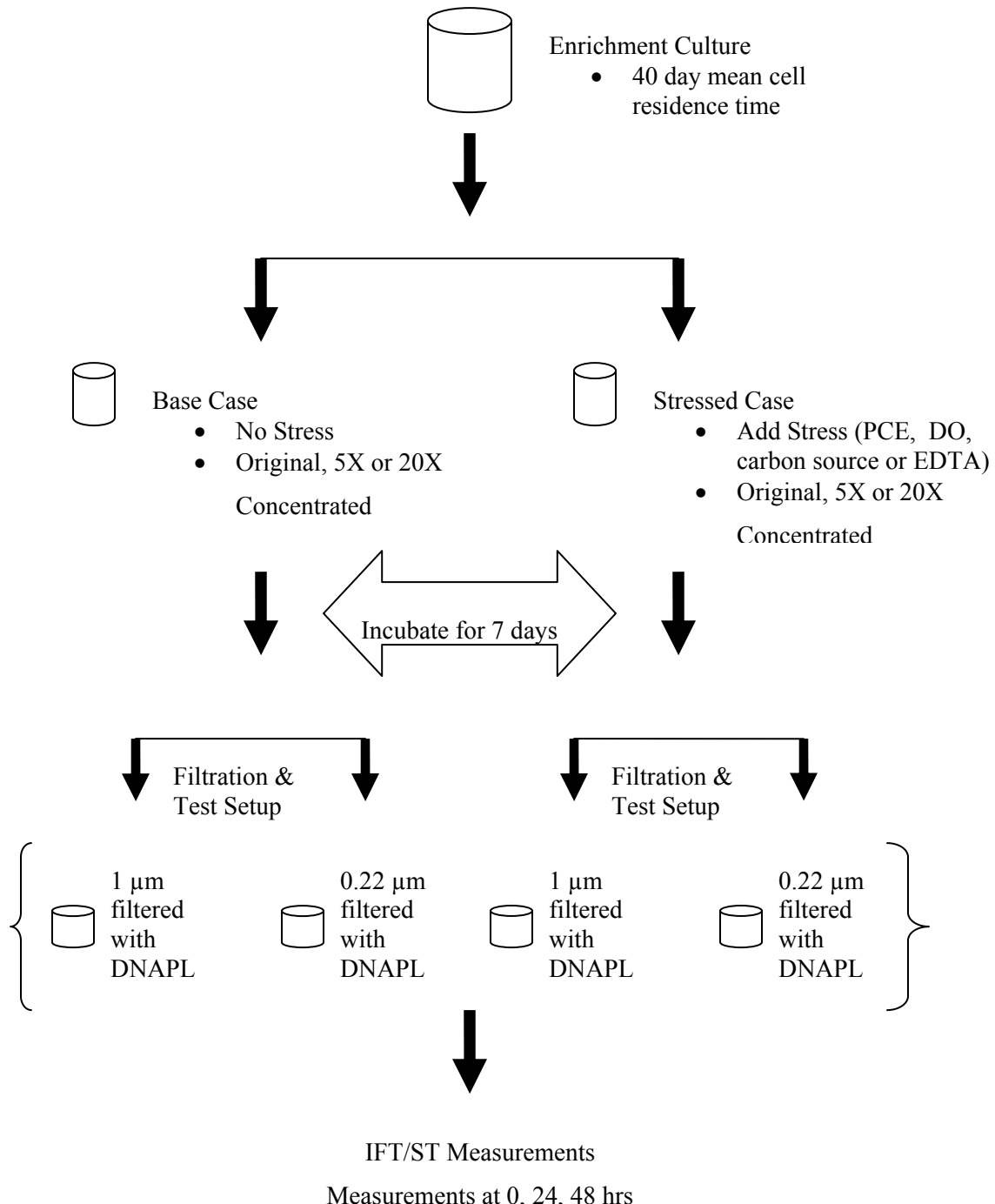


Figure 6.2: Microcosm preparation schematic

PCE stressed microcosms. PCE is a toxic organic solvent that historically has been a widespread contaminant at SRS. However, the culture used to generate SRS2 came from a part of the site free of PCE DNAPL contamination. Organisms that have little exposure to certain compound may lack the ability to produce enzymes for biodegradation. Therefore, cultures lacking this ability would be stressed by the presence of these compounds. In order to determine that the culture did not contain organisms that would dechlorinate PCE, neat PCE was added at lower concentrations of 27.05 mg/L (1 μ l) to

microcosms prepared identical to that of the base case, incubated for one week and monitored for PCE dechlorination over the duration of the incubation. Samples were monitored by using a gas chromatograph (GC) as detailed below. No dechlorination was observed in any of the SRS2 samples.

High PCE concentrations, at approximately saturation level (190 mg/L), were also prepared. These samples again were prepared identical to that of the base case with the exception of receiving of 7 μ L of neat PCE prior to incubation.

Dissolved oxygen (DO) stressed microcosms. Oxygen was added at different concentrations in order to determine whether this stress on the anaerobic cultures would alter interfacial and surface tension. In order to produce these samples, microcosms were first created, again, as described above. However immediately before incubation, oxygen was delivered to the samples. This was achieved by inserting a large deflected point septum penetration needle through the septum to the bottom of each sample microcosm. In addition, a second, short needle was inserted through the septa into the headspace above the sample, which acted as a vent to equalize the pressure in the vial. The samples were essentially "purged" with oxygen in this manner for a pre-determined amount of time, in order to achieve a desired dissolved oxygen concentration. Various preliminary tests were completed to gauge the correct gas pressure, flowrate, and contact time required to achieve desired levels of dissolved oxygen. Samples were sacrificed after a given time period to measure DO using an YSI Model 57 Oxygen Meter (YSI Inc, Yellow Springs, Ohio).

Altered Carbon Source Stress. Altered carbon sources were the first variable studied with the Cornell enrichment culture since it had been maintained using butyrate only. Lactic and propionic acid amended samples were created with the initial culture, following the procedure outlined above. However, these carbon sources were fed to samples at the same molar ratio as the butyric acid in the base case samples, and main enrichment culture. Initial base case samples were fed 0.052 moles of butyrate every 24 hrs. Alternatively, lactic or propionic acid was added to result in equal molar amounts of 0.052 moles of each carbon source every 24 hrs.

EDTA Amendments. EDTA is a complexing agent known to significantly alter the aqueous chemistry of trace metals in solution. EDTA-amended samples were produced to determine whether the change in the aqueous chemistry of the culture media would produce significant changes in interfacial properties. EDTA amended samples were created with the Cornell culture by adding EDTA stock solution at a final concentration of 200 mg/L to microcosms produced as described above. The EDTA amendment was completed immediately following the addition of culture to the samples, which were then incubated for a week under the same conditions and feeding regimen as the Cornell enrichment culture.

Abiotic Controls. In addition to the culture samples, a number of abiotic controls were created and tested, which included testing the abiotic media, and a number of abiotic particles including goethite, latex, and silica particles filtered to the same filtrate specifications. This ensured that any observed impact was directly due to microbial activity, and not simply a physical process induced by the presence of inorganic particles.

PCE analysis. Gas chromatography was completed on all samples, to monitor PCE biodegradation. PCE and its biodegradation byproducts, or intermediates, were analyzed using a Hewlett Packard HP 5790 Series II gas chromatograph equipped with an electron capture detector (ECD) and headspace sampler (Agilent HP7694). The column was 60 meters long, with a 0.25 mm inside diameter, and a 0.25-micron film (J&W Scientific, Cat. # 1225062, DB-5). An argon/methane mixture was used as the carrier gas. The following method was employed for PCE analysis: Inlet temperature of 250°C, detector temperature of 300°C, an initial column temperature of 40°C maintained for 2 minutes, followed by a 10°C per minute increase until 220°C is reached, then a 40°C increase per minute until 300°C. 5-mL diluted samples were placed in 20-mL headspace vials with Teflon lined septa and aluminum crimp caps.

Surface and Interfacial Tension Measurements. After incubation, surface tension (ST) and interfacial tension (IFT) measurements were completed on each sample filtrate. Approximately 25 ml of filtrate was added to a 75-ml beaker. 25 ml of TCE was then drawn into a syringe, which was inserted through the filtrate to the bottom of the beaker and carefully dispensed into the beaker, creating a two-phase system, with TCE as the model DNAPL. Separate beakers were prepared to analyze the ST or IFT after 0, 24 or 48 hours to allow the phases to equilibrate. Surface tension (ST) of the filtrates and interfacial tension (IFT) of both the particulate and the particle-free filtrates and TCE were measured. All ST and IFT measurements were conducted using a Du Nuoy ring tensiometer (FISHER Surface Tensiomat, Model 21) following ASTM D-971. Observed reductions in ST together with IFT in either particulate filtrate or particle-free filtrate may be indicative of the presence of biosurfactants accumulating at the interfaces. Observed reductions in IFT measurements with particulate filtrate only while showing little affect on ST indicate the accumulation of organisms at the NAPL/filtrate interface (microbial adhesion). Any observed reductions in IFT measurements with particle-free filtrate would only indicate biosurfactant accumulation at the NAPL/filtrate interface. In this manner, the samples were screened for biosurfactant production and/or adhesion at the interface. Four replicates were used for all surface or interfacial tension measurements.

Bacterial Cell Counts. Live/Dead® *BacLight*™ (Kit L-7007; Molecular Probes, Inc.) counts were completed on all cultures, in order to determine the concentration of cells in the culture, as well as to verify that the cultures were active. This kit contains nucleic acid stains SYTO® 9 green-fluorescent and propidium iodide, which is red-fluorescent. Due its small molecular size SYTO® 9 will stain all cells, while propidium stains only DNA of membrane compromised cells (i.e. “dead” organisms).

Each sample was diluted 1/1000 of which ten milliliter final sample dilutions were completed in triplicate for each representative sample and stained with the green and red stains. Each 10-mL sample received 1.5 μ L of each stain (red and green). The dye-culture mixture was then vortexed for approximately 15 seconds to ensure it is well mixed, and then allowed to rest in darkness for 15 minutes, during which time the dyes attach to the corresponding “live” and “dead” cells. Samples were then filtered onto black 0.22 μ m filter paper and counted using fluorescent microscopy at 1250X magnification. Cell numbers on each filter were quantified using a Olympus BX51 microscope equipped with a Photometrics Cool SNAP™ ES digital camera and an image analysis system (MetaMorph®; Universal Imaging Corporation™). Thirty representative locations per filter were used to count live/dead cells. Each set contained a blank particle free DI stained sample for quality control purposes.

It was determined that the Cornell culture was approximately 20 times more concentrated than was the SRS1 and 10 times more that SRS2 cultures.

6.4 Results

The anaerobic cultures were compared with respect to their net effect on DNAPL/water interfacial properties under basic growth conditions and when stressed by environmental scenarios that may conceivably occur at PCE/TCE contaminated sites. All cultures were exposed to elevated concentrations of PCE and dissolved oxygen. In addition, a number of different variables were considered for the Cornell culture, including several carbon sources and the addition of EDTA. All samples were incubated for one week, and tested at 0, 24, and 48 hours after incubation and filtration. All other samples were then compared to the base-case (non-stressed) samples and to the abiotic control in order to determine the relative extent and significance of each variable tested on ST and IFT. As described below, for the PCE degrading cultures, increased PCE concentrations and DO concentrations produced the greatest reductions of interfacial tension, which seem to be mediated by accumulation of organisms at the DNAPL/water interface. However, the background anaerobic culture (SRS2) exhibited significant surfactant production under normal growth conditions, which was significantly inhibited once stress was imposed.

6.4.1 Base Case Scenarios

Surface tension and interfacial tension measurements were conducted on both the particulate and particle-free filtrates of the base-case samples. ST and IFT data after 48 hours equilibration between phases in the beaker are shown in Table 6.7. Data for earlier times are presented in Table 6.8 and discussed here with standard deviations listed in parenthesis. For comparison purposes, the ST of pure water is 72.8 dynes/cm and the IFT for TCE and water is 34.5 dynes/cm (Demond and Linder 1993). All of the measured ST values were below the ST of pure water as would be expected for contaminated samples. IFT values range from very close to that of pure TCE and water to significantly lower values.

The Cornell culture sample surface tensions averaged 69.8 (0.3) dynes/cm, for the particulate filtrate, and 63.6 (1.3) dynes/cm for particulate-free filtrate, when tested immediately after incubation and filtration. Cornell culture base-case samples tested after 24 hours yielded ST averages of 69.4 (0.4) dynes/cm for the particulate filtrate, and 65.9 (0.5) dynes/cm for particulate-free filtrate (Table 6.7). Interfacial tension results from the base-case samples averaged 36.0 (0.8) dynes/cm for the particulate filtrate, and 35.1 (0.9) dynes/cm for particulate-free filtrate at 0 hours. After 24 hours, base-case samples yielded IFT averages of 30.4 (0.8) dynes/cm for the particulate filtrate, and 28.8 (1.8) dynes/cm for particulate-free filtrate (Table 6.7). Concentrating SRS1 culture to levels comparable to the Cornell culture resulted in similar surface activity of both unstressed cultures. An IFT of 27.0 dynes/cm after 48 hrs was measured for the concentrated culture (Table 6.8).

For all three cultures, the ST did not change significantly with time, although they did vary among cultures. The surface tension for SRS2 was significantly lower than for the other two cultures and the abiotic control, indicating that SRS2 may have produced a biosurfactant that accumulated at the air/water interface. The IFT for all three cultures, however, decreased for the first 24 hrs of sample analysis (Table 6.8) indicating that particles or other surface active compounds accumulated at the TCE/water interface over time. IFT of SRS2 was lower than both other cultures.

Table 6.7: Base-case culture interfacial activity after 48 hrs (mean±standard deviation).

Parameter		Abiotic Control ¹	Cornell	SRS1		SRS2
Cell concentration [cells/mL]		0	9.4x10 ⁸	5.0x10 ⁷	7.7x10 ⁸	8.9x10 ⁸
ST [dyn/cm]	Particulate	68.2	68.6±0.4	67	68.3	64.8±0.3
	Particle free	66.4	67.1±0.5	67		64.1
IFT [dyn/cm]	Particulate	33.7	28.7±0.8	35	27.0	25.3
	Particle free	32.3	28.6±1.8	35		25.0

¹Abiotic control consists of TCE/basal media surface and interfacial tension measurements

Table 6.8: Comparison of ST and IFT of non-stressed Cornell and Concentrated SRS Cultures at similar cell concentrations.

	Filtrate	0 Hrs	24 Hrs	48 Hrs
Base Case Cornell Culture	Particulate ST	69.8	69.4	68.6
	Particle Free ST	63.6	65.9	67.1
	Particulate IFT	36.1	30.4	28.7
	Particle Free IFT	35.1	28.8	28.6
Concentrated SRS1 Culture				
	Particulate ST	68.1	68.0	68.3
	Particulate IFT	33.4	27.7	27.0
Concentrated SRS2 Culture	Particulate ST	64.1	64.6	64.8
	Particle Free ST	64.0	62.6	64.1
	Particulate IFT	32.3	25.6	25.3
	Particle Free IFT	31.6	24.3	25.0

6.4.2 Abiotic Controls

Control microcosms were developed in order to determine the effect of inorganic particles accumulating at the TCE/water interface on IFT. Controls were treated identically to the biological microcosms. Inorganic particle size was similar to microorganism size. It is clear that the colloidal particles, which have different surface charge properties than bacteria at the same pH values (neutral pH), did not have significant effect on the IFT or on the surface tension (Figure 6.3). In addition, the effect of pure media on the interfacial tension after 48 hours (30 dynes/cm) was very similar to the effect the original culture after 48 hours (28.7 dynes/cm). This suggests that abiotic colloids were not responsible for the interfacial tension decreases observed for either particulate or particulate free samples.

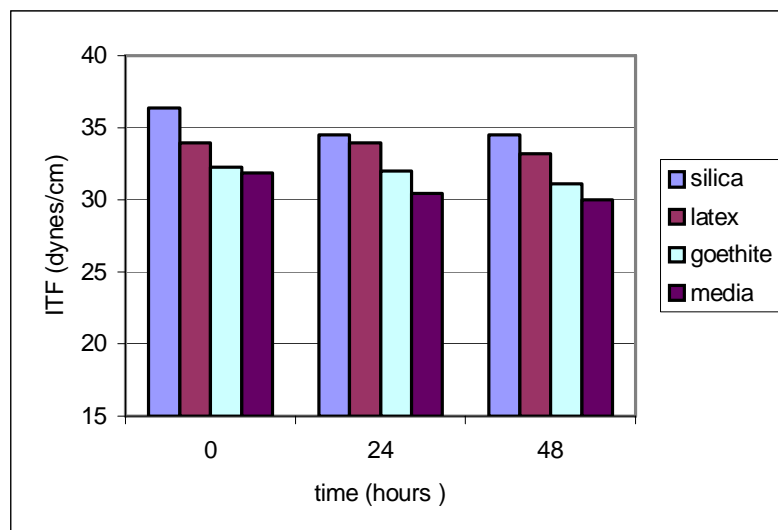


Figure 6.3: Mineral colloids, and pure media controls effect on interfacial tension

6.4.3 Stressed Culture Results.

EDTA and Carbon Source Amendments. EDTA-amended samples were produced with the Cornell culture, to determine the effects of increased availability trace metals in the growth media would induce culture surface activity. The EDTA-amended samples resulted in slight, statistically not significant (less than 10%) decreases in ST and IFT averages as compared to the original base-case (Table 6.9), and were therefore not studied further.

Samples were also produced in which lactic and propionic acid replaced butyrate as the carbon source during incubation. These systems produced ST and IFT data similar to that of the EDTA-amended samples, and were therefore also not studied further (Table 6.9).

Table 6.9: EDTA and Carbon Source Amendments Results for Cornell Culture

ST & IFT (dynes/cm)	Base Case	Propionic	Lactic	EDTA
Particulate ST	66.2	68.0	68.1	69.3
Particle-Free ST	66.6	66.8	66.4	68.0
Particulate IFT	26.2	26.5	24.8	32.9
Particle-Free IFT	30.3	29.8	32.9	32.8

Increased PCE Concentration Amendments. Samples were studied in which the concentration of PCE administered during the one-week incubation was increased tenfold (i.e. 190 mg/L) for the PCE degrading cultures (Cornell and SRS1) while PCE was introduced at two levels (27 and 190 mg/L) for the non-dechlorinating culture SRS2. For the Cornell culture particulate filtrate (filtered through 1 μ m filter) surface tensions remained relatively constant over the 48-hour period, yet were approximately 10% to 12% lower than the initial base case samples ($p=0.042$, $n=9$) (Figure 6.4). The IFT measurements for particulate filtrate showed significant reductions. The particulate samples were then left undisturbed for 2 days, during which IFT measurements were taken every 24 hours. Average IFT measurements of the stressed culture containing a PCE concentration of 190 mg/L were reduced to 19 dyn/cm, as compared to 30.4 dyn/cm in the base case samples, after 24 hrs of incubation ($p<0.0001$, $n=9$) (Figure 6.4). No further decline after the initial 24 hrs period was observed.

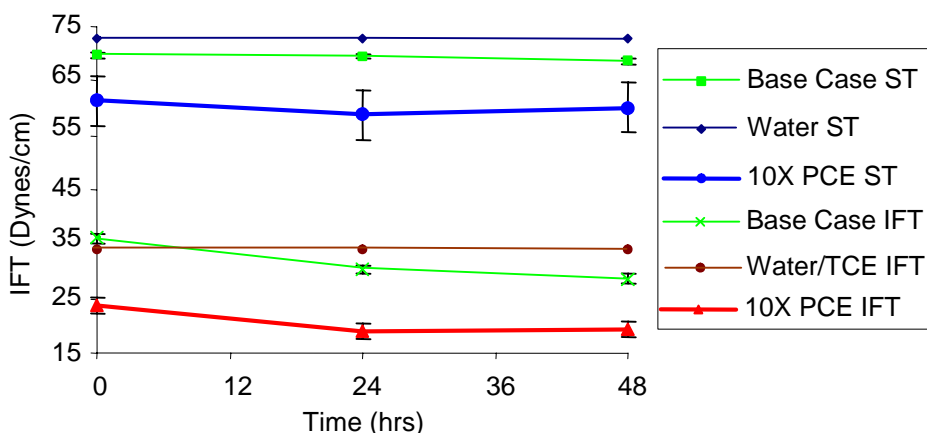


Figure 6.4: ST and IFT of particulate sample from Cornell butyrate culture stressed with 190 mg/L PCE for 1-week. Error bars represent one standard deviation of three replicate measurements

SRS1 microcosms stressed with 190 mg/L PCE exhibited relatively little change in interfacial properties. Observed particulate and particle-free IFT reductions compared to the non-stressed control were not statistically significant ($p=0.16$, $n=3$) over the 48-hour period. The bacterial concentration of the

SRS1 culture was approximately 10 times lower than the Cornell enrichment culture (5.0×10^7 vs. 9.4×10^8 #/mL). Experiments conducted for SRS1 at higher cell concentrations of the non-stressed culture exhibited similar surface activity than the Cornell culture (Table 6.8). Unfortunately stressed experiments could not be conducted due to the limited availability of the enrichment culture volume.

Stress to concentrated (5X) SRS2 cultures was evaluated. After one week of incubation of the culture at a cell concentration comparable to Cornell culture (8.9×10^8 #/mL vs. 9.4×10^8 #/mL), ST and IFT using TCE as the model DNAPL were measured at 0, 24, and 48 hours and were compared to the corresponding 5X concentrated base case samples (particulate samples) (Figure 6.5). While initial (0 hr) reductions of IFT relative to the unstressed control were observed in the presence of 190 mg/L PCE, reductions were not statistically significant for later time points ($p = 0.2$) (Table 6.10).

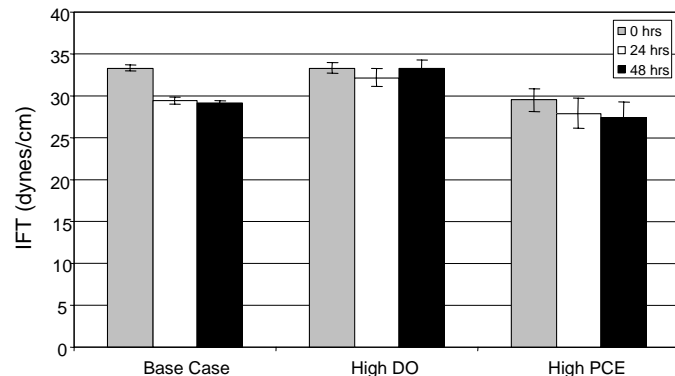


Figure 6.5: Effect of PCE (190 mg/L) and oxygen (1.5 mg/L) stress on SRS2 IFT at a cell concentration of 8.9×10^8 #/mL (5X). (1 μ m Filtered (particulate samples))

Table 6.10: Effect of PCE (190 mg/L) and Oxygen (1.5 mg/L) Stress on SRS2 at a cell concentration of $8.9 \times 10^8 \text{ #/mL}$. Statistical Significance IFT Measurements, 1 μm Filtered

5X Concentrated TCE DNAPL			
1 μm , IFT, 0 hr	Base Case	High DO	High PCE
p value		0.50	0.00
Mean \pm one standard deviation	33.3 \pm 0.3	33.3 \pm 0.6	29.5 \pm 1.4
% difference (based on mean) *		0.0%	11.4%
1 μm , IFT, 24 hr	Base Case	High DO	High PCE
p value		0.01	00.22
Mean \pm one standard deviation	29.4 \pm 0.4	32.2 \pm 1.0	27.9 \pm 1.8
% difference (based on mean) *		-9.7%	4.9%
1 μm , IFT, 48 hr	Base Case	High DO	High PCE
p value		0.01	0.21
Mean \pm one standard deviation	29.2 \pm 0.3	33.2 \pm 1.1	27.4 \pm 1.9
% difference (based on mean) *		-13.9%	6.0%

* negative values indicate an increase in IFT relative to the unstressed culture

Dissolved Oxygen Amendments. Samples containing various concentrations of DO were tested with the Butyrate culture. Sample sets with DO concentrations of 0, 1.5, and 2.8 mg/l were produced (Figure 6.6). Significant ($p=<0.0001$, $n=9$) ST reductions of greater than 10% were observed at both oxygen levels (DO=1.5 mg/L and DO=2.8 mg/L), in both particulate and particle-free filtrates. These changes were comparable to the changes induced by the 10X PCE stress experiments.

Observed IFT reductions were significant ($p=0.0008$, $n=9$) at both oxygen stress levels (DO=1.5 mg/L and DO=2.8 mg/L) for both particulate and particle-free filtrates. The greatest reduction was observed in the DO=1.5mg/L sample's particulate filtrate, which produced a 43% reduction of IFT from the original base-case samples. This DO concentration appears to have the most significant impact on the Cornell culture with respect to observed surface activity of the culture media.

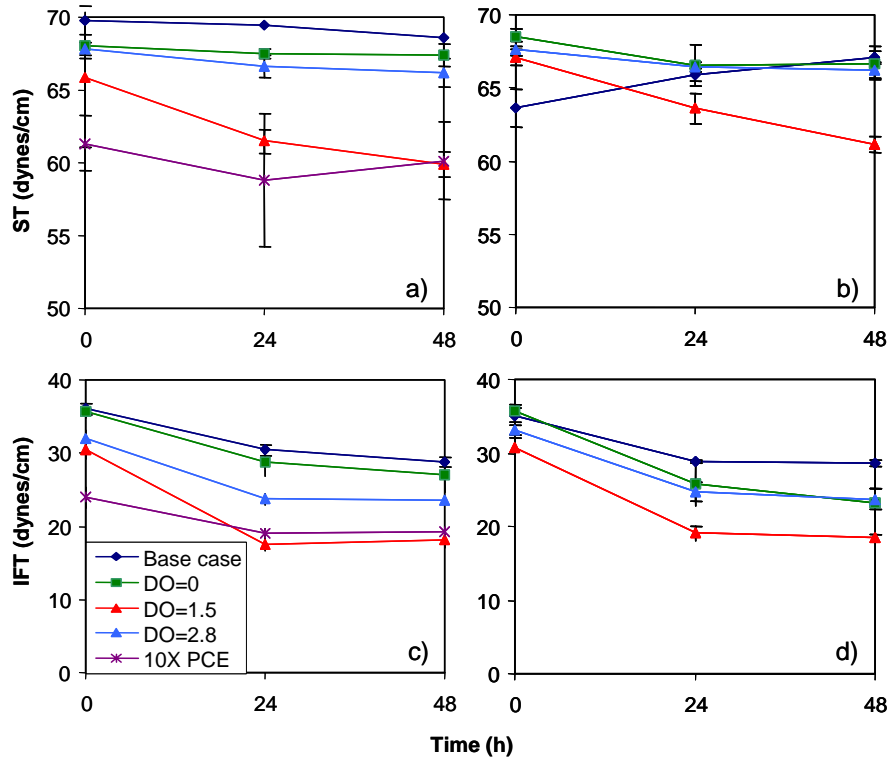


Figure 6.6: Effect of oxygen stress on interfacial properties (ST: a), b) and IFT: c), d)) of Cornell Culture after one-week of incubation. DO concentrations in mg/L. Media filtered through 1 μ m filter paper (particulate samples: a, c)) and 0.22 μ m (particulate free samples: b), d)). Error bars of one standard deviation included

Two oxygen stress levels were tested with enrichment culture SRS1 (0.8 mg/L and 1.5 mg/L). Results of IFT measurements did not produce any significant reductions for either oxygen level ($p=0.163$, $n=9$) compared to base case values.

The cell concentration within the microcosms of SRS1 was 5.0×10^7 cells/ml compared to 9.4×10^8 cells/ml of the Cornell culture. To determine the significance of cell concentrations on observed results, the SRS1 culture was concentrated via centrifugation under anaerobic conditions to a concentration approximately equal to the butyrate culture (7.7×10^8 cells/ml). The concentrated SRS culture sample was then tested in order to determine the significance of cell concentrations on the SRS culture. Significant IFT ($p=0.038$, $n=9$) reductions of approximately 20% below base case conditions were observed, from 34.0 dynes/cm in the base case, to 27.0 dynes/cm in the concentrated non-stressed sample. These results illustrate that conclusions of organisms' potential to affect interfacial properties depend on cell concentrations and it is unclear whether SRS1, at higher cell concentrations, would have exhibited increased surface activity upon oxygen stress (as did the Cornell culture).

Unlike that of the original concentrated SRS2 culture, oxygen (1.5 mg/L) stressed samples did not affect IFT. In fact IFT for the oxygen stressed SRS2 culture were statistically significantly higher than the non-stressed culture ($p=0.01$ at both 24 and 48 hrs) (Figure 6.5). IFT for particle-free filtrate in the 1.5 mg/L samples increased approximately 20% and 16% respectively compared to the non-stressed base culture.

Effect of cell concentration on SRS2 surface activity. In order to determine the effect of cell concentration on interfacial properties three sets of microcosms were generated using culture SRS2. The three concentrations were generated by (1) mixing 10 mL of the enrichment stock culture with 50 mL,

50 mL enrichment culture with 10 mL media and (3) centrifugation of 200 mL enrichment culture followed by resuspension in 60 mL carbon-free anaerobic media. Cell concentrations were quantified at the end of the one-week incubation period. IFT and ST were measured using PCE as the model DNAPL. IFT and ST for 5-times concentrated culture were consistently lower than the original and 20-times concentrated microcosms (Table 6.11). When compared to the other two cultures at similar cell concentrations, SRS2 exhibited the lowest IFT and ST at non-stressed conditions (Table 6.8). While increased cell concentration for SRS1 increased surface activity, increasing concentration above 9E8 cells/mL resulted in a decline in apparent surface activity of SRS2. If surface active compounds are produced in the enrichment reactor, increasing the cell concentration in the microcosms by changing the ratio of enrichment culture to fresh media would result in an increase in the surfactant concentration. Similarly, centrifugation with subsequent resuspension of the culture would remove all the original surfactant, thus less surface activity would be observed.

Table 6.11: Base Case Comparison of Mean Values of ST and IFT (dynes/cm)
at 0, 24, 48 hrs for Varying Cell Concentrations

1 μm (particulate) ST Base Case Comparison								
Concentration	Original	5X				20X		
Cells/microcosm	1.77E+08	8.85E+08				5.73E+09		
DNAPL	PCE	PCE	PCE	TCE	TCE	PCE	PCE	
Test	NA	1	2	3	4	5	6	
Mean @ 0 hrs	66.7	62.7	66.3	62.0	66.2	67.7	67.8	
Mean @ 24 hrs	66.8	59.9	65.1	63.3	65.9	68.0	67.6	
Mean @ 48 hrs	66.5	63.0	65.6	62.3	67.3	68.1	67.2	
1 μm (particulate) IFT Base Case Comparison								
Concentration	Original	5X				20X		
Cells/microcosm	1.77E+08	8.85E+08				5.73E+09		
DNAPL	PCE	PCE	PCE	TCE	TCE	PCE	PCE	
Test	NA	1	2	3	4	5	6	
Mean @ 0 hrs	32.1	32.9	35.1	31.2	33.3	34.9	37.2	
Mean @ 24 hrs	32.2	28.0	30.8	21.8	29.4	39.3	39.9	
Mean @ 48 hrs	31.8	27.4	28.8	21.4	29.2	37.4	37.3	
0.22 μm (particulate free) ST Base Case Comparison								
Concentration	Original	5X				20X		
Cells/microcosm	1.77E+08	8.85E+08				5.73E+09		
DNAPL	PCE	PCE	PCE	TCE	TCE	PCE	PCE	
Test	NA	1	2	3	4	5	6	
Mean @ 0 hrs	58.7	54.8	63.7	62.9	65.0	67.9	65.4	
Mean @ 24 hrs	61.2	54.8	63.5	60.2	64.9	68.2	67.5	
Mean @ 48 hrs	63.3	59.0	62.0	61.2	67.0	68.1	66.3	
0.22 μm (particulate free) IFT Base Case Comparison								
Concentration	Original	5X				20X		
Cells/microcosm	1.77E+08	8.85E+08				5.73E+09		
DNAPL	PCE	PCE	PCE	TCE	TCE	PCE	PCE	
Test	NA	1	2	3	4	5	6	
Mean @ 0 hrs	28.3	30.7	34.4	29.9	33.2	34.5	34.8	
Mean @ 24 hrs	30.1	25.8	28.0	25.8	28.7	40.2	40.6	
Mean @ 48 hrs	31.1	26.3	25.8	20.4	29.5	38.0	33.9	

Summary of Stresses towards SRS2. While both PCE degrading cultures (Cornell and SRS1) seemed to respond similarly towards oxygen and PCE stress, the background culture SRS2 responded very differently (Figure 6.7). For the non-concentrated culture, ST and IFT were lowest under no-stress conditions and increase slightly (not statistically significant) when stressed at any stress level with either PCE or oxygen. The data suggests that oxygen or PCE induced stress removes any surface active components from solution during the one-week incubation.

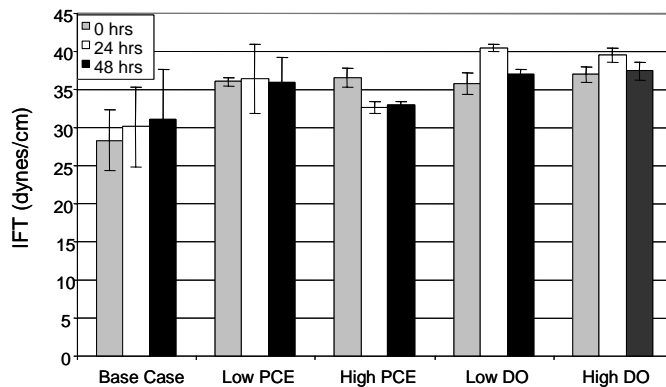


Figure 6.7: IFT for SRS2 sample - Original Concentration, 0.22 μm Filtered

At higher cell concentrations, the response to stress remained similar with respect to the exposure to oxygen (ST and IFT increase upon oxygen stress). A slight decline (less than 10%) in IFT and ST was observed when the 5X or 20X concentrated SRS2 cultures were incubated in the presence of 190 mg/L PCE. This decline, however, is significantly smaller than was observed for the Cornell culture.

6.5 Discussion

Observed activity at DNAPL/water or air/water interfaces may be (1) due to the presence of biosurfactants in solution or (2) due to the accumulation of microorganisms at interfaces whose cell membranes may be particularly surface active. If biosurfactants are responsible for the observed activity, samples should maintain their activity even after removal of all biological particulate matter (i.e. filtration through 0.22 μm). While there has been some evidence of cells smaller than 0.2 μm , most organisms will be removed by a filter with 0.22 μm pores. Therefore, comparing IFT and ST of “particulate-free” with “particulate” samples will allow for the determination of the predominant pathway to alter surface activity.

Any reduction in surface tension, in both the particulate and particle-free filtrates, can be attributed to biosurfactant production, whereas reduced IFT values observed in the particulate filtrate could be due to one of three scenarios. The presence of a biosurfactant may also cause an accumulation of surfactant at the NAPL/water interface, thereby reducing IFT as well as ST. Alternatively, organisms present in solution may settle through the aqueous phase to the interface over a period of time, accumulating or adhering at the DNAPL-water interface and lowering the IFT. The third scenario is a combination of both mechanisms. The combination of bacterial adhesion and surfactant accumulation may therefore also be the cause of the observed IFT reductions. In order to determine which mechanism(s) are responsible for the IFT reductions, the IFT values of the particle-free filtrate must also be considered. Since the majority of colloids and organisms are removed from the particle-free filtrate, any observed reductions in particulate-free IFT values are due to biosurfactant accumulation at the NAPL-water interface only. Particulate and particle-free filtrates of the Cornell culture at DO= 1.5mg/L, and samples with increased PCE concentrations produce some degree of ST reductions. This would be indicative of the presence of biosurfactants. This culture and oxygen stress also resulted in decreases in the IFT of both particulate and particulate-free samples. The IFT of the particulate sample decreased 43%

relative to the control, whereas there was less decrease for particulate free sample (33%). These results suggest that the stressed Cornell culture produced surfactants (as illustrated by ST and particle-free IFT reduction) and the cell surface was surface active since particulate IFT reduction was larger than particle-free filtrate. Such reductions in IFT may significantly alter the distribution of the NAPL present in the system.

It is possible that bacteria produced polymeric compounds that have aggregated and settled or adsorbed at the TCE water interface. Klein and Dhurjati (1995) studied CheY protein aggregation kinetics in *Escherichia Coli* and showed that proteins (polymers of α -amino acids) are able to aggregate in soluble and insoluble forms, and that the aggregation was time dependent. In addition, many studies showed that proteins could be adsorbed at interfaces and reduce the interfacial tension (Beverung et al., 1999; van der Vegt et al., 1996; Keshavarz et al., 1979). Furthermore, He et al. (1998) showed that bacteria under certain growth condition are able to produce polymer compounds. They showed that the Strain *pseudomonas* strain stutzeri coded 1317 isolated from contaminated soil was able to produce polyhydroxyalkanoates when grown in glucose and soybean oil as carbon source. Majid et al. (1999) also showed that the *Erwinia* sp. USMI-20 was found to produce poly(3-hydroxybutyrate) from either palm oil or glucose. They also found that this bacteria is able to produce the copolymer poly(3-hydroxybutyrate-*co*-3-hydroxyvalerate) using a combination of palm and another carbon source such as propionic acid but the effect of these polymers on the interfacial tension remains unclear. In addition, Lefebvre et al., (1997) studied the effect of dissolved oxygen concentration on polymer production by *Alcaligenes eutrophus* bacteria. Their study showed that under low dissolved oxygen concentrations and nitrogen limiting conditions, an increase of poly (3-hydroxybutyrate-*co*-3-hydroxyvalerate) was observed. This was likely due to the low glucose uptake caused by the low dissolved oxygen concentration.

In contrast to the Cornell culture, the background culture SRS2 exhibited surface activity during normal growth conditions but stress conditions inhibited the surface activity. The ST and IFT for the non-stressed SRS2 culture were lowest among the three cultures (Table 6.7). Low ST and IFT of the particulate-free sample indicate the presence of biosurfactants. Surface activity is increased for SRS2 when microcosms were generated using a larger concentration of enrichment culture (Table 6.7). However, when increasing the cell concentration through centrifugation and resuspension in fresh media, the apparent surface activity vanished. A biosurfactant present in the enrichment culture would have been removed through centrifugation, thus a reduction in surface activity would be expected. Once stressed with either PCE or dissolved oxygen, the SRS2 IFT (Figure 6.7) and ST increased. This response is opposite to both PCE-degrading enrichment cultures.

The data presented here illustrate that under certain environmental conditions, and at significant cell concentrations, microorganisms possess the ability to significantly alter the interfacial properties of NAPL-water systems, through both adhesion and biosurfactant production. Whether this surface tension reduction is a means to enhance mass transfer of PCE to enter the aqueous phase during reductive dechlorination (Maier et al. 2000), or a fortuitous effect due to the excretion of surface active by-products is unknown. However, in either case, it would increase the probability that the DNAPL can enter smaller pore spaces in the subsurface.

Observed surface activity for all cultures was clearly a function of cell culture concentration. In order to determine whether the observed effects could occur at contaminated sites, cell concentrations at the DNAPL/water interface in laboratory experiments would have to be compared to environmental systems. Using the cell concentrations used in the microcosms, and by computing the area of the beakers ($r = 2.3\text{cm}$), used to measure IFT, the total number of cells per square millimeter of DNAPL/water interface was determined for each culture. The original SRS1 culture consisted of approximately 7.4×10^5 cells/ mm^2 of interface area assuming all bacteria were settled to the interface after 48 hrs. The concentrated SRS1 culture produced approximately 1.1×10^7 cells/ mm^2 , and cell concentration of the Cornell culture was approximately 1.4×10^7 cells/ mm^2 .

Results from initial samples from the SRS site (Grimberg 2000) determined total cell concentrations of approximately 100×10^6 cells per gram of soil at the SRS site. Assuming a spherical particle of 0.3 mm in diameter, and a density of 2.64 g/cm^3 , a cell concentration of approximately 8.5×10^{10} cells per gram of soil would be estimated to achieve similar bacterial surface coverage than in the DNAPL/water samples. While this estimate is approximately three orders of magnitude higher the DNAPL/water interface in soil systems is significantly smaller than the water/soil interface. In addition, soil heterogeneity could result in large concentration variations. Thus, it is not inconceivable to encounter in environmental samples cell concentrations at DNAPL/water interfaces at levels similar to the observed in the laboratory setting.

6.6 Conclusions – Task 2

Significant IFT reductions have been observed under a number of varied environmental stress conditions with both the Cornell and SRS dechlorinating cultures, including the presence of DO, and increased PCE concentrations. This IFT reduction may significantly alter NAPL distribution in NAPL-water systems. Under the same stress conditions, surfactant production of the background culture was inhibited.

As illustrated, when organisms encounter certain environmental conditions, they may become stressed, during which imbalanced growth may occur. Specifically, imbalanced growth within the two dechlorinating cultures considered here can be attributed to low concentrations of DO and high concentrations of PCE. Either of these conditions created unfavorable environments for these cultures, which in turn lead to increased microbial adhesion and biosurfactant production, both of which play significant roles in altering the interfacial properties of NAPLs. The microbial mechanisms stimulated under these conditions are ultimately responsible for altering the distribution of DNAPLs in the subsurface.

On the other hand, the response to the same stresses is not universal. Surface activity of the non-dechlorinating culture was reduced upon exposure to PCE or DO. Whether this is a universal trend or just representative for the three enrichment cultures studied requires further investigation. The research however, provides evidence that stress due to the presence of PCE or oxygen may alter the surface activity of cultures significantly, at cell concentrations representative to environmental samples, which will impact the fate of DNAPL in subsurface systems.

6.7 References

Beverung, C. J., Radke, C. J and. Blanch, H. W. (1999). Protein adsorption at the oil/water interface: characterization of adsorption kinetics by dynamic interfacial tension measurements. *Biophysical Chemistry* 81(1): 59-80.

BHI, 1996. *Design, Operations, and Maintenance of the Soil Vapor Extraction Systems for the 200 West Area Carbon Tetrachloride Expedited Response Action*. BHI-00365, Rev. 0, Bechtel Hanford, Inc., Richland, Washington.

Chanmugathas, P., Bollag, J.M. (1988). A Column Study of the Biological Mobilization and Speciation of Cadmium in Soil. *Arch. Environ. Contam. Toxicol.* 17: 229.

Demond, A.H.; Lindner, A.S. (1993). Estimation of Interfacial Tension between Organic Liquids and Water. *Environ. Sci. Technol.*, 27(12), 2318-2331

DiStefano, T.D., J.M. Gossett, and S.H. Zinder (1992). Hydrogen as an Electron Donor for Dechlorination of Tetrachloroethene by an Anaerobic Mixed Culture. *Applied and Environmental Microbiology*. 58(11): 3622-3629.

Dohse, Dirk M. and Lion, Leonard W. (1994). Effect of Microbial Polymers on the Sorption and Transport of Phenanthrene in a Low-Carbon Sand. *Environmental Science and Technology*. 28(4): 541-548.

Gossett, James M., Fennell, Donna E., and Zinder, Stephen H. (1997). Comparison of Butyric Acid, Ethanol, Lactic Acid, and Propionic Acid as Hydrogen Donors for the Reductive Dechlorination of Tetrachloroethene. *Environmental Science and Technology*. 31(3): 918-926.

Gossett, James M., Smatlak, Concordia R., and Zinder, Stephen H. (1996). Comparative Kinetics of Hydrogen Utilization for Reductive Dechlorination of Tetrachloroethene and Methanogenesis in an Anaerobic Enrichment Culture. *Environmental Science and Technology*. 30(9): 2850-2858.

Grimberg, S. J., Powers, S. E., Denham, M., and Chen, K. "Field Study to Correlate Chlorinated Solvent Concentrations and Microbial Distributions in the Unsaturated Zone." *Symposium on Chemical-Biological Interactions in Contaminant Fate at the 220th ACS National Meeting*, Washington, DC.

He, T., Tian, W., Zhang, G., Chen, G., and Zhang, Z. (1998) production of novel polyhydroxyalkanoates by pseudomonas stutzeri 1317 from glucose and soybean oil. *Ferm Microbiology letters*. 169: 45-49.

Hurst, C.J., Knudsen, G.R., McInerney, M.J., Stetzenbach, L.D. and Walter, M.V. (1996). *Manual of Environmental Microbiology*. ASM Press.

Keshavarz, E., and Nakai, S. (1979). The relationship between hydrophobicity and interfacial tension of proteins. *Biochimica et Biophysica Acta - Protein Structure*. 576(2): 269-279

Knox, K., Jones, P.H. (1979). Complexation Characteristics of Sanitary Landfill Leachates. *Water Res.*, 13: 839-846.

Maier, R. M., Pepper, I. L., and Gerba, C. P. (2000). *Environmental Microbiology*, Academic Press.

Majid, M. I. A., Akmal, D. H., Few, L. L., Agustien, A., Toh, M. S., Samian, M. R., Najimudin, N., Azizan, M. N. (1999). Production of poly(3-hydroxybutyrate) and its copolymer poly(3-hydroxybutyrate-*co*-3-hydroxyvalerate) by *Erwinia* sp. USMI-20. *International Journal of Biological Maromolecules*. 25: 95-104.

Marshall, K. C. (1991). "The importance of studying microbial cell surfaces." *Microbial Cell Surface Analysis*, N. M. Mozes, P. S. Handley, H. J. Busscher, and P. G. Rouxhet, eds., VCH-publishers, New York, 3-20.

Maymo-Gatell, X., Chien, Y., Gossett, J. M., and Zinder, S. H. (1997). "Isolation of a bacterium that reductively dechlorinates tetrachloroethene to ethene [see comments]." *Science*, 276(5318), 1568-71.

van der Vegt, W., Norde, W., van der Mei, H. C., and Busscher, H. J. (1996). Kinetics of Interfacial Tension Changes during Protein Adsorption from Sessile Droplets on FEP-Teflon. *Interface Science*. 179(1): 57-65.

Yang, Y., and McCarty, P. L. (2002). "Comparison between donor substrates for biologically enhanced tetrachloroethene DNAPL dissolution." *Environmental Science and Technology*, 36(15), 3400-3404.

Zehnder, A. (1976). Titanium (III) Citrate as a NONTOXIC oxidation-Reduction Buffering System for the Culture of Obligate Anaerobes. *Science*. 194:4270-4271.

7.0 Characterization of DNAPL from DOE Savannah River Site¹ (Task 3)

7.1. Introduction

The U.S. Department of Energy's Savannah River Site (SRS) is a 320 square mile facility near Aiken, South Carolina that was used for the production of nuclear materials from the 1950s until 1985. In 1981, significant levels of groundwater contamination were identified at SRS. The presence of a dense, non-aqueous phase liquid (DNAPL) in the subsurface was one source of the groundwater contamination. In 1991, a clear, orange-colored DNAPL was found in two wells on the northwest side of the M-area settling basin in a quantity sufficient for recovery from the subsurface [Pickett et al., 1985].

The 30,000 m³ M-area settling basin was used as a hazardous waste management facility for several SRS buildings. Waste effluents from the fuel and target fabrication facilities that were discharged to the settling basin contained an array of aqueous and organic fluids, including degreasers, acids, caustics and metals [Pickett et al., 1985]. The use of chlorinated solvents evolved over the operating period of SRS. Discharges to the M-area basin included 144,000 kg of trichloroethene (TCE) from 1952 to 1970, 820,000 kg of tetrachloroethene (PCE) from 1962 to 1979, and 8,600 kg of 1,1,1 trichloroethane (TCA) from 1979 to 1982 [Pickett et al., 1985].

Preliminary analysis of the DNAPL from the SRS site showed that it is comprised primarily of PCE (80-98%, mole basis) and TCE (2-20% mole basis) [Looney, et al., 1992]. However, numerous other trace constituents have also been detected in the DNAPL, including polychlorinated biphenyls (75 mg/L), and a suite of long chain alkyl esters (~500 mg/L; e.g., butyl hexadecanoate) [Crump, 1997]. Raman spectroscopy of the DNAPL samples showed a high broad background signal indicating the presence of petroleum oils. This spectrum was matched to hydraulic oil historically used at the site [Rossabi et al., 2000]. These additional constituents could have contaminated the chlorinated solvent mixture during degreasing operations, co-disposal with other wastes, or through subsurface biogeochemical processes.

DNAPLs are a significant contributor to groundwater contamination. The behavior of DNAPL in the subsurface is very complex, depending on the spill history, DNAPL properties and geologic heterogeneity. This renders efforts to locate the DNAPL in the subsurface and subsequent remediation of these sites difficult and, consequently, results in a long-term contamination source of groundwater. When spilled, the DNAPL will vertically travel through the subsurface due to gravity. Heterogeneities in grain size or moisture content can cause significant horizontal flow of the DNAPL. This occurs when the DNAPL does not have sufficient head to overcome the entry pressure of a fine-grained or water saturated region of the unsaturated zone. The DNAPL pressure required to overcome the pore entry pressure of a geological layer is defined through the Young-Laplace equation as a function of the DNAPL interfacial tension (IFT), system wettability and the distribution of the pore radii. For a given pore size, the entry pressure is lower for systems that are not strongly water wetting or for DNAPLs that have low interfacial tensions. For these cases, the DNAPL can more readily infiltrate into low permeability regions of the subsurface.

Several recent studies have shown that DNAPLs collected from the subsurface often have interfacial tensions that are much lower than expected based on the predominant constituents. For example, reported IFT values of chlorinated solvent mixtures range from ~8-15 mN/m for degreasing solvents collected from the subsurface at U.S. Air Force Bases [Dwarakanath, 2002] to 21 – 34 mN/m for DNAPL from a variety of industrial facilities [Harrold et al., 2003]. The presence of stabilizers in industrial grade solvents, such as low concentrations of triethylamine, or oils and greases dissolved into the solvent during degreasing operations can contribute to reduced interfacial tensions compared with

¹ Manuscript in preparation for submission to the *Journal of Contaminant Hydrology*

laboratory grade solvents [Harrold et al., 2003]. Coal tars and creosotes also have low interfacial tensions (< 5 - 20 mN/m), especially under basic conditions [Barranco and Dawson, 1999; Zheng and Powers, 2003]. Zheng and Powers [2003] and Lord et al. [1997] showed that acidic macromolecule constituents in a DNAPL can play a significant role in lowering the interfacial tension of these complex mixtures. A study by Pfeiffer et al. [2005], determined that the mixing of soy oil in TCE or PCE can linearly decrease the IFT between the DNAPL and water as a function of the soy oil mole fraction to approximately 10 mN/m.

The wettability of a water-DNAPL-porous medium system can also be affected by the presence of trace constituents in any of the three phases [Powers et al., 1996; Harrold et al., 2001; Standal et al., 2001; Zheng and Powers, 1999]. Wettability, which is often quantified with contact angle measurements, is the ability of a liquid to spread on a solid surface in the presence of another immiscible liquid. Typically, porous media are assumed to be strongly water wetting, where the water covers the sand grains as a thin film occupying the small pores, while oil occupies the large pores.

Factors influencing wettability have been widely studied [Buckley, 1989; Hirasaki, 1991; Seo, 2006]. Buckley et al. [1997] proposed that rock wettability can be changed by four mechanisms: polar interactions, surface precipitation, acid/base dissociation, and specific interaction between charged sites and higher valent ions. The wettability of most minerals is dictated by the stability of the water film between the rock and the oil phase, which is related to the zeta-potentials of the oil–water and water–rock interfaces, and the charge of rock–water interface [Strand, 2006]. Combinations of trace or primary constituents that result in unlike charges at the mineral–water and NAPL–water interfaces can cause sufficient attraction between these interfaces to reduce the thickness of the water film and enable contact between the NAPL and mineral surfaces [Zheng and Powers, 1999]. This can effectively convert a water-wet system to an intermediate or oil-wet system.

The combined influences of lowered interfacial tension and wettability other than strongly water wetting can reduce the displacement pressure controlling DNAPL entry into fine grained media. Thus, we would expect to find that DNAPL can penetrate strata that are difficult to remediate. This has been a problem for the SRS site when soil vapor extraction (SVE) and steam extraction systems were employed for remediation purpose. The remediation efficiency of SVE, to a large extent, depends on the accessibility of remediation fluids to the DNAPL. Though SVE has proven to be a generally effective remediation strategy, wide variability in the effectiveness has been observed and it has shown to be less effective than anticipated at the SRS [Rohay, 1999].

DNAPL that is immobilized as discrete ganglia or pooled on an impermeable layer can continue to contaminate the groundwater. The dissolution process depends primarily on the effective solubility of the organic constituents comprising the DNAPL. The effective solubility can be altered through the presence of surfactants or co-solvents that were co-disposed with the DNAPL, potentially increasing the aqueous phase saturations. Co-solvents can enhance the overall NAPL mobility through different complementary mechanisms including: reduction of interfacial tension between the aqueous and NAPL phases; enhanced effective solubility of the NAPL constituents; swelling of the NAPL relative to the aqueous phase; and, under certain conditions, complete miscibility of the aqueous phase and NAPL. The relative importance of these different mechanisms depends on the ternary (water, cosolvent, NAPL) phase behavior of the specific system [Falta, 1998]. Surfactants can reduce the interfacial tension between water and NAPL, and enhance the extent of NAPL dissolution [Pennell, 1994; Imhoff, 1995; Saba, 2001].

Based on the work presented above and preliminary characterization of the DNAPL, it was hypothesized that the presence of trace constituents in the SRS DNAPL could substantially lower surface and interfacial tensions and increase the solubility of PCE and TCE. Thus, the goal of this work was to identify both trace and primary constituents in the SRS DNAPL and further characterize the DNAPL–water partitioning and interfacial properties. While the co-disposal of a wide range of organic and inorganic contaminants into the M-area lagoon at this site may make this DNAPL unique, it is typical that

chlorinated solvent wastes contain an array of chemicals that may alter DNAPL properties [Harrold et al, 2003]. Characterization of these properties could aid in identifying suitable remediation techniques and can provide the basis for more realistic multiphase flow modeling efforts.

7.2. Experimental Approach

An experimental plan was developed to identify constituents in the organic phase and water equilibrated with the organic phase, and to characterize interfacial properties. The measurements summarized in Table 7.1 were chosen based on knowledge of the co-disposed wastes and findings of other researchers cited above.

Table 7.1: Overview of experimental approach

Characteristic / Experimental test	Comments/references
Organic composition (DNAPL and equilibrated water):	
¹ H NMR	GC-FID for quantitative analysis of primary constituents.
GC-FID, GC-MS	MS detection for identifying trace constituents.
HPLC-MS	High MW hydrocarbons expected from degreasing operations
Inorganic composition (DNAPL and equilibrated water):	
ICP-MS	Possible metal constituents partitioned to organic phase during co-disposal at extreme pH values
Partitioning:	
Effective solubility of primary DNAPL constituents	Low IFT could be caused by co-solvent or surfactant constituents that also increase the solubility of the organic phase [Van Valkenburg, 2002]
Interfacial tension and related :	
IFT - Pendant drop shape analysis	Zheng et al. [1999] showed that low interfacial tension correlated to acidic constituents in other DNAPLs
Acid number – potentiometric titration	
Wettability and related:	
Wettability Bottle test	Qualitative means of assessing wettability with relevant mineral surfaces [Powers et al, 1996]
Electrophoretic mobility	Positively charged DNAPL surfaces more likely to wet negatively charged mineral surfaces [Zheng and Powers, 2003]

7.2.1 Materials

A DNAPL sample collected from the Savannah River site in the vicinity of the M-area basin was used as the site DNAPL. Tetrachloroethene (99.5%, Sigma Aldrich Co) and trichloroethene (99.5%, Sigma Aldrich Co) were used as a surrogate DNAPLs for comparison purposes.

All aqueous phase solutions were prepared with deionized water. An Orion pH meter model 420A was used in all pH measurements. For the electrophoretic mobility experiments, the pH was

adjusted with 0.1N HNO₃ and 0.1N KOH solutions and the ionic strength was adjusted using 99% NaCl (Fisher Scientific) from 0.01 to 0.1 N.

Soils used in wettability experiments included quartz sand and two SRS samples. The quartz sand (U.S silica, Ottawa, IL), was sieved to obtain a 0.425-0.6 mm fraction diameter. The sand was cleaned with concentrated HNO₃ (50%), washed several times with acetone and water, and dried at 103°C for 24 hours. SRS sand samples were received from a core (SB-3) collected at the A-area outfall area of SRS in May 2001. Two different soils were used in our experiments due to differences in their mineral surface composition as determined by electron dispersive spectroscopy. The SRS clay, collected from 3.46 – 4.06 m below ground surface (bgs), contained 15% each (atom %) aluminum and silica with a low percentage of iron. The yellow color of the SRS sand (12.3 - 12.5 m bgs) was indicative of its higher iron content (7.8%). Silica (13.7%) and aluminum (9.8%) were still predominant in the sand.

7.2.2 Methods

Organic Composition

A Hewlett Packard HP 5890 Series II gas chromatograph (GC) with a flame ionization detector (FID) and an Agilent HP7694E Headspace Sampler were used for bulk organic compound analysis. The GC was equipped with a Supelco Vocol™ column (60m long, 0.25mm inside diameter with 0.25µm film). Highly purified helium was used as the carrier gas and an air-hydrogen mixture as flame gases. The following conditions were employed for our experiments: Inlet temperature of 250°C, detector temperature of 300°C, and initial column temperature of 80°C maintained for 2 minutes followed by a rate of 6°C /min increase until 180°C is reached and this temperature was maintained for 2 minutes. 2-mL samples were placed in 5-mL headspace vials with Teflon lined septa and aluminum crimp caps.

Triplet samples of the SRS DNAPL and aqueous phase samples that had equilibrated with the DNAPL were prepared and analyzed. Samples were diluted by a factor of 5, 8 or 25 times to reduce the concentrations as appropriate for analysis. Methanol and DI water were used as blanks. Reagent grade PCE and TCE were used for standards and to verify the accuracy of solubility measurements.

Gas chromatography with mass spectrometer (GC/MS) has long been recognized as an efficient instrument to characterize unknown organic samples due to its high sensitivity and accuracy [Durand, 2004; Cai, 2006]. In this research, a Finnigan Trace Ultra gas chromatograph (San Jose, CA) equipped with a PolarisQ ion trap mass spectrometer (ThermoFinnigan, Austin, TX) was used. The sample was prepared by transferring 10µL of SRS DNAPL to a 2ml amber vial. For identification of carboxylic acids, the aliquot was derivatized with N,O-bis(Trimethylsilyl)trifluoroacetamide (BATFA) with Trimethylchlorosilane (TMCS). Briefly, a 10µL aliquot of BSTFA + TMCS (1%, 10%) was added to the vial which was capped and heated at 70°C for 1 hr. The vial was then cooled and 350µL of hexane was added. Then sample was immediately analyzed via GC/MS.

Individual organic constituents were identified and individual peaks were resolved using a 60m × 0.25mm × 0.25µm DB-XLB column (J&W Scientific, Folsom, CA). The injector was configured in splitless mode with a constant temperature of 250°C. The initial oven temperature was set to 40°C then ramped to 310°C at 2°C /min. The mass spectrometer was set to scan mode with ion source and transfer line temperatures set to 200 and 300°C, respectively. Compounds were tentatively identified using the NIST mass spectra library. Confirmation was not possible due to the lack of authentic standards for the compounds listed.

NMR spectroscopy is an analytical technique used to characterize and determine the structure of functional groups using common elements as hydrogen [Totsche, 2003]. In this study, NMR was used to determine the presence of acid functional group in the SRS DNAPL that would be detected by looking at the presence of hydrogen atom. SRS DNAPL sample for the NMR was prepared by dissolving 5mg of DNAPL in a 0.6mL of deuterated chloroform (CDCl₃, 99.9%, fisher scientific). The solution was then

placed in a 5mm NMR tube and analyzed using the Bruker Acance NMR model DMX 400 (Bruker BioSpin Corporation, Billerica, MA).

Inorganic Compositions

Inductively coupled plasma mass spectrometry (ICP/MS) has been increasingly used for precise and accurate determination of isotope ratios of long-lived radionuclides at the trace and ultratrace level due to its excellent sensitivity, good precision and accuracy [Becker, 2005]. An X series using Plasma Hot Screen (Thermo Electron Corp., USA) was used in this study for qualitative analysis of SRS DNAPL. Two milliliters of the SRS sample was dried in digestion vessel at 120°C overnight to evaporate the organic solvent. The residue was digested with 10mL HNO₃ (optima, Fisher scientific Co.) at 15 minutes ramp to 200°C and held for 15 minutes in a CEM MARS-X microwave accelerated reaction system (CEM Corp., USA). Five milliliter more of concentration HNO₃ was added and the sample was digested a second time. Digested samples were diluted to 100mL with 18.5 MΩ-cm DI water. The same amount (2mL) of PCE was used as a blank for quality control.

Interfacial Tension

A ring tensiometer (Fisher surface tensionmat, model 21) was used to determine the surface (ST) and interfacial tension (IFT) at room temperature (25±1 °C) according to the ASTM method for interfacial tension of oil against water by the ring method [ASTM 1991]. ST and IFT measurements were made in triplicate for the SRS DNAPL, with PCE used as a control.

Time-varying interfacial tensions were also measured with an OCA 15+ goinometer (Dataphysics Company, Bethpage, NY). This goinometer is equipped with SCA10 software which can automatically calculate surface tension and IFT by analyzing the shape of pendent drop using Laplace-Young equation (Figure 7.1).

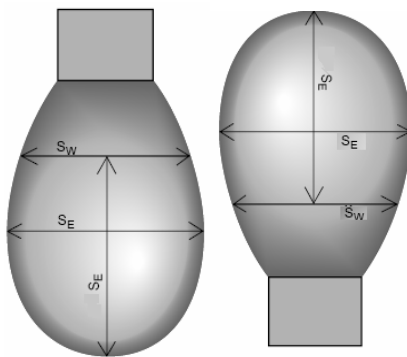


Figure 7.1: Pendent drop ST/IFT measured by OCA 15+

Left: $\rho_{drop} > \rho_{ambient}$; Right: $\rho_{drop} < \rho_{ambient}$

By measuring the dimension S_E and S_W shown in Figure 6.1, the ST/IFT is calculated as:

$$\gamma = \frac{\Delta\rho g S_E^2}{H} \quad (7.1)$$

where, $\Delta\rho$ the difference of density of bulk phase and the drop, in the case of ST or the difference of the drop density and the ambient air density; g is the acceleration of gravity; S_E is the equatorial diameter (Figure 7.1), which is measured automatically by the software; S_W is the diameter measured a distance S_E from the tip of the droplet; H is an empirical value that depends on the ratio of S_W/S_E

Continuous measurements of the DNAPL/water IFT were conducted in two ways. Droplets of DNAPL were suspended in water using a straight needle and droplets of water were suspended in DNAPL using an upright needle. IFTs were recorded for three hours or until the droplet separated from the needle. The IFT was measured for at least three droplets for each fluid pair system.

Wettability

Bottle test experiments developed by Powers et al. [1996] were employed to evaluate the wettability changes for a given porous media/DNAPL/aqueous phase system for various pH values and ionic strengths. These tests equilibrate water, DNAPL and mineral phases and use qualitative assessment of the fluid phase that coats the mineral. Oil red-O (electrophoresis grade, Fisher Scientific Co) was added to the DNAPL as a dye at concentrations of 0.1 g/L when needed for clear observation. The aqueous phases included pH 4.7, 7.2, and 10.3 at ionic strengths of 0.01 and 0.1 M. Quartz sand, SRS clay and SRS sand were used as the porous media.

Electrophoretic Mobility

Electrophoresis is one of the basic analytical tools for the estimation of the surface property of a charged entity in a dispersion medium [Lee, 2004]. Electrophoretic mobility of the SRS DNAPL was measured using a Zeta PALS instrument (Brookhaven Instruments Corporation). A DNAPL emulsion was prepared by mixing the SRS DNAPL with deionized water at a volume ratio of 1:2. The emulsion (100 μ L) was then diluted with 15 mL of 0.01 M KCL solution. The pH was adjusted with either KOH or HCl depending upon the pH target. Ionic strength was measured using a Cole Parmer conductometer (model 014816-61).

Acid Number

The acid content of the SRS DNAPL was determined using a non-aqueous potentiometric titration following the method used by Zheng and Powers [2003]. Acid content is expressed as an acid number, which is defined as the quantity of base, in milligram of potassium hydroxide per gram of sample, required to titrate a sample to a specific end point [ASTM, 1995]. Separate glass and indicating electrodes were used to improve the accuracy of the electromotive force reading. An inverted sleeve junction type calomel electrode (model 39420, Beckman, Fullerton CA) and a glass electrode (model 39322, Beckman, Fullerton CA) were used as the reference and indicating electrodes, respectively. Saturated NaClO₄ in 2-propanol was used as the electrolyte. The DNAPL was diluted in methyl isobutyl ketone (MIBK) (98.5%, Fisher Scientific Co), which is known to be a versatile solvent [Bruss and Wyld, 1957]. The titrant used was tetrabutylammonium hydroxide (Fisher Scientific Co).

As the titrant was added to the sample, the measured emf (mV) was plotted as a function of titrant added. The derivative of this curve was then calculated and plotted to obtain the inflection point. The corresponding volume of titrant at the inflection point was used to calculate the neutralization capacity or acid number of the sample. A known amount of stearic acid was added to the samples to obtain well-defined inflection points.

7.3. Results and Discussion

7.3.1 Composition of the SRS DNAPL

The characterization of the SRS DNAPL using GC-FID showed that the organic composition of this field DNAPL is 94.7% PCE and 4.7% TCE (mole fraction). This result is consistent with earlier analysis reported for the SRS DNAPL [Looney, 1992].

GC/MS chromatography (Figure 7.2) gives the qualitative characterization of SRS DNAPL. In addition to the chlorinated hydrocarbons (PCE and TCE), several carboxylic acid derivatives and fuel hydrocarbons (hopane, etc.) were found. Phthalates are commonly added to plastics to increase their flexibility.

- a. Hexadecanoic acid butyl ester
- b. Octadecanoic acid butyl ester
- c. Pentadecanoic acid methyl ester
- d. Hexadecanoic acid derivative
- e. Hopanes and mixed hydrocarbons
- f. Phthalate
- g. TCE
- h. PCE

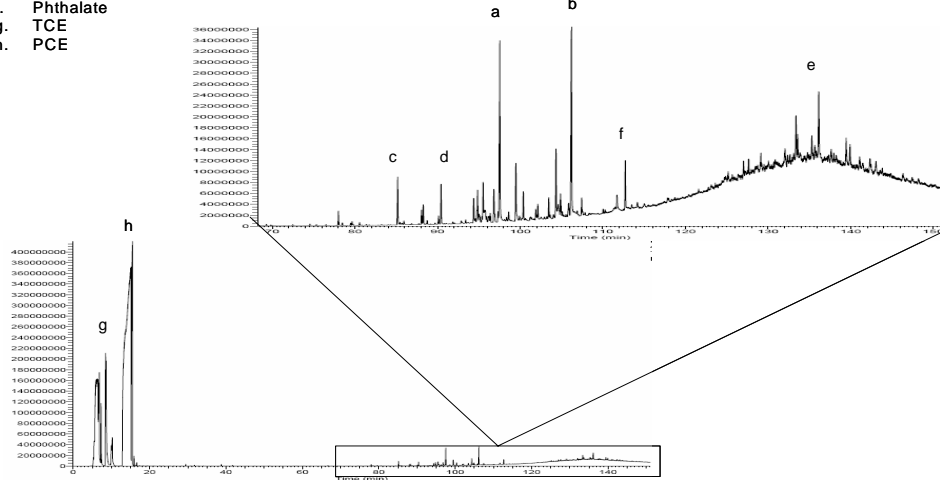


Figure 7.2: SRS DNAPL chromatography from GC/MS

^1H NMR was used to characterize the acid functional group in the SRS DNAPL (Figure 7.3). Carboxylic acids would most likely appear downfield at around 10 ppm. Although this range is not shown on Figure 7.3, no peaks were detected on the spectrum that would suggest the presence of hydroxyl groups. It is possible that low concentrations of species would not be detected with ^1H NMR. The spectrum did, however, show the presence of a long chain hydrocarbon with the CH_3 , CH_2 and CH groups appearing upfield between 0.8 and 1.6 ppm, which are very similar to the signature of the hydraulic oil (Figure 7.3b). A singlet appearing at 6.5 ppm indicates the presence of TCE in the DNAPL. (a bearing and circulating oil at 1% concentration (DTE oil heavy medium Mobil, number 6001638))

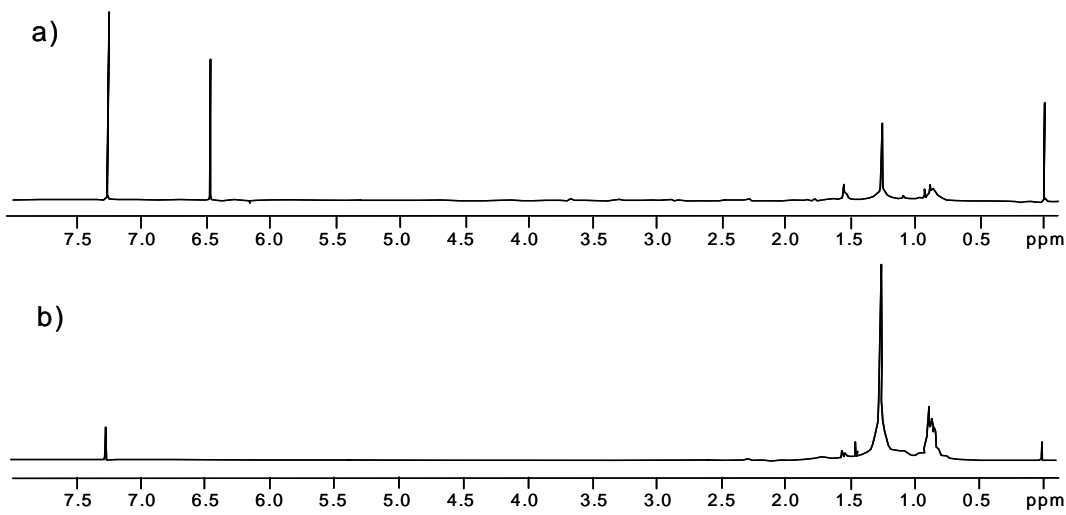


Figure 7.3: ^1H NMR spectra for SRS DNAPL (a) and TCE with hydraulic oil (b)

The ICP/MS semi-quantitative analysis of SRS DNAPL showed the presence of several metal species (Table 7.2). Despite our uncertainty in quantifying the concentrations of these elements, Table 7.2 shows the presence of elemental species that include both those that could have been derived

from subsurface minerals, as well as others that cannot be attributed to subsurface minerals. Tin and boron are the most notable elements that can be correlated to the waste disposal history during plutonium production in SRS.

Table 7.2: Detected metals in SRS DNAPL

Major elements	Si; Ca; Na; K; Fe; Cr; Al; Cu; B
Trace elements	Sn; Zn; Mn; Pb; In; Ni; Sr; Cd; Ba;

Note: Metals are listed in order of their mass concentration in the SRS DNAPL

The local mineralogy and groundwater chemistry could account for the Al, Si, Ca, Fe and probably the Zn. K and Na were also used in processing, as was boric acid. Borates are also common components of detergents (e.g. Borax). Ni, Sn and In are commonly used metals in industry for alloying, soldering and plating, which are common to many metal finishing operations.

7.3.2 Effective solubility of SRS DNAPL constituents

The SRS DNAPL was equilibrated with water to determine the effective solubility of constituents in the DNAPL. Reagent grade PCE and TCE were used as controls. The resulting aqueous phase samples were diluted and analyzed by GC/FID. Results of the solubility experiments are shown in Table 7.3. The measured solubility of pure TCE and PCE are comparable to literature values 1100 mg/kg and 200 mg/kg (Mackay, 1993), respectively. The large standard deviations resulted from the need to dilute samples prior to analysis. The standard deviations are generally ~8% of the mean, except for the TCE concentration in water equilibrated with the SRS DNAPL, where the standard deviation was 60% of the mean.

Table 7.3: SRS DNAPL solubility in water (mg/kg; mean \pm standard deviation)

	Pure PCE	Pure TCE	SRS DNAPL	
			PCE	TCE
Solubility – measured in the aqueous phase	202 \pm 16	1118 \pm 80	180 \pm 13	59.7 \pm 25
Solubility – estimated from Raoult's law	--	--	191	52.5

Mixtures of chlorinated solvents are generally assumed to behave in a thermodynamically ideal manner when equilibrated with water. That is, their activity coefficients in the organic mixture are equal to one. With this assumption, Raoult's law can be used to estimate the effective aqueous phase solubility (S_i) of a chemical constituent equilibrated with the DNAPL mixture based on the mole fraction in the DNAPL (X_i) and the pure phase solubility of this component in water (s_i) [Banerjee, 1984; Burris, 1985, Broholm, 1995].

$$S_i = X_i s_i \quad (7.2)$$

With the application of Raoult's law (eqn. 7.2) using the pure phase solubility of PCE and TCE (Table 7.3) and the measured mole fractions for the SRS DNAPL, the expected effective solubilities for these components in water were calculated and are presented in Table 6.3. The calculated solubilities are within one standard deviation of the measured, implying that Raoult's law is applicable for this DNAPL mixture. Thus, the trace constituents in the DNAPL do not solubilize the primary chlorinated solvent constituents.

7.3.3 SRS DNAPL – Interfacial properties

The surface tension of water equilibrated with the SRS DNAPL and the SRS DNAPL-water interfacial tension were significantly lower than for the PCE system used as a control (Table 7.4). pH

values before and after equilibration were also measured. These data show that the SRS DNAPL has a very low interfacial tension and high acidity. In contrast, the IFT for the reagent-grade PCE is well over an order of magnitude higher and showed no significant aqueous pH change. The measured PCE IFT is very close to published values (44.4 mN/m; Demond and Lindner, 1993), confirming the accuracy of the ring tensiometer technique.

If the SRS DNAPL was a simple mixture of PCE and TCE, its interfacial tension could be adequately estimated by the sum of the interfacial tensions of the individual constituents times their mole fractions [Seo and McCray 2002]. Based on published interfacial tension data ($\gamma_{\text{PCE}} = 44.4 \text{ mN/m}$; $\gamma_{\text{TCE}} = 34.5 \text{ mN/m}$ [Demond and Lindner, 1993]), and measured mole fractions, we would expect that the interfacial tension of a PCE/TCE mixture would be $\sim 42 \text{ mN/m}$ – which is more than an order of magnitude higher than measured for the SRS DNAPL. Thus, the minor constituents appear to contribute significantly to the interfacial behavior of this DNAPL.

Table 7.4: Surface tension of water equilibrated with the DNAPLs and water-DNAPL interfacial tensions measured with a ring tensiometer (average \pm standard deviation)

	ST (mN/m)	IFT (mN/m)	Initial pH	Eq'm pH
SRS DNAPL	39.8 ± 0.9	1.2 ± 0.2	6.3	3.8
PCE	72.8^*	44.2 ± 0.4	6.4	6.3

* published value from Demond and Linder [1993]

These results collectively indicate that a sufficient amount of surface-active species accumulate on the interface of DNAPL and water after equilibration that can significantly reduce the IFT. The solubility experimental results, however, indicate that this interfacial tension change is not due to the presence of co-solvents or certain classes of surfactants that also solubilize an organic phase.

The accumulation of surface active species at the DNAPL-water interface can be a dynamic process, limited by partitioning of species between phases or diffusion to the interface. Multiple interfacial tension measurements with DNAPL droplets suspended in DI water and DI droplets suspended in DNAPL were completed. Quantitative results are included in Figure 7.4 with photographs of the droplets over time shown in Figure 7.5.

Observation of the shape and size of the drops in these two different systems alone suggests that there are significant differences over time and as a function of the relative volumes of DNAPL and water. Stable drops of DNAPL quickly formed in water. These drops had a much lower interfacial tension (16 mN/m) than pure PCE, but higher than measured using the ring tensiometer (Table 7.4). Water droplets suspended in the DNAPL, however, showed a longer-term decrease in the IFT, with a final measured IFT (3.5 mN/m) that was much closer to results with the ring tensiometer. Figure 7.5 illustrates the significant changes in the shape of the water droplet over this time. The droplet became elongated and appeared to have a wrinkled interface.

A white precipitate was observed to form a semi-rigid film on the water droplets suspended in the DNAPL (Figure 7.5) and the DNAPL water interface in the ring tensiometers beakers – both of which had simultaneous measurements of low IFT. In contrast, no precipitate was observed on the DNAPL droplet suspended in water. Thus, it appears that the presence or composition of this precipitated material is instrumental in lowering the interfacial tension. Differences between the DNAPL droplet-in-water and water-in-DNAPL systems suggest that inorganic constituents partition from the DNAPL to the water. Though there have been reports of organic compounds adsorbing on the interfaces to change the interfacial properties [Dietz and Freiser, 1986; Shioya, 1998; Staszak and Prochaska, 2004], the role of partitioning inorganic constituents between DNAPL and water has not previously been addressed in literature describing subsurface systems. Further analysis of this mechanism is on-going.

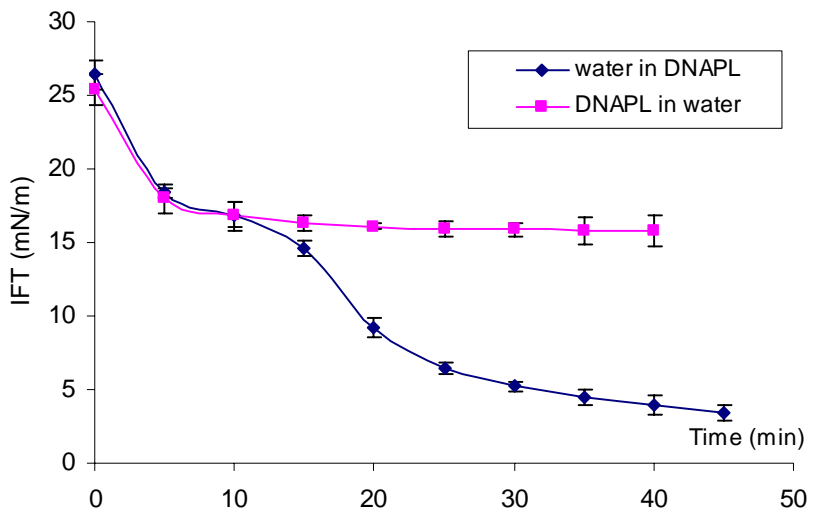


Figure 7.4: Dynamic changes of IFT between DNAPL/water over time. Error bars are standard deviation calculated from triplicate measurements.

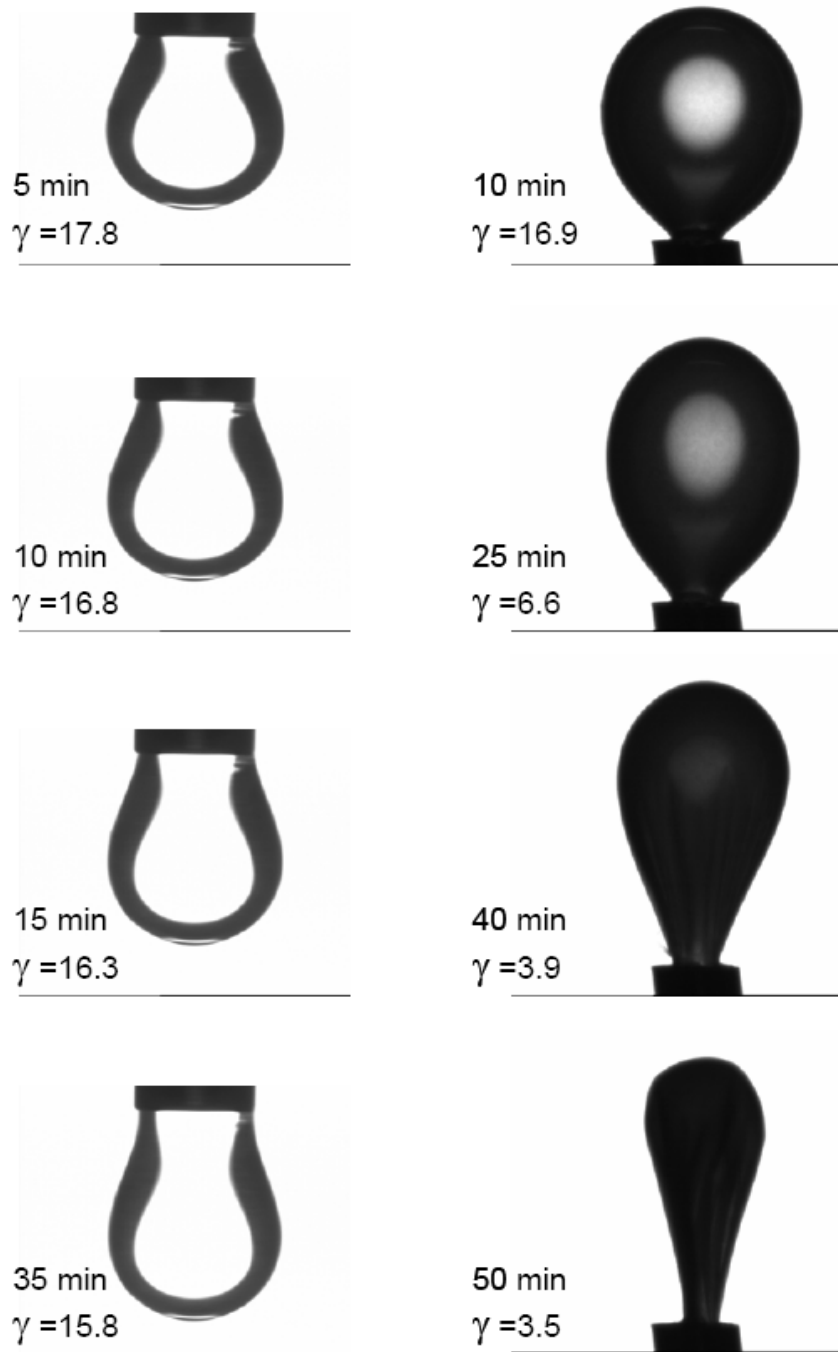


Figure 7.5: Pendant drops from tensiometer (IFT in mN/m). Left column – time series of DNAPL droplets in water show little change with time. Right column – time series of water droplets in DNAPL show more significant changes and the formation of a semi-rigid film as white precipitate (not visible in photo) accumulates at the interface.

7.3.4 Wettability

Bottle tests were used to determine the wettability of SRS DNAPL/water/soil systems since this has been an issue with other complex DNAPL mixtures [e.g., Dwarakanath, 2002]. Experiments were completed over a range of pH values and with three different porous media. In all cases, water strongly wet the soil surfaces - there were no changes in the wetting properties following exposure to the SRS DNAPL at any pH or ionic strength tested. Thus, the surface active constituents in the DNAPL did not partition to and coat the soil surfaces, at least not to the extent required to alter their surface properties.

Had a shift in wettability occurred, it would have indicated that the surface charge of two interfaces are opposite to overcome the electrostatic repulsion force between the interfaces [Zheng and Powers, 2003]. The electrophoretic mobility of the SRS soil and DNAPL (Figure 7.6) shows negatively charged surfaces for the SRS clay, sand, and DNAPL. Thus, it appears that the repulsive forces between the like-charged DNAPL and the soil were sufficient to overcome van der Waal's attractive forces to maintain the water-wetting nature of this system. The relatively high proportion of silica (isoelectric point ~ 2) contributed to the net negative charge at the sand and clay surfaces despite the presence of aluminum and iron at these surfaces.

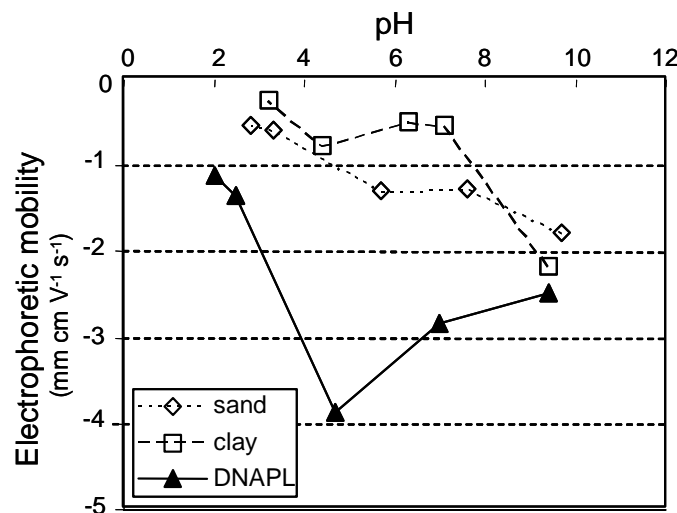


Figure 7.6: Electrophoretic mobility of SRS soils and DNAPL

7.3.5 Acidity

The observed reduction in the pH of unbuffered water equilibrated with the SRS DNAPL to pH < 4 (Table 7.4) suggests the presence of acid constituents within the DNAPL. The effect of acids on the interfacial tension depends on their nature, concentration, and distribution within the DNAPL and water system [Lord et al., 1997; Standal et al., 1999; Zheng and Powers, 2003].

The amount of acid present in the SRS DNAPL was determined by a non-aqueous potentiometric titration and expressed as an acid number. As shown in Figure 7.7, the titration curve of the SRS DNAPL shows a clear inflection point at ~ 4 mL of titrant added, corresponding to a calculated acid number of 4.1 ± 0.8 mg (as KOH)/g of DNAPL. Compared to previous studies, this amount of acid is significant and may be responsible for the low interfacial tension of the SRS DNAPL. Ovalles et al. [1998] studied the interfacial tension of a crude oil and found that an acid number of 3.7 mg KOH/g of crude oil corresponded to an IFT < 1 mN/m. Zheng and Powers [2003] showed that the interfacial tension of coal tar and creosote NAPLs decrease with increasing acid number. The highest observed acid number (3.2 mg KOH/g creosote) corresponded to an IFT < 10 mN/m. The acid content of the SRS DNAPL is higher

than others reported for crude oil, creosote or coal tar, possibly indicating that organic or inorganic acids co-disposed at the SRS M-area lagoon partitioned into the DNAPL.

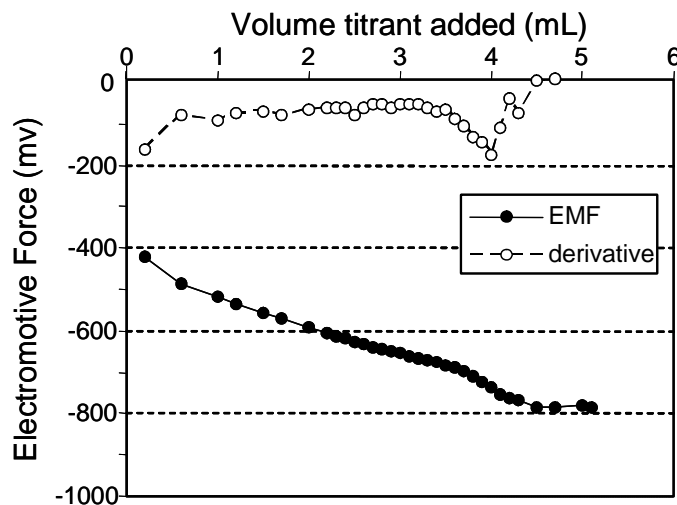


Figure 7.7: Electromotive force measured during non-aqueous titration of SRS DNAPL spiked with stearic acid. The derivative of this curve is used to determine the inflection point and acid number.

The strength of the acid can be estimated based on the electrophoretic mobility of the sample [Barbosa, 2001]. The pK_a determination is based on the principle that a solute exhibits a maximum electrophoretic mobility when it is fully ionized, a minimum electrophoretic mobility when it is fully protonated and an intermediate mobility in the regions surrounding its pK_a [Perez-Urquiza and Beltran, 2001]. The electrophoretic mobility of the SRS DNAPL showed a minimum value – or maximum protonation – at approximately pH = 4.7 (Figure 7.6). Carboxylic acids have pK_a 's in this vicinity.. The GC-MS results suggested the presence of high molecular weight carboxylic acids, such as hexadecanoic acid that could contribute to the acidity of the DNAPL. NMR analysis, however, failed to confirm the presence of protons associated with carboxylic acids. It is most likely that the concentration was insufficient for detection by this analytical technique.

7.4. Conclusions and Implication – Task 3

The composition of chlorinated hydrocarbon DNAPLs from field sites can be substantially different than the material originally purchased for use as a solvent. Disposal practices at the DOE SRS facility included co-disposal of a wide range of organic and inorganic wastes. The characterization of the DNAPL collected from the vicinity of the disposal lagoon suggests that numerous constituents partitioned into the DNAPL during its use as a solvent, co-disposal and ultimate migration through the subsurface. Trace constituents in the DNAPL include high molecular weight hydrocarbons, alkyl esters, acids, and metals from processing operations, co-disposal practices, and subsurface minerals.

This complex mixture results in DNAPL-water interfacial properties that are substantially different than would be expected from a simple mixture of PCE and TCE. Acidic components from the DNAPL partition into the aqueous phase, dropping the pH to below 4, possibly causing the precipitation and surface accumulation of inorganic precipitates. This accumulation could contribute to the interfacial tension that is over an order of magnitude lower than expected for a PCE/TCE mixture. Other surface active constituents in the DNAPL could also contribute to low IFT. The specific mechanisms contributing to this are currently under investigation.

The extreme low interfacial tension between the SRS DNAPL and water substantially lowers the entry pressure of the DNAPL allowing it to enter to the fine soil pores of the vadose zone that typically have a higher moisture content than coarser layers. The small pores and high soil water content jointly

decrease the air permeability in the region, resulting in reduced contact between the DNAPL contamination and any fluids used for remediation [Yoon, 2002]. This can directly reduce the effectiveness of remediation efforts such as SVE.

The low surface and interfacial tension will alter the migration and entrapment of the DNAPL in the subsurface. Decreasing the interfacial tension between a DNAPL and water in the vadose zone could alter a non-spreading DNAPL, such as PCE, into a spreading NAPL [McBride, 1992]. This change in the distribution of the DNAPL as pendular rings towards a system where the DNAPL forms a thin film over the water-wet porous media would increase the surface area for mass transfer. However, at the same time, the low IFT would enable the DNAPL to enter pore spaces that are an order of magnitude smaller and become entrapped in low permeability regions of the subsurface. Both of these changes in the distribution of the DNAPL would affect remediation techniques such as SVE. The presence of the DNAPL in low permeability lenses could have contributed to SVE efforts at SRS that were not as successful as anticipated [Rohay, 1999].

7.5 Acknowledgements

This research was supported by the Office of Science (BER), U.S. Department of Energy, Grant No. DE-FG02-03ER63660. Chemical analysis was supported by the Clarkson University Center of Air Resources Engineering and Science. This paper is #XXX in the Clarkson Center for the Environment paper series.

7.6 References

ASTM. Standard test method for interfacial tension of oil against water by the ring method. Designation D 971-91, ASTM International, West Conshohocken, Pennsylvania, USA, 1991

ASTM Standard Test Method for Acid Number of Petroleum Products by Potentiometric Titration. Designated D 664-95, ASTM International, West Conshohocken, Pennsylvania, USA, 1995

Banerjee S. Solubility of Organic Mixtures in Water. *Environ. Sci. Technol.* 1984: 18:587–591

Barbosa, J.; Barron, D.; Jimenez-Lozano, E.; Sanz-Nebot, V. Comparison Between Capillary Electrophoresis, Liquid Chromatography, Potentiometric and Spectrophotometric Techniques for Evaluation of pK_a Values of Zwitterionic Drugs in Acetonitrile–Water Mixtures. *Analytica. Chemica. Acta.* 2001, 437, 309-321

Barranco, F.T.; Dawson, H.E. Influence of aqueous pH on interfacial properties of coal tar. Influence of Aqueous pH on the Interfacial Properties of Coal Tar. *Environ. Sci. Technol.* 1999, 33, 1598-1603

Becker, J.S. Inductively Coupled Plasma Mass Spectrometry (ICP-MS) and Laser Ablation ICP-MS for Isotope Analysis of Long-Lived Radionuclides *International Journal of Mass Spectrometry* 2005, 242: 183–195

Broholm K, Feenstra S. Laboratory Measurements of the Aqueous Solubility of Mixtures of Chlorinated Solvents. *Environ Toxicol Chem.* 1995, 14:9–15

Bruss, D. B., and G. E. A. Wyld. Methyl Isobutyl Ketone as Wide-Range Solvent for Titration of Acid Mixtures and Nitrogen Bases. *Anal. Chem.* 1957, 29: 232–235

Buckley, J.S.; Takamura, K. and Morrow, N.R. Influence of Electrical Surface Charges on Wettability Properties of Crude Oils. *SPE Reservoir Engineering*, 1989: 332-340

Buckley, J.S.; Liu, Y.; Xie, X. and Morrow, N.R. Asphaltenes and crude oil wetting - The effect of oil composition. *SPEJ*, 1997: 107-119

Burris DR, MacIntyre WG. Water Solubility Behavior of Binary Hydrocarbon Mixtures. *Environ Toxicol Chem.* 1985 4:371–377

Cai, L.S.; Koziel, J.A.; Davis, J.; Lo, Y.C. and Xin, H.W. Characterization of Volatile Organic Compounds and Odors by In-vivo Sampling of Beef Cattle Rumen Gas, by Solid-Phase Microextraction, and Gas Chromatography-Mass Spectrometry-Olfactometry. *Analytical and Bioanalytical Chem.* 2006, 386 (6): 1791-1802

Crump, S. Memo to J. Rossabi (WSRC): GC/MS Analytical Results for M-Area Seepage Basin DNAPL. April 17, 1997

Demond, A.H.; Lindner, A.S. Estimation of Interfacial Tension between Organic Liquids and Water *Environ. Sci. Technol.* 1993, 27(12): 2318-2331

Dietz, M.L. and Freoser, H. Adsorption of Neutral Metal Chelates at Liquid-Liquid Interfaces *Langmuir* 1987, 3: 467-470

Durand, C.; Ruban, V.; Ambles, A. ; et al. Characterization of the Organic Matter of Sludge: Determination of Lipids, Hydrocarbons and PAHs from Road Retention/Infiltration Ponds in France. *Environmental Pollution* 2004, 132 (3): 375-384

Dwarakanath, V.; Jackson, R. E.; Pope, G. A. Influence of Wettability on the Recovery of NAPLs from Alluvium. *Environ. Sci. Technol.* 2002, 36(2): 227-231

Falta, R.W. Using Phase Diagrams to Predict the Performance of Cosolvent Floods for NAPL Remediation, *Ground Water Monitoring and Remediation* 1998, 18(3): 94-102

Harrold, G.; Goody, D.C.; Lerner, D.N.; and Leharne, S.A. Wettability Changes in Trichloroethylene-Contaminated Sandstone. *Environ. Sci. Technol.* 2001, 35: 1504-1510

Harrold, G.; Goody, D. C.; Reid, S.; Lerner, D. N.; Leharne, S. A. Changes in Interfacial Tension of Chlorinated Solvents following Flow through U.K. Soils and Shallow Aquifer Material Changes in Interfacial Tension of Chlorinated Solvents following Flow through U.K. Soils and Shallow Aquifer Material. *Environ. Sci. Technol.* 2003, 37(9):1919 -1925

Hirasaki, G.J. Wettability: Fundamentals and Surface Forces. *SPE Formation Evaluation*, 1991: 217-226

Imhoff, P.T.; Simon, N.G.; McBride, J.F.; Vancho, L.A., Okuda, I. and Miller, C.A. Cosolvent-Enhanced Remediation of Residual Dense Nonaqueous Phase Liquids: Experimental Investigation. *Environ. Sci. Technol.* 1995, 29: 1966-1976

Lee, E.; Tai, C.S., Hsu, J.P. and Chen, C.J. Electrophoresis in a Carreau Fluid at Arbitrary Zeta Potentials. *Langmuir*, 2004, 20: 7952-7959

Looney, B.B., et.al. Assessing DNAPL Contamination, A/M-Area, Savannah River Site: Phase I Results Westinghouse Savannah River Company, Aiken, SC. 1992 WSRC-RP-92-1302

Lord, D.L.; Hayes, K.F.; Demond, A.H.; Salehzadeh, A. Influence of Organic Acid Solution Chemistry on Subsurface Transport Properties. 1. Surface and Interfacial Tension Influence of Organic Acid Solution Chemistry on Subsurface Transport Properties, 1. Surface and Interfacial Tension. *Environ. Sci. Technol.* 1997, 31(7): 2045-2051

Mackay, D., W-Y Shiu, and K-C Ma. 1993. *Illustrated Handbook of Physical-chemical Properties and Environmental Fate for Organic Chemicals: Vol. III Volatile Organic Chemicals*. Lewis Publishers. Ann Arbor, Michigan.

McBride, J. F.; Simmons, C. S.; and Cary, J. W. Interfacial Spreading Effects on One-dimensional Organic Liquid Imbibition in Water-Wet Porous Media. *J. Contam. Hydrol.*, 1992, 11: 1-25

Ovalles, C.; Garcia, M.; Lujano, E.; Aular, W.; Bermudez, R.; Cotte, E. Structure/Interfacial Activity Relationships and Thermal Stability Studies of Cerro Negro Crude Oil and its Acid, Basic and Neutral Fractions. *Fuel* 1998, 77: 121-126.

Pennell, K.D., Minquan, J., Abriola, L.M. and Pope, G.A., Surfactant Enhanced Remediation of Soil Columns Contaminated by Residual Tetrachloroethylene. *J. Contam. Hydrol.* 1994, 16: 35–53

Perez-Urquiza, M.; Beltran, J.L. Determination of the Dissociation Constants of Sulfonated and Dyes by Capillary Zone Electrophoresis and Spectrophotometry Methods. *J. Chromatography A.* 2001, 917: 331-336.

Pfeiffer, P.R.; Bielefeldt, A.R. et. al. Physical Properties of Vegetable Oil and Chlorinated Ethene Mixtures. *J. Environ. Engin.* 2005, 10: 1447-1450

Pickett, J.B.; Colven, W.P.; Bledsoe, H.W. Environmental Information Document: M-Area Settling Basin and Vicinity. DPST-85-703. Report prepared for the U.S. DOE, 1985.

Powers, S.E.; Anckner, W.H.; and Seacord, T.F. The Wettability of NAPL-Contaminated Sands. *J. Environ. Engin.* 1996 122(10): 889-897

Rohay, V. J. et. al..(1999) Performance Evaluation Report for Soil Vapor Extraction Operations at the Carbon Tetrachloride Site, February 1992 - September 1998

Rossabi, J.; Riha, B.D.; Haas III, J.W.; Eddy-Dilek, C.A.; Lustig Kreeger, A.G.; Carrabba, M.; Hyde, W.K.; Bello, J. Field Tests of a DNAPL Characterization System Using Cone Penetrometer-based Raman Spectroscopy. *Ground Water Monitor. Remed.* 2000, 20: 72-81.

Saba, T.; Illangasekare, T.H. and Ewing, J. Investigation of Surfactant-Enhanced Dissolution of Entrapped Nonaqueous Phase Liquid Chemicals in a Two-Dimensional Groundwater Flow Field. *J. Contam. Hydrol.* 2001, 51: 63-82

Seo, J. and Lee, L. P. Effects on Wettability by Surfactant Accumulation/Depletion in Bulk Polydimethylsiloxane (PDMS). *Sensors and Actuators B-chemical*, 2006, 119 (1): 192-198

Shioya T. Nishizawa, S. and Teramae, N. Complexation of 5-Alkyloxymethyl-8-quinolinolins at Liquid-Liquid Interfaces As Studied by Dynamic Interfacial Tensiometry. *Langmuir* 1998, 14: 4552-4558

Soe, H.S.; McCray, J.E. Interfacial Tension of Chlorinated Aliphatic DNAPL Mixtures as a Function of Organic Phase Composition. *Environ. Sci. Technol.* 2002, 36(6): 1292-1298.

Standal, S.; Haavik, J.; Blokhus, A.M.; Skauge, A. Effect of Polar Organic Components on Wettability as Studied by Adsorption and Contact Angles. *J. Petrol. Sci. Eng.* 1999, 24: 131-144.

Standal S. H., T. Barth, A. M. Blokhus, and A. Skauge The Effect of Crude Oil Acid Fractions on Wettability as Studied by Interfacial Tension and Contact Angles. *J. Petrol. Sci. and Eng.*, 2001 (30): 91-104

Staszak, K. and Prochaska, K. Interfacial Activity of Copper(II) Complexes with Chelating Ligands and Individual Hydrophobic Extractants in Model Extraction Systems I. Study of Equilibrium Interfacial Tension at the Hydrocarbon/Water Interface for Systems with Copper(II) Complexes with Chelating Ligands and Individual Hydrophobic Extractants. *J. of Colloid Interface Sci.* 2004, 280: 184-191

Strand, S.; Hognesen E. J. and Austad T. Wettability Alteration of Carbonates—Effects of Potential Determining Ions (Ca^{2+} and SO_4^{2-}) and Temperature. *Colloids and Surfaces A: Physicochem. Eng. Aspects*, 2006, 275: 1–10

Totsche, K.U.; Kogel-Knabner, I.; Haas, B.; Geisen, S. and Scheibke, R. Preferential Flow and Aging of NAPL in the Unsaturated Soil Zone of a Hazardous Waste Site: Implications for Contaminant Transport. *J. of Plant Nutrition and Soil Science*, 2003, 166 (1): 102-110

Van Valkenburg, M.E. and Annable, M.D. Mobilization and Entry of DNAPL Pools into Finer Sand Media by Cosolvents: Two-Dimensional Chamber Studies. *J. Contam. Hydrol.* 2002, 59: 211-230

Yoon, H., Kim, J.H., Liljestrand, H.M., et al. Effect of Water Content on Transient Nonequilibrium NAPL-gas Mass Transfer During Soil Vapor Extraction. *J. Contam. Hydrol.* 2002, 54 (1-2): 1-18

Zheng, J.; Powers, S. E. Organic Bases in NAPLs and their Impact on Wettability. *J. Contam. Hydrol.* 1999, 39, 161-181

Zheng, J.; Powers, S.E. Identifying the Effect of Polar Constituents in Coal-Derived NAPLs on Interfacial Tension. *Environ. Sci. Technol.* 2003, 37, 3090-3094

8.0 Mechanisms for interfacial tension reductions in the presence of metals and metal-ligand complexes (Task 4)

8.1 Introduction

DNAPLs (dense non-aqueous phase liquids) have been widely used in a variety of industrial and cleaning processes since the 1930s. Frequent spills, leakage from underground storage tanks, and disposal to the ground by industrial users, coupled with their unique physicochemical properties, render chlorinated solvents one of the most common and insidious sources of groundwater contamination [Mackay, 1989; Lohman, 2002].

DNAPLs are a significant contributor to groundwater contamination. The behavior of DNAPL in the subsurface is very complex, depending on the spill history, DNAPL properties and geologic heterogeneity. This renders efforts to locate the DNAPL in the subsurface and subsequent remediation of these sites difficult and, consequently, results in a long-term contamination source of groundwater. When spilled, the DNAPL will travel vertically through the subsurface due to gravity. Heterogeneities in grain size or moisture content can cause significant horizontal flow of the DNAPL. This occurs when the DNAPL does not have sufficient head to overcome the entry pressure of a fine-grained or water saturated region of the unsaturated zone. The DNAPL pressure required to overcome the pore entry pressure of a geological layer is defined through the Young-Laplace equation as a function of the DNAPL interfacial tension (IFT), system wettability and the distribution of the pore radii. For a given pore size, the entry pressure is lower for systems that are not strongly water wetting or for DNAPLs that have low interfacial tensions. For these cases, the DNAPL can more readily infiltrate into low permeability regions of the subsurface.

A low interfacial tension, which has been widely reported for NAPLs recovered from the subsurface [Powers, 1996; Harrold, 2001; Dwarakanath, 2002, Dou et al., 2007], will enhance the mobility of the NAPL and hence is not favorable for remediation efforts. Our previous study showed that a DNAPL from U.S. Department of Energy (DOE) Savanna River Site (SRS) has a very low interfacial tension (less than 3 mN/m) [Dou et al., 2007]. It also contains an array of higher molecular weight organic compounds and metals, and has a high acidity. Current understanding of the constituents within the DNAPL and mechanisms contributing to the low interfacial tension is lacking. The low interfacial tension could result from surfactants or some other surface-active chemicals or particles absorbed on the interface. This paper presents a laboratory study designed to explore factors contributing to low interfacial tensions. The literature cited below was used as a basis to identify potential mechanisms that could lead to significant reductions in IFT.

DOE sites such as SRS have a long history of co-disposal of many types of industrial wastes, including an array of surfactants and ligands. Tributyl phosphate (TBP) and dibutyl butylphosphonate (DBBP) have been identified by the DOE [Riley, 1992] as representative compounds in the class of alkyl phosphates. They are widely used for metal extraction and as antifoaming agents [Jha et al, 1999] due to their surfactant and solvent properties. The effectiveness of TBP in metal extraction is increased by its capability of increasing the partitioning of acidic molecules such HNO_3 from the aqueous phase into the oil phase [Baaden et al, 2001a]. TBP has a surface tension of 27 mN/m, an acid number ≤ 0.05 mg KOH/g [Bayer TIB, 2003], is biodegradable [Thomas and Macaskie, 1996], and can undergo a hydrolysis in the presence of a strong acid leading to the formation of dibutyl ether and dibutyl phosphoric acid [Stoyanov, 1997]. The surface activity the TBP at the oil/water interface depends on its concentration and the acidity of the aqueous phase [Baaden et al, 2001b]. DBBP is another colorless to light-yellow liquid. It exhibits a synergistic effect with TBP, so they are commonly used together for the extraction of heavy metals [D'Olieslager et al, 1985]. The polarity of TBP and DBBP or their protonation could lead to their adsorption to surfaces in the subsurface, thereby reducing the interfacial tension.

Several researchers showed that some metal-ligand complexes used in liquid-liquid extraction process can adsorb on the interface or partition into the organic phase and reduce the interfacial tension of the system [Dietz and Freiser, 1986; Staszak and Prochaska, 2004; Shiya, 1998; Sengupta, 1999; Prochaska and Staszak, 2005]. The extent of this partitioning depends on the solubility of the metal complex in the two phases. With the existence of chelating agents and/or ligands that were used during the degreasing or some other industrial operations, metal ions may partition into the bulk DNAPLs as hydrophobic metal-ligand complexes.

Besides co-disposal, another possible source of chelating agents or ligands may be the natural water system. Turner et al. (2004) reported the hydrophobicities of dissolved Al, Cu, Mn, and Pb in natural water and their octanol-water partitioning coefficients. The ligands used in the experiment were salicylic acid, ethylxanthic acid and oxine that are possibly present in natural water after been used for industry or agriculture purpose. Oxine copper (cupric 8-quinolinoxide), for example is a fungicide used extensively for preserving wood, paper and seeds. Although highly non-soluble in water, it is found with increasing frequency in environmental systems. The results showed that metals might become hydrophobic either by neutralizing relatively hydrophilic ligands or by combining with ligands that are intrinsically hydrophobic themselves. The hydrophobicity was characterized by their partitioning into the organic phase octanol.

The connection between metal-ligand complexes in the environment and DNAPL-water interfacial tension has not been established or studied adequately to date. The most closely related study was published by Harrold et al. [2005], who showed that a chlorinated solvent mixture, which contained a surfactant additive and which had been in contact with a sandstone core containing goethite (Fe_2O_3), had an extremely low interfacial tension. The evidence suggested that the exposure to sandstone and goethite, particularly the detachment of iron oxide particles from the sandstone surface, was instrumental in creating this low IFT system. It would seem clear that the role that additives might play in TCE DNAPL transport and fate in the sub-surface environment can be substantially attenuated through interactions between the additives and mineral surfaces. Harrold et al. [2005] did not investigate the role of iron species alone without the surfactant additive.

The chlorinated solvent DNAPL from the SRS has an extreme interfacial tension (< 3 mN/m) (Dou et al., 2007). A semi-rigid film which was observed to form at the DNAPL-water interface could lower the interfacial tension. Similar interfacial films have been observed by other studies with crude oil [Sun, 2003], coal tar [Luthy, 1993] and field waste TCE sample [Harrold, 2001]. In the case of crude oil, these films are the result of the adsorption of high molecular weight polar molecules at the crude oil-water interface [Sun, 2003]. The investigations by Nelson et al. [1996] concluded that the formation of an interfacial film on coal tar-water interface was due to weak, reversible bonding between water molecules and the coal tar constituents. No investigations have been carried out with the film formed on the interface of chlorinated hydrocarbon DNAPLs and water.

Based on the known disposal history and preliminary observations, it is the hypothesis in this research that the interfacial tension of the SRS DNAPL could have been substantially altered by the presence of other constituents in the waste or subsurface, including:

- Surfactants,— especially TBP, DBBP
- The formation of metal- organic ligand complexes that partition between DNAPL and water and accumulate at the interface
- Metal precipitates that accumulate and/or react at the DNAPL/water interface

The objective of the research here was to thoroughly investigate these mechanisms to identify their potential for altering the IFT of chlorinated solvents. An experimental plan was developed to isolate these mechanisms and consider them independently to the extent possible.

8.2 Materials and Methods

8.2.1 Overview

The experimental plan (Table 8.1) included conditions necessary to test the three hypothesized mechanisms presented above. Variables and controls were defined to isolate these mechanisms to determine their impact on the DNAPL-water interfacial tension. Supplemental analyses were designed to confirm the phenomena. Tetrachloroethene (PCE) and trichloroethylene (TCE), as typical chlorinated solvents, were used in our experiment as surrogate DNAPLs. Oxine was identified as a suitable ligand due to its hydrophobicity and environmental relevance (Turner et al., 2004). Iron and copper were employed as metals because they are common in industrial processes and iron also ubiquitous in mineral systems. Copper is a relatively simple species in aqueous systems, whereas iron exists in numerous different mineral and hydroxide species with both Fe(II) and Fe(III) oxidation states found under environmental conditions. The investigation of the role of metal hydroxide precipitates on the IFT identified an additional possible mechanism that was also investigated – dechlorination reactions enabled by iron oxidation.

Vials which were used for metal experiments were acid cleaned in a 4 N HNO₃ solution, and then together with other vials, were put in a muffle furnace at 400 °C for 4 hours to burn off the residual organic compounds. All the experiments were performed as duplicates or triplicates for quality control purposes.

Table 8.1: Overall plan for research

Mechanism	Variables	Controls	Measurements
Surfactants	Surfactant type and concentration <ul style="list-style-type: none">• TBP• DBBP	DI water	IFT
Metal-ligand complexes	Type and concentration <ul style="list-style-type: none">• Cu-Oxine• Fe-Oxine	DI water Cu alone Fe alone	IFT Equilibrium PCE concentration
Metal precipitates	Type and concentration: <ul style="list-style-type: none">• Fe(II)• Fe(III)	DI water	IFT pH SEM-EDS of film
Dechlorination	Concentration: <ul style="list-style-type: none">• Fe(II)	DI water Fe(III) Other chlorinated and non-chlorinated solvents	IFT PCE degradation

8.2.2 Chemicals

Organic solvents used in this study included tetrachloroethene (PCE, 99%, Acros), trichloroethene (TCE, 99%, Acros), toluene (99%, J.T. Baker), 3-chlorotoluene (3-CT, 98% GC, TCI), 4-chlorotoluene (4-CT, 98%, TCI), and n-heptane (99.9%, HPLC grade, FisherChemicals). Ligands and surfactants used included 99% tributylphosphate (Sigma Aldrich Co), 90% dibutyl butylphosphonate (Sigma Aldrich Co), and 8-hydroxyquinoline (Oxine, 99%, Alfa Aesar). Metal salts are ferric chloride (99%, FisherChemicals), ferrous chloride (4-hydrated, 99%, FisherChemicals), and copper chloride (anhydrous, 98%, Alfa Aesar). The water used in this study was all de-ionized. The properties of the organic solvents used are listed in Table 8.2.

Table 8.2: Properties of organic solvents tested

Property	PCE	TCE	n-Heptane	Toluene	3-Chlorotoluene	4-Chlorotoluene
Solubility (mg/l)	200 ¹	1,100 ¹	2.78 ²	543 ²	19 ³	106 ⁴ ; 40 ⁵
Interfacial tension (mN/m)	47 ⁶	35 ⁶	52 ²	34 ²	52 ³	45 ⁶

References: 1: Mackay, 1993; 2: Derived from Demond and Linder, 1993; 3: Basak, 2005; 4: Kemp, 2001; 5: Schlottmann, 2005; 6: Measured in this study.

8.2.3 Methods

Interfacial tension measurements

All interfacial tension values were measured using an OCA 15+ drop shape analyzer (Dataphysics Company, Bethpage, NY). This type of instrument has been widely adopted in laboratories for interfacial tension, contact angle and wettability studies [del Rio et al., 1997; Harrold et al., 2005; Sztukowski and Yarranton, 2005]. The CCD digital camera [Teli, Toshiba, Japan] captured the shapes of drops. Once captured, the profile was extracted and numerically fitted to the Young-Laplace equation [del Rio et al., 1997] using SCA10 software to generate the interfacial tension values automatically.

A detailed experiment procedure used for interfacial tension measurement can be found in literature [Harrold et al., 2003]. The interfacial tension measurements commenced by dispensing an aqueous drop into the organic phase. Initial experiments showed that changes in the interfacial tension are more significant for this method versus dispensing organic phase droplet into aqueous phase. Both an upright or U-shape needle and a straight needle were used, depending on the density of the organic phase relative to the density of water. The interfacial tension between PCE and DI water was measured each day of analysis as quality control. The IFT measurement errors were within the range of ± 0.4 mN/m.

Dechlorination experiments

The experimental set-up to determine if PCE is dechlorinated in the presence of Fe(II) was adapted from the methods reported by Hwang et al. [2005] and Liu et al. [2006]. The samples were prepared in the atmospheric environment at room temperature ($\sim 23.5^\circ\text{C}$). Stock solutions were prepared by adding 20 μL of PCE to 200mL DI to make PCE concentration close to 100 ppm. The actual concentration was determined by GC-FID with headspace sampler. An ultrasonic cleaner (Aquasonic Model75T, VWR Scientific) was used to help dissolve the PCE in water. After the PCE dissolved, ferric or ferrous chloride was added to duplicate bottles to make a 0.01 mol/L metal cation solution. Water with PCE but no iron was used as a control.

Solutions from the 200-mL vials were transferred to borosilicate glass vials (12ml) with crimp tops for use as reaction vessels. The vials were completely filled with solutions to minimize gas phase partitioning of PCE. Duplicate samples were prepared and triple GC headspace sample were made from each vial. Sets of vials were analyzed at 5 day increments for a total of 30 days. No pH buffers were added to the vials but pH values were monitored at every sample time. PCE concentrations were analyzed on GC-FID equipped with headspace sampler. The experiment was performed at room temperature (25°C).

Analytical methods

PCE concentrations: A Hewlett Packard HP 5890 Series II gas chromatography (GC) with a Flame Ionization Detector (FID) and an Agilent HP7694E Headspace Sampler was used for organic compound analysis. The GC was equipped with a 60m long, 0.25mm inside diameter with $0.25\mu\text{m}$ film

Supelco Vocol TM column. Highly purified helium was used as the carrier gas and an air-hydrogen mixture as flame gas. The following conditions were employed for our experiments: an inlet temperature of 250°C, detector temperature of 300°C, and initial column temperature of 80°C maintained for 2 minutes followed by a rate of 6°C/min increase until 180°C was reached. This temperature was maintained for 2 minutes. Two-ml samples were placed in 5-ml headspace vials with Teflon lined septa and aluminum crimp caps. DI water was used as blanks. The detection limit of this method was 2 ppm for PCE.

SEM-EDS: Due to its quick and effective characteristics, scanning electron microscopy and energy dispersive spectrometer (SEM-EDS) has been used widely to identify metal species [Liu, 2006]. SEM/EDS (JSM 6300 by Japan Electron Optics Laboratory) was employed in this study to analyze precipitated particles that accumulated at the DNAPL-water droplet interface. The EDS technique identifies and quantifies elemental constituents of the sample. Two particle samples were collected from the needle tip resulting from the suspension of aqueous solutions (0.01 mol/L FeCl_3 and 0.01 mol/L FeCl_2) in PCE. The samples were then coated with gold for analysis.

pH measurements: All pH values were measured with an Orion 525A⁺ pH, mV, ORP, Temperature Meter with a standard size glass double-junction combination electrode (Accumet). Before every measurement, the pH meter was calibrated using 3 buffer solutions, pH 4.01, 7.00 and 10.01 respectively (Fisher Scientific). The measurement followed EPA standard method 9040B pH electrometric measurement. Each measurement as duplicated and the average value calculated.

8.4 Results and Discussion

8.4.1 Surfactants

Interfacial tensions measured for TCE containing the DOE-relevant surfactants DBBP and TBP are shown in Figure 8.1. The short error bars, which represent one standard deviation, indicate reproducible results. The interfacial tension measured for pure TCE was 34.9 mN/m with a standard deviation of 0.1 mN/m, which is quite comparable with the reported value of 34.5mN/m [Demond and Lindner, 1993]. The TCE/water interfacial tension decreased as much as 28% with TBP and 33% with DBBP, both at a concentration of 7% by weight. This shows that these additives do impact the interfacial tension, but not as substantially as observed for DNAPLs collected from some field sites.

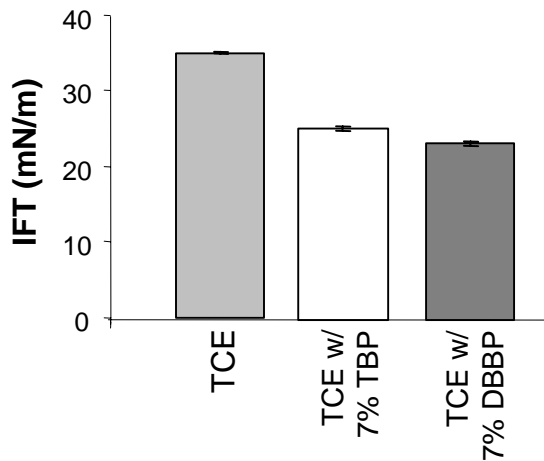


Figure 8.1: Interfacial tension of TCE/water with surfactants TBP and DBBP.

8.4.2 Metal-Oxine Complexes

According to our hypothesis, it is expected that certain ligand-metal complexes will partition between organic and aqueous phases, and accumulate at the interface, thereby reducing the interfacial tension. Such ligand-metal complexes would have relatively high octanol-water partition coefficient so

they partition from the aqueous phase to the organic phase. Oxine was chosen as a test ligand since it has a high octanol-water partition coefficient (36.4 in natural waters) [Turner and Mawji, 2004].

The matrix in Table 8.3 shows the variables and results for experiment with copper as the metal ion. The incipient precipitation pH for oxine-Cu complex is about 2.3 [Martell & Calvin, 1952], the pH value of most of the aqueous phases in this experiment was adjusted to less than this value using diluted HCl. Those that have higher values were set for comparison purposes.

The organic and aqueous phases were equilibrated on a rotator overnight before interfacial tension analysis. After equilibration, it was observed that the colorless organic and aqueous phases both changed to green/yellow for all the systems containing both oxine and Cu(II). This indicates the formation of the oxine-Cu complex [Giraudi, 1999].

Measured interfacial tension values for PCE and water in the presence of Cu-oxine are given in Table 8.3 and shown in Figure 8.2. Generally, interfacial tension values of samples with high oxine concentrations (#7, 13, 15) are lower than other samples and are statistically different than the controls. This indicates that the oxine and oxine-Cu complex are interfacially active at a high concentration. However, from a DNAPL migration perspective, none of the measured interfacial tensions were substantially decreased, even those systems with observable Cu-oxine complex precipitates at interface (#13, 15). The results from control samples sample 1 and sample 2 show that pH alone does not have an effect on the interfacial tension of PCE and water. The pH changes after equilibration were due to the oxine chemistry.

Fe-oxine complexes were also evaluated to determine their impact on interfacial tension. The matrix of experiments completed with iron oxine complexes is shown in Table 8.4. After introducing an iron-contaminated aqueous solution with an oxine-contaminated PCE solution, the two phases separated well and the interfaces were clearly seen. However, both phases changed to a green/yellow color, indicating that the oxine-Fe complex had been formed.

Table 8.3: Variable matrix of Oxine-Cu interfacial tension experiment

No.	Oxine (mol/l)	Cu(II) (mol/l)	Initial Aqueous pH	Final Aqueous pH	Equilibrated IFT (mN/m)	P-value
1	0	0	8.34	8.13	47	-
2	0	0	2.15	2.14	47	0.960
3	0	0.5×10^{-4}	2.03	2.08	46	0.156
4	0	0.5×10^{-2}	2.03	2.08	47	0.189
5	10^{-4}	0	2.04	2.06	46	0.109
6	10^{-2}	0	2.04	2.05	46	0.034
7	10^{-1}	0	2.04	3.98	38	0.000
8	10^{-4}	0.5×10^{-4}	2.03	2.13	45	0.527
9	10^{-4}	0.5×10^{-2}	2.05	2.13	46	0.410
10	10^{-2}	0.5×10^{-4}	2.03	2.68	45	0.003
11*	10^{-2}	0.5×10^{-2}	2.03	2.01	45	0.001
12	10^{-1}	0.5×10^{-4}	2.02	4.00	41	0.000
13*	10^{-1}	0.5×10^{-2}	2.03	3.59	36	0.000
14	10^{-1}	0.5×10^{-4}	6.43	7.64	40	0.000
15*	10^{-1}	0.5×10^{-2}	5.94	3.59	35	0.000

Notes:

1. *: Precipitates were observed on interface for samples 13 and 15

2. A p-value less than or equal to 0.05 (see bold entries) indicates that the sample is statistically different than the control (samples 1 and 2) at 95% level; a p-value larger than 0.05 indicates that there is not a statistically significant difference at this level.

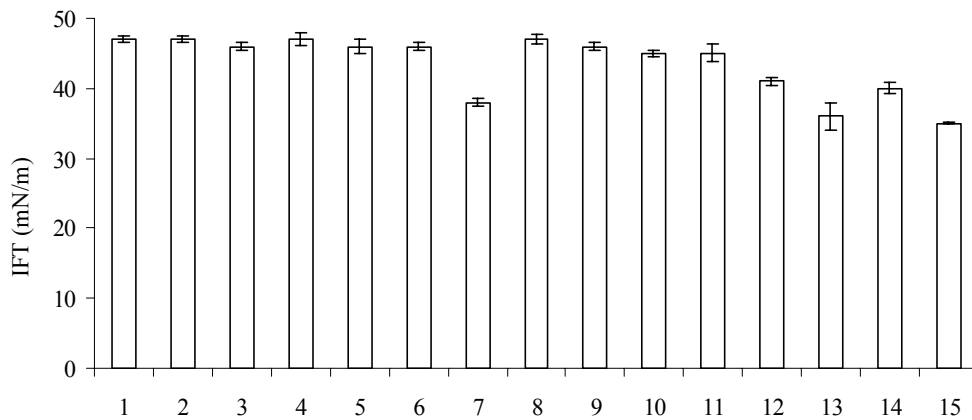


Figure 8.2: Interfacial tension of PCE (with oxine) and water (with Cu(II)). The interfacial tensions were measured 20 minutes after the drops dispense in order for the equilibration of the two phases. Sample numbers are defined in Table 3.

Table 8.4: Variable matrix of Oxine-Fe interfacial tension experiment

No.	Oxine (mol/l)	Fe(III) (mol/l)	Initial Aqueous pH	Final Aqueous pH	Equilibrated IFT ((mN/m)	p-value
1	0	0	5.83	5.86	47	-
2	10^{-4}	0	5.78	5.69	47	0.932
3	10^{-2}	0	5.81	5.79	46	0.216
4	0	10^{-2}	2.44	2.43	38	0.001
5	0	10^{-4}	3.78	3.82	43	0.003
6	10^{-4}	10^{-4}	3.78	7.44	44	0.007
7	10^{-2}	10^{-4}	3.78	7.32	44	0.017
8	10^{-4}	10^{-2}	2.44	2.20	44	0.016

Notes:

1. Interfacial tensions were measured at 20 mins after drops dispensed.
2. A p-value less than or equal to 0.05 (see bold entries) indicates that the sample is statistically different than the control (samples 1 and 2) at 95% level; a p-value larger than 0.05 indicates that there is not a statistically significant difference at this level.

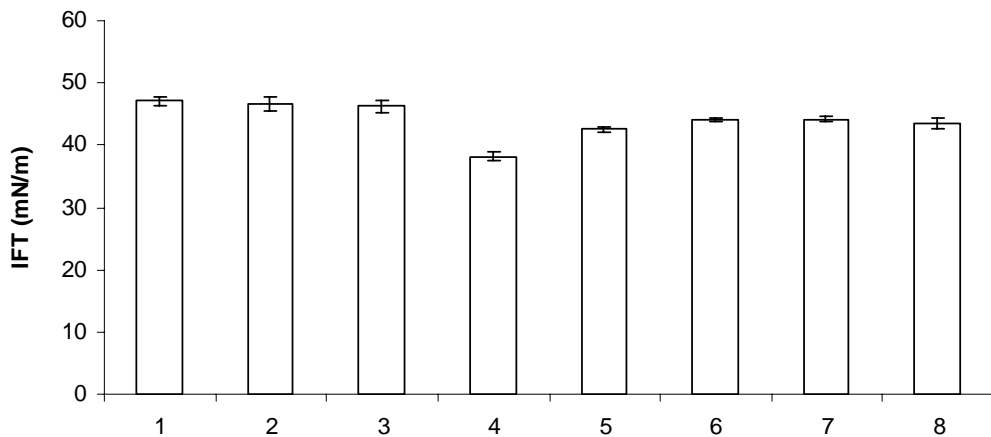


Figure 8.3: Interfacial tension of PCE (with oxine) and water (with Fe(III)). The interfacial tensions were measured 20 minutes after the drops dispense in order for the equilibration of the two phases. Sample numbers are defined in Table 2.

Figure 8.3 shows the results of this experiment. The interfacial tension of systems with oxine-Fe complexes were all close to or greater than 40 mN/m, indicating that, although the changes were statistically different from the control ($\alpha=0.05$), there was very little change from a physically relevant perspective. The lowest measured IFT was with Fe(III) alone, without the oxine ligand, suggesting that the ferric cation and ferric hydroxide species could affect IFT. In this sample (#4), a film-like skin was observed surrounding the aqueous drop. Longer drop equilibration times resulted in the more substantial deposition of solid particulates and the near complete disappearance of the aqueous phase droplet. This will be expanded below.

PCE solubility experiments in the presence of oxine and metals (Cu and Fe) were conducted to investigate the effect of metal-oxine complex on NAPL dissolution in the aqueous phase. Based on the visible presence of hydrophobic metal-ligand complexes, the potential for colloid-facilitated transport was considered [e.g., Prechtel, 2002; Laegdsmand, 2004 ; Bekhit, 2005; Simunek, 2006]. The variable matrix of this experiment and the observations of the phases – organic, inter and aqueous are shown in Table 5.

Table 8.5: Variable matrix of PCE solubility experiment

No.	Oxine (mol/l)	Fe (III) (mol/l)	Cu(II) (mol/l)	Observation of phases			Solubility (ppm)	p- value
				Aqueous	Interface	Organic		
1	0	0	0	-	-	-	205	-
2	0	10^{-2}		brown	-	-	182	0.072
3	0	0	10^{-2}	-	-	-	187	0.058
4	10^{-1}	0	0	-	-	-	185	0.056
5	10^{-4}	10^{-2}	0	brown	-	-	191	0.077
6	10^{-2}	10^{-4}	0	Light brown	-	-	205	1.000
7	10^{-2}	10^{-2}	0	Dark green	Precipitates	Grey/green	360	0.000
8	10^{-1}	10^{-2}	0	Bulky yellow precipitates	Precipitates	Yellow precipitates	238	0.280

Notes:

- ‘-’ Clear or no color change.
- A p-value less than or equal to 0.05 (see bold entries) indicates statistically significant difference at 95% level from the control.

The aqueous phases, which initially only contained metal ions (Fe or Cu), turned color to indicate the presence of Fe-oxine (green) or Cu-oxine (yellow) complexes after equilibration with the PCE containing oxine. In the sample No. 8 (Table 8.5), which has the highest concentrations of both Cu(II) and oxine, most of the precipitates aggregated in the aqueous phase and accumulated near the interface. The organic phase was yellow too, with comparatively lesser amount of complex precipitates. This suggests that even though Cu-oxine complex has a large octanol-water partition coefficient, [Turner and Mawji, 2004], the precipitates tend to stay in aqueous phase and do not partition through the interface to a substantial extent.

Figure 8.4 shows the results of PCE solubility with presence of metals (Cu and Fe) and oxine, together with the controls. A t-test at 95% confidence level was done to test the statistical differences between the samples and controls. The t-test results from controls 2, 3 and 4 show that the presence of oxine, Cu, or Fe individually does not affect the aqueous solubility of PCE. Samples 5 and 6, with low (10^{-4} M) concentrations of oxine or Fe(III), are also comparable to the controls. This indicates that the metals and ligand do not affect the solubility of PCE in aqueous phase at these low concentrations. However, the higher Fe(III) and oxine concentrations in samples 7 and 8 resulted in a substantially increased PCE solubility. The results of this analysis had significant uncertainties. Aqueous phase samples collected for analysis contained precipitates. PCE could adsorb on or be entrained with these aggregated precipitates. Thus, while the apparent solubility may indeed be higher, it could be the result of the presence of additional phases, not a true aqueous phase solubility.

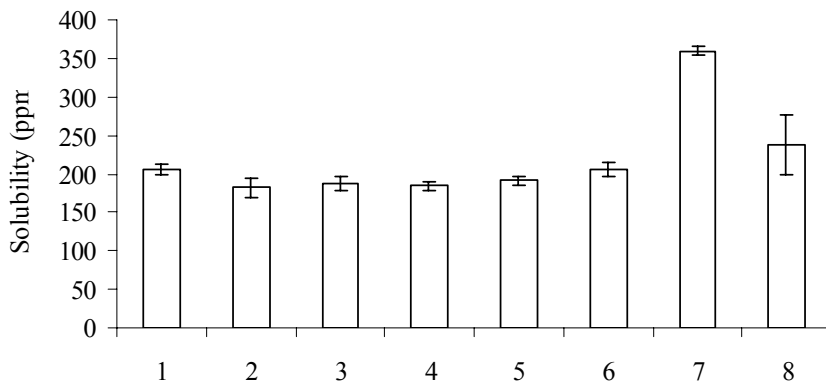


Figure 8.4: PCE solubility in metal complex solutions. Sample numbers are defined in Table 8.5.

The report from McCarthy [1989] showed that the non-polar organics have a high affinity for binding to particulate organic matter. Based on the evidence from sample 7, it could be argued that the Cu-oxine complex could serve as the adsorbent of PCE and hence facilitated the transfer of PCE into aqueous phase when the complex partitioned on the interface. The inorganic or organic chemical must bind strongly and essentially irreversible to the colloids for colloid-facilitated transport to occur [Sen and Khilar, 2006]. The strength and irreversibility of PCE sorption to Cu-oxine precipitates were not evaluated here to confirm the potential for colloid facilitated transport.

8.4.3 Fe(III) and Fe(II) precipitation and surface reactions

Based on the analysis of Fe-oxine complexes, it was observed that the control experiment with Fe(III), but without oxine, had the most significant decrease in IFT (Table 8.4). The precipitation of iron hydroxides and the observed formation of a surface film at the PCE-water interface could have contributed to this change. Additional experiments with a wider range of sample times, NAPLs, and iron species and concentrations were conducted.

Figure 8.5 shows the temporal change in the interfacial tension of NAPLs contacted with 0.01 mol/l Fe(II) and Fe(III) solutions. These data show that the IFT of the chlorinated solvents change substantially with either Fe(II) or Fe(III) in solution compared with the control experiments in the absence of iron. Whereas the IFTs of non-chlorinated NAPLs, toluene, and especially heptane, varied much less between the iron-containing and iron-free aqueous phases. An interfacial tension for PCE as low as 17 mN/m was recorded for the aqueous phase droplet containing 0.01 M Fe(III) at 60 minutes. Of all of the samples, the lowest measurable IFT was 5 mN/m, which was recorded for 4-chlorotoluene in contact with a 0.01M Fe(II) solution.

In systems with the greatest changes in the IFT (PCE, TCE and 4-CT), a surface film or precipitate coating appeared to develop at the surface of the water droplet (Figure 6). This film was only formed when an aqueous drop containing iron was dispensed into the organic phase. The surface film is apparent for water droplets containing both Fe(II) and Fe(III) at 60 minutes or longer. The droplets continued to change over time, past the point where reliable IFT measurements could be made. The Young-LaPlace equation failed to fit droplet shapes that had elongated and deformed. After additional time, the droplets burst, releasing their aqueous phase content to float away yet retaining the yellowish-orange surface film that appears analogous to a punctured balloon.

The formation of a surface film was not observed when an organic phase drop was dispensed into the aqueous phase. The difference between these experimental conditions was the volume ratio of organic phase to aqueous phase. The beaker containing the bulk phase is about 7-ml and the volume of a drop is about 5 μ L. The ratio of the bulk phase to the drop phase is then around 1000:1. Thus, when the

bulk phase is aqueous, it can serve as either a ‘source pool’ or a ‘reservoir’ for any type of surface reaction making it more difficult to observe changes.

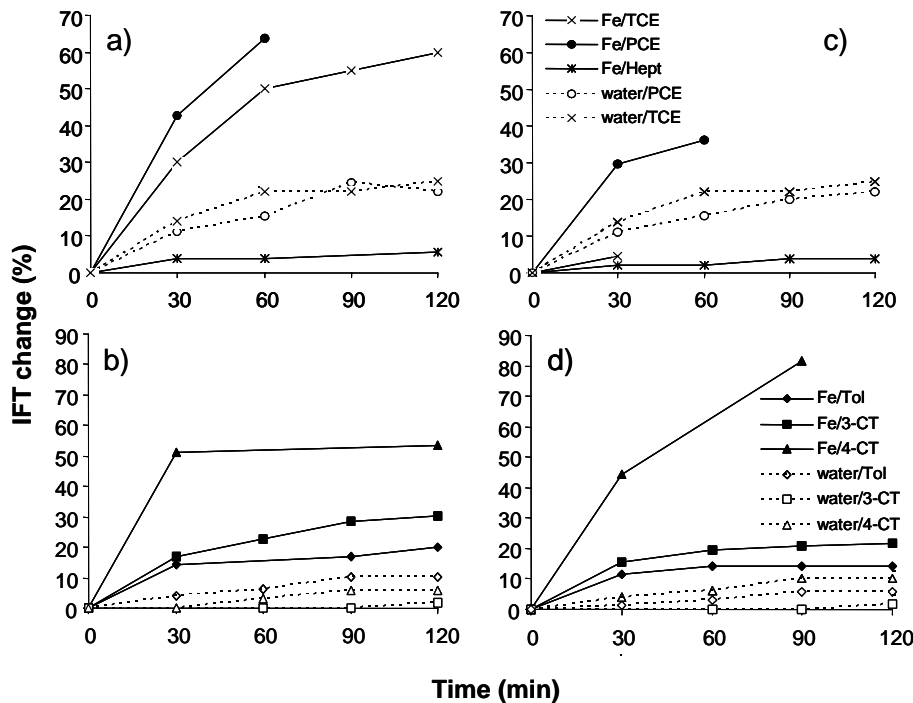


Figure 8.5: Percentage change in the interfacial tension of NAPLs contacted with a) and b) 0.01 mol/L Fe(III) or c) and d) 0.01 mol/L Fe(II) solutions

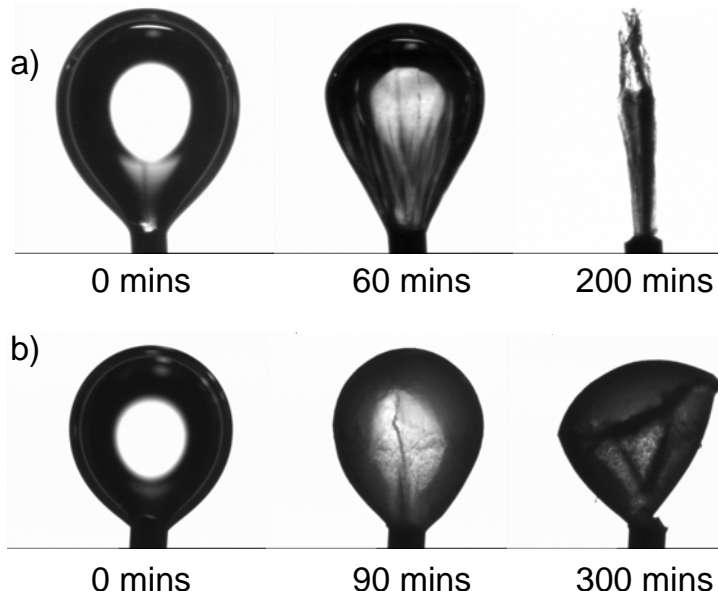


Figure 8.6: Film formation when dispense 0.01 mol/L a) Fe(III) and b) Fe(II) aqueous solution droplets in PCE. A semi-rigid surface film is apparent on drops that aged at least 60 minutes. The white center of the droplets is an artifact of the light reflected from the liquid surface during photography.

The residual film was collected from the needle tip after the Fe(III) experiment and quantified by SEM-EDS analysis. It had an iron/oxygen elemental molar ratio of 0.72, which is very close to that of

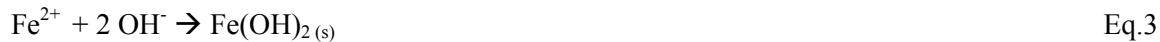
Magnetite (Fe_3O_4). The collective evidence from IFT measurements and identification of Fe species in the surface film leads to the indication that surface chemical reactions between Fe(II) or Fe(III) and chlorinated hydrocarbons can generate a precipitate that causes the formation of a semi-rigid film at the DNAPL-water interface when the chlorinated solvent is in excess compared to the aqueous phase. Both Fe(II) and Fe(III) can undergo hydrolysis reactions forming insoluble precipitates and polymeric species. These species can continue to undergo further transformations to create stable species such as magnetite. These reactions are pH and Eh dependent, but not clearly related to the chlorine content of the DNAPL. Fe(II) can, however react with chlorinated hydrocarbons to oxidize the Fe and dechlorinate the hydrocarbon. This reaction provides an additional pathway to transform between Fe(II) and Fe(III) species, thereby affecting the diversity of insoluble iron species precipitating on the interface, regardless of the initial form of iron used. These chemical reactions are described in more detail below.

It has been reported that the structure and composition of film coated on zero-valent iron could vary depending on the formation mechanism [Cornell, 1996]. In the case of fresh cathodically cleaned iron surface, a quasi-bulk $\text{Fe(OH)}_2/\text{Fe}_3\text{O}_4$ film would be expected [Liu, 2006]. An Fe^{3+} film should form on a pre-oxidized iron surface, which would then be reduced to form a $\text{Fe}_3\text{O}_4/\text{Fe(OH)}_2\cdot2\text{FeOOH}$ film (Odziemkowski, 1998). And in both cases, the main surface product of the aged film is magnetite (Fe_3O_4) [Liu, 2006].

Equations 1 [Liu, 2006] and 2 [Cornell, 1996] can be applied in this case. However, the reaction presented in Eq. 1 needs an increase of pH and eq. 2 requires a reducing environment. In the experiments conducted here, the Fe(III) solution was clear and colorless right after it was made from FeCl_3 . While after about half day, it turned to a brown and turbid color, which indicates the precipitates suspended in solution. The precipitate formation is due to the slow hydrolysis of ferric chloride [Flynn, 1984].



The consumption of H^+ results in the rise of pH. Thus, it causes the precipitation of ferrous hydroxide. Eq. 3 applies here.



Ferrous hydroxide is a relatively insoluble solid phase that can exist for several weeks if in the absence of oxygen and at low temperatures, particularly when synthesized in the laboratory. Nevertheless, it is intrinsically thermodynamically unstable and will convert to magnetite (Fe_3O_4) [Odziemkowski, 1998]. The reaction (Eq. 4) converting ferrous hydroxide to magnetite is known as the Schikorr reaction [Aligizaki, 2000].



Coupled with the iron oxidation reactions, chlorinated organic compounds can undergo dechlorinated reactions. Three pathways (Eq. 5 to Eq. 7) of dehalogenation were presented by Matheson and Tratnek [1994].



The first dehalogenation step (Eq. 5) involves zero-valent iron which is not present in the experiments considered here; hence, it is not applicable. Since Eq. 2 generates Fe^{2+} and Eq. 4 generates H_2 gas, the later two reactions (Eq. 6 and Eq. 7) could occur to dechlorinate the chlorinated solvents and generate precipitates that could accumulate at the interface.

To evaluate the hypothesis that dechlorination reactions occurred and contributed to the apparent reduction in the interfacial tension, n-Heptane and toluene, which are not chlorinated and include a wide range of solubilities, were employed in our study as controls. 3-chlorotoluene and 4-chlorotoluene were also considered for comparison purposes. As discussed above there was no substantial change in the IFT over time relative to the control experiment with no iron (Figure 8.5), photographs presented in Figure 8.7 illustrate that no surface film was observed on these non-chlorinated species. Figure 8, however, shows that precipitates were observed around or inside the drop in 4-chlorotoluene. This might be explained by the strong hydrophobicity of the 3-chlorotoluene which retarded the accessibility of chlorine for the reaction. The study by Burris [1998] showed that the hydrophobicity of chlorinated compound limits its sorption/mass transfer to cast iron and hence, limits the dechlorination rate.

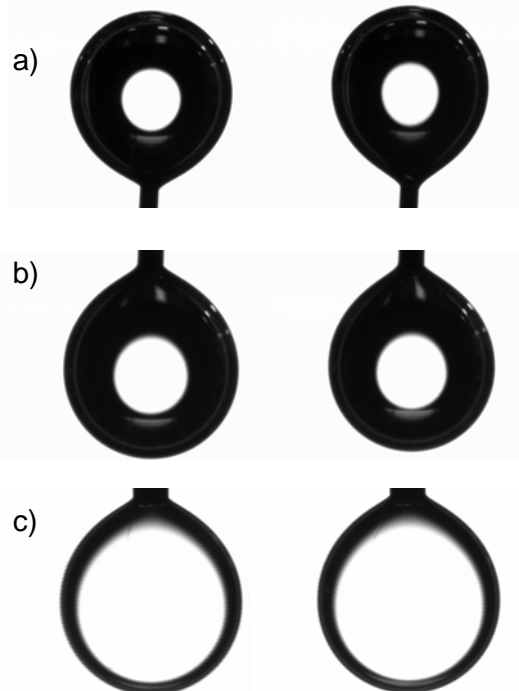


Figure 8.7: Fe(III) aqueous solution droplets suspended in NAPLs: a) 3-chlorotoluene; b) toluene; and, c) heptane at 0 mins (left) and 120 mins (right)

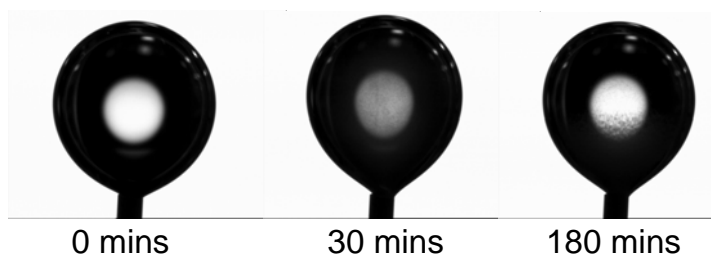


Figure 8.8: Precipitate formation observed when a 0.01 mol/L Fe(III) aqueous solution drop was dispensed in 4-chlorotoluene.

8.4.4 PCE degradation and pH change of aqueous phase

Although the interfacial tension measurements clearly show that the IFT can be reduced substantially when iron and chlorinated hydrocarbons are both present. This is not sufficient, however, to

identify dechlorination reactions as a critical step in the overall mechanism. To further substantiate the importance of dechlorination reactions in the observed film formation and IFT reduction, an experiment to assess the degradation of PCE in solutions of Fe(II) or Fe(III) was conducted. The results are shown in Figure 8.9. Volatile losses were observed in the control experiment with no iron. The results presented are normalized to account for these losses. Interpretation of the results is somewhat complicated by variability in the initial PCE concentrations. This experiment is currently being replicated to improve on the existing experimental artifacts.

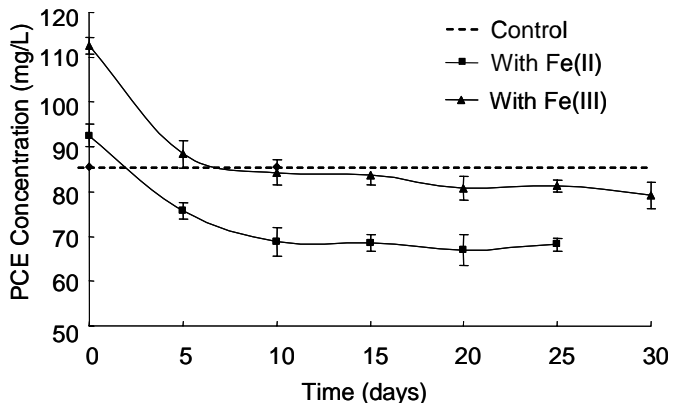


Figure 8.9: PCE degradation with 0.01 mol/l Fe^{3+} and 0.01 mol/l Fe^{2+}

Figure 8.9 shows that the addition of Fe(III) or Fe(II) facilitates the losses rate of PCE relative to the control. With similar losses, however, in both Fe(II) and Fe(III) vials, we cannot substantiate the hypothesis that dechlorination reactions are contributing to the overall set of chemical reactions since only Fe(II) can participate in dechlorination reactions. Further work is required to verify these results before making any final conclusions.

The pH values of the solutions were also monitored (Figure 8.10). The control and ferric chloride solution showed slight change. The ferrous chloride solution pH changed from 4.4 to 3.4. Student's t-tests were done on a 90% confidence level; no statistically significant differences were observed over time.

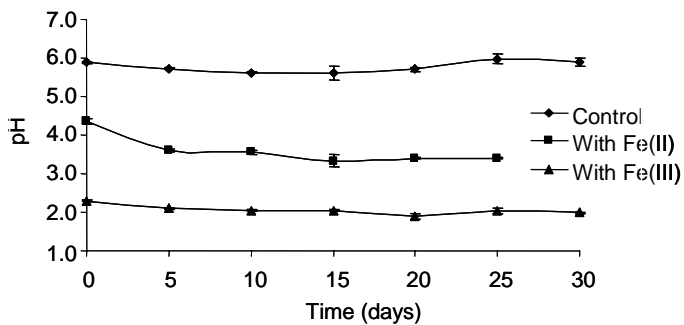


Figure 8.10: pH change of PCE degradation with 0.01 mol/l Fe^{3+} and 0.01 mol/l Fe^{2+}

8.5 Conclusions – Task 4

Low interfacial tensions have been observed for DNAPLs collected from the subsurface [Powers, 1996; Harrold, 2001; Dwarakanath, 2002], although little research has been carried out to investigate the mechanisms. Based on the general types of contaminants co-disposed with DNAPLs and related phenomena reported in the literature, three mechanisms were identified as possible contributors to low interfacial tensions. The conclusions are as following:

Surfactants DBBP and TBP, which are relevant to many DOE sites caused a modest change in the interfacial tension. These changes were much less substantial than observed at field sites, especially for the DOE SRS DNAPL.

The formation of complexes between metals and hydrophobic organic ligands was hypothesized as a mechanism to facilitate the partitioning of metal complexes into the organic phase and enable accumulation of surface active species at the DNAPL-water interface. In the oxine-Cu and oxine-Fe system studied, there was no reduction in the IFT of the DNAPL relative to control experiments. It is possible that this mechanism could be important, however our experimental matrix did not identify relevant metal-ligand combinations.

The most substantial changes in the IFT of chlorinated solvents occurred during their equilibration with Fe(II) or Fe(III) aqueous solutions. The substantial reductions in IFT were observed only for chlorinated solvents. In these cases, semi-rigid surface films formed on water droplets suspended in the solvent. The film was characterized as magnetite (Fe_3O_4), which can form from ferrous hydroxide. The role of the chlorinated versus non-chlorinated solvents on the formation of a semi-rigid surface film and interfacial tension are not yet understood. Preliminary experiments to quantify dechlorination reactions did not show significant differences between Fe(II), which can be oxidized during dechlorination reactions, and Fe(III), which cannot be further oxidized. Further testing is on-going to better identify the specific mechanistic steps in this system.

8.5 Acknowledgements

This research was supported by the Office of Science (BER), U.S. Department of Energy, Grant No. DE-FG02-03ER63660. Chemical analysis was supported by the Clarkson University Center of Air Resources Engineering and Science. This paper is #XXX in the Clarkson Center for the Environment paper series.

8.6 References

Aligizaki, K.K.; de Rooij, M.R. and Macdonald, D.D. Analysis of Iron Oxides Accumulating at the Interface between Aggregates and Cement Paste. *Cement and Concrete Research*. 2000, 30(12): 1941-1945.

Baaden, M.; Berny, F.; Wipff G. The Chloroform / TBP / Aqueous Nitric Acid Interfacial System: a Molecular Dynamics Investigation. *J. Mol. Liq.* 2001, 90: 1-9.

Baaden, M.; Burgard, M.; Wipff. G. TBP at the Water - Oil Interface: the Effect of TBP Concentration and Water Acidity Investigated by Molecular Dynamics Simulations. *J. Phys. Chem. B* 2001, 105: 11131-11141.

Basak, S.C.; and Mills, D. Prediction of Partitioning Properties for Environmental Pollutants Using Mathematical Structural Descriptors, *Arkivoc* 2005 (ii): 60-76
http://www.arkivoc.org/ARKIVOC%5CJOURNAL_CONTENT%5Cmanuscripts%5C2005/NA-1214FP%20as%20published%20mainmanuscript.pdf

Bayer. Technical Information Bulletin: Tributyl Phosphate. (TIB 2003-10-16), Bayer AG, Leverkusen, 2003.

Bekhit, H.M.; and Hassan, A.E. Two-dimensional Modeling of Contaminant Transport in Porous Media in the Presence of Colloids. *Advances in Water Resources*. 2005, 28 (12): 1320-1335.

Burris, D.R.; Allen-King, R.M.; Manoranjan, V.S.; et. al. Chlorinated Ethane Reduction by Cast Iron: Sorption and Mass Transfer. *J. Environ. Engrg. – ASCE*. 1998, 124(10): 1012-1019.

Cornell, R.M.; and Schwertmann, U. *The Iron Oxides*. VCH publishers, New York, 1996.

del Rio, O.I.; Neumann, A.W. Axisymmetric Drop Shape Analysis: Computational Methods for the Measurement of Interfacial Properties from the Shape and Dimensions of Pendant and Sessile Drops. *J. Colloid Interface Sci.* 1997, 196(2), 136–147.

Demond, A.H.; and Lindner, A.S. Estimation of Interfacial Tension between Organic Liquids and Water. *Environ. Sci. Technol.* 1993 (27): 2318-2331.

Dietz, M.L.; and Freiser, H. Adsorption of Neutral Metal Chelates at Liquid-Liquid Interfaces. *Langmuir.* 1987, (3): 467-470.

D'Olieslager, W.; Sannen, L.; De Jonghe, M. Synergism of Tributylphosphate (TBP)-Dibutylbutylphosphate (DBBP) Mixtures in the Extraction of Tm(III) with Benzoyltrifluoroacetone (HBTA). *J. Less Common Metals.* 1985, 112: 235-242.

Dou, W.; Powers, S. E.; et.al. Characterization of DNAPL from DOE Savannah River Site in preparation for submission to *J. Cont. Hydrol.* 2007.

Dwarakanath, V.; Jackson, R.E. and Pope, G.A. Influence of Wettability on the Recovery of NAPLs from Alluvium. *Environ. Sci. Technol.* 2002, (36): 227-231.

Flynn, C.M. Jr. Hydrolysis of Inorganic Iron(III) Salts. *Chem. Rev.* 1984, 84: 31-41.

Giraudi, G.; Giraudi, G.; Baggiani, C.; Giovannoli, C.; Marletto, C. And Vanni, A. Synthesis and Characterisation of 8-Hydroxyquinoline Bovine Serum Albumin Conjugates as Metal Ion Chelating Proteins. *Analytica Chimica Acta*, 1999, 378 (1-3): 225-233.

Guasp, E. and Wei, R. Dehalogenation of Trihalomethanes in Drinking Water on Pd-Fe Bimetallic Surface. *J. Chemical Technology and Biotechnology.* 2003, 78 (6): 654-658

Harrold, G.; Goody, D. C.; et. al. Wettability Changes in Trichloroethylene-Contaminated Sandstone. *Environ. Sci. Technol.* 2001 (35): 1504-1510.

Harrold, G.; Goody, D. C.; Reid, S.; Lerner, D. N.; Leharne, S. A. Changes in Interfacial Tension of Chlorinated Solvents following Flow through U.K. Soils and Shallow Aquifer Material. *Environ. Sci. Technol.* 2003, 37(9):1919 -1925.

Harrold, G., Lerner, D., and Leharne, S. The Impact of Additives Found in Industrial Formulations of TCE on the Wettability of Sandstone. *J. Contam. Hydrol.* 2005, 80: 1-17.

Hwang, I.; Park, H.J.; et. al. Reactivity of Fe(II) / Cement Systems in Dechlorinating Chlorinated Ethylenes. *J. of Hazard. Mater.* 2005 (B118): 103-111.

Jha. B.K.; Patist, A.; Shah, D.O. Effect of Antifoaming Agents on the Micellar Stability and Foamability of Sodium Dodecyl Sulfate SolutionsEffect of Antifoaming Agents on the Micellar Stability and Foamability of Sodium Dodecyl Sulfate Solutions. *Langmuir.* 1999, 15: 3042-3044.

Johnson T.L.; Fish W.; Gorby Y.A.; et al. Degradation of Carbon Tetrachloride by Iron Metal: Complexation Effects on the Oxide Surface. *J. Contam. Hydrol.* 1998, 29 (4): 379-398.

Kemp, S.B. Occidental Chemical Corporation Physical-Chemical Properties of Specific HPV Chemicals. Sept. 2001 <http://www.epa.gov/chemrtk/pubs/summaries/pchlrtol/c13214.pdf>

Laegdsmand, M.; de Jonge, L.W.; Moldrup, P.; et al. Pyrene Sorption to Water-Dispersible Colloids: Effect of Solution Chemistry and Organic Matter. *Vadose Zone Journal.* 2004, 3 (2): 451-461.

Liu, C.C.; Tseng, D.H.; Wang, C.Y. Effects of Ferrous Ions on the Reductive Dechlorination of Trichloroethylene by Zero-Valent Iron. *J. of Hazard. Mater.* 2006 (B136): 706-713.

Lohman, J.H., A History of Dry Cleaners and Sources of Solvent Releases from Dry Cleaning Equipment. *Environ. Forensics* 2002, 3: 35– 58.

Luthy, R.G.; Ramaswami, A.; et. al. Interfacial Films in Coal Tar Nonaqueous-Phase Liquid-Water Systems. *Environ. Sci. Technol.* 1993 (27): 2914-2918.

Matheson, L.J.; and Tratnyek, P.G. Reductive Dehalogenation of Chlorinated Methanes by Iron metal. *Environ. Sci. Technol.* 1994, 28: 2045-2053.

Mackay, D.M.; Cherry, J.A. Groundwater Contamination— Pump-and-Treat Remediation: 2. *Environ. Sci. Technol.* 1989, 23(6): 630– 636.

Mackay, D.; Shiu, W-Y.; and Ma, K-C. *Illustrated Handbook of Physical-chemical Properties and Environmental Fate for Organic Chemicals: Vol. III Volatile Organic Chemicals.* 1993, Lewis Publishers. Ann Arbor, Michigan

Martell, E.; and Calvin, M. *Chemistry of the Metal Chelate Compounds.* Prentice-Hall, New York, N. Y., 1952.

McCarthy, J. F.; and Zachara J. M. Subsurface Transport of Contaminants. *Environ. Sci. Technol.* 1989 23: 496-502.

Mercer, J.W.; Cohen, R.M. A Review of Immiscible Fluids in the Subsurface: Properties, Models, Characterization and Remediation. *J. Contam. Hydrol.* 1990, 6 (2): 107–163.

Nelson, E.C.; Ghoshal, S.; et al. Chemical Characterization of Coal Tar-Water Interfacial Films. *Environ. Sci. Technol.* 1996, 30: 1014-1023.

Odziemkowski, M.S.; Schuhmacher, U.; Gillham, R.W.; and Readon, E.J. Mechanism of Oxide Film Formation on Iron in Simulating Groundwater Solutions: Raman Spectroscopic Studies. *Corros. Sci.* 1998, 40: 371-389.

Poulsen M. M.; and Kueper B. H. A Field Experiment to Study the Behavior of Tetrachloroethylene in Unsaturated Porous Media. *Environ. Sci. Technol.* 1992, 26: 889-895.

Powers, S.E.; Anckner, W.H.; and Seacord, T.F. The Wettability of NAPL-Contaminated Sands. *J. Environ. Engrg.* 1996, 122(10): 889-897.

Prechtel A.; Knabner, P.; Schneid, E.; et al. Simulation of Carrier-Facilitated Transport of Phenanthrene in a Layered Soil Profile. *J. Contam. Hydrol.* 2002, 56 (3-4): 209-225.

Prochaska, K. and Staszak, K. Adsorption at the Liquid/Liquid Interface in Mixed Systems with Hydrophobic Extractants and Modifiers I. Study of Equilibrium Interfacial Tension at the Hydrocarbon/Water Interface in Binary Mixed Systems Extractants. *J. Colloid and Interface Science.* 2005 (285): 1-8.

Riley, R.J.; Zachara, G.M. Chemical Contaminants on DOE Lands and Selection of Contaminant Mixtures for Subsurface Science Research. Report prepared for U.S. DOE Office of Energy Research, Subsurface Science Program DOE-ER 0547T. 1992.

Ritter, K.; Odziemkowski, M.S.; and Gillham, R.W. An In Situ Study of the Role of Surface Films on Granular Iron in the Permeable Iron Wall Technology. *J. Contam. Hydrol.* 2002, 55(1-2): 87-111.

Schlottmann, U. SIDS Initial Assessment Report for SIAM 20 Paris, France, 19 – 22 April 2005 <http://www.chem.unep.ch/irptc/sids/OECDSIDS/106434.pdf>.

Sen, T.K.; and Khilar, K.C. Review on Subsurface Colloids and Colloid-Associated Contaminant Transport in Saturated Porous Media. *Advances in Colloid and Interface Science.* 2006, 119(2-3): 71-96.

Sengupta, T.; Yates, M. and Papadopoulos, K.D. Metal Complexation with Surface-Active Kemp's Triacid. *Colloid and Surfaces A: Physicochemical and Engineering Aspects.* 1999 (148): 259-270.

Shioya, Y.; Nishizawa, S. and Teramae, N. Complexation Kinetics of 5-alkyloxymethyl-8-quinolinols at Liquid-Liquid Interfaces as Studied by Dynamic Interfacial Tensiometry. *Langmuir*. 1998, (14): 4552-4558.

Shirin, S.; Buncel, E. and VanLoon, G. Effect of Cyclodextrins on Iron-Mediated Dechlorination of Trichloroethylene - A Proposed New Mechanism. *Canadian J. of Chemistry*. 2004, 82 (12): 1674-1685.

Simunek, J.; He, C.M.; Pang, L.P.; et al. Colloid-Facilitated Solute Transport in Variably Saturated Porous Media: Numerical Model and Experimental Verification. *Vadose Zone Journal*. 2006, 5(3): 1035-1047.

SRC PhysProp Database <http://www.syrres.com/esc/physdemo.htm>

Staszak, K.; and Prochaska, K. Interfacial Activity of Copper(II) Complexes with Chelating Ligands and Individual Hydrophobic Extractants in Model Extraction Systems I. Study of Equilibrium Interfacial Tension at the Hydrocarbon/Water Interface for Systems with Copper(II) Complexes with Chelating Ligands and Individual Hydrophobic Extractants. *J. Colloid and Interface Science*. 2004, (280): 184-191.

Stoyanov, E.S. Compositon, Structure and IR Spectra Peculiarities of Proton Hydratosolvates $H+(H_2O)_n Lm$ Forming in the Tributylphosphate Solutions of Strong Acid $HFeCl_4$. *J. Chem. Soc., Faraday T rans.* 1997, 93:4165-4175.

Sun, T.L.; Zhang, L.; et.al Dynamic Dilational Properties of Oil-Water Interfacial Films Containing Surface Active Fractions from Crude Oil. *J. of Disper. Sci. Technol.* 2003, 24(5): 699-707.

Sztukowski, D.M.; and Yarranton, H.W. Rheology of Asphaltene - Toluene/Water Interfaces. *Langmuir*. 2005, 21(25): 11651-11658.

Thomas, R.P.; Macaskie, L.E. Biodegradation of Tributyl Phosphate by Naturally Occurring Microbial Isolates and Coupling to the Removal of Uranium from Aqueous Solution. *Environ. Sci. Technol.* 1996, 30: 2371-2375.

Turner, A.; Mawji, A. Hydrophobicity and Octanol-Water Partitioning of Trace Metals in Natural Waters. *Environ. Sci. & Technol.* 2004, (38): 3081-3091.

9.0 Research Products

9.1 Papers:

Powers, S.E., Omrane, K., and Grimberg S.J., Unique Interfacial Properties of the Chlorinated Solvent DNAPL at Savannah River National Laboratory. In: Extended Abstracts, Environmental Division of the American Chemical Society (Anahiem CA, March 2004), (on CD).

Hwang, S.I., K.P. Lee, D.S. Lee, S.E. Powers, "Effects of fractional wettability on capillary pressure-saturation-relative permeability relations of two-fluid systems." *Advances in Water Resources*, 29(2): 212-226, 2006.

Dou, W., K. Omrane, S.J. Grimberg, M. Denham and S.E. Powers, "Interfacial Properties of a Chlorinated Solvent DNAPL from the Savannah River DOE Facility." in preparation for submission to *J. Cont. Hydrology*.

Denham, M.E., S.J. Grimberg, M. R. Millings, S.E. Powers. Vadose zone DNAPL distributions relative to physical, chemical and biological sources of heterogeneity at a field site. in preparation for submission to *J. Cont. Hydrology*.

Grimberg, S.J., T. Doty, L. Bertrand, K. Omrane, S.E. Powers, The Role of PCE degrading Microorganisms on DNAPL Interfacial Properties. In preparation.

9.2 Presentations at Conferences:

Powers, S.E., Omrane, K., Dou, W., and Grimberg S.J., Unique Interfacial Properties of the Chlorinated Solvent DNAPL at Savannah River National Laboratory. Presented at the American Chemical Society National Meeting, Anahiem CA, March 30, 2004.

Bertrand, L.J., S.J. Grimberg, S.E. Powers, M. Denham, T.D. Doty, "Microbial Heterogeneity in the Subsurface and its Effects on DNAPL Interfacial Properties" Poster presented at the annual AGU conference, San Francisco CA Dec. 14, 2004.

Dou, W., S.E. Powers, "Colloids Partitioning between Organic and Aqueous Phase Cause the Low Interfacial Tension of DNAPL. Presented at the ACS Colloids and Surfaces Conference, Clarkson University, Potsdam NY, June 2005.

Bertrand, L.J., S.J. Grimberg, S.E. Powers, T.D. Doty, M. Denham, "Microbial Heterogeneity in the Subsurface and its Effects on DNAPL Interfacial Properties." Poster presented at the 2005 AEEPS Research and Education Conference, Clarkson University, Potsdam NY, July, 2005.

Dou, W., S.E. Powers, "Mechanisms Contributing to Low DNAPL-Water Interfacial Tension (IFT)." Presented at the 2006 NYWEA Conference, New York City, February 2006.

9.3 Invited Lectures

Grimberg, S.J. (2003) Bacteria/DNAPL Interactions and Their Role on DNAPL Interfacial Properties. Presented to the Department of Inorganic, Analytical and Applied Chemistry, University of Geneva, Switzerland, June 6, 2003.

Grimberg, S.J. (2003) The role of microorganisms on DNAPL interfacial properties and DNAPL distribution. Presented under the Environmental Sciences Series of the EAWAG, Switzerland, May 23, 2003.

Powers, S.E. "What's in that DNAPL and Why does it Matter?" NIEHS DNAPL Source Zone Workshop, University of Arizona, Tucson AZ, February 2005.

9.4 Graduate Thesis

Tom Doty (2003), The Role of Microorganisms on DNAPL Interfacial Properties and Distribution, Masters Thesis, Clarkson University, Potsdam NY.

Kamel Omrane (2003), Factors affecting the interfacial properties in the subsurface at the Savannah River Site, Masters Thesis, Clarkson University, Potsdam NY.

Laura Bertrand (2006), Analysis of background microbial concentrations and impacts on DNAPL-water interfacial tension, Masters Thesis, Clarkson University, Potsdam NY.

Wenqian Dou (2007, expected) Mechanisms and components causing low interfacial tension of chlorinated NAPLs, PhD Dissertation, Clarkson University, Potsdam NY